# CONTROL OF SUBSYNCHRONOUS RESONANCE USING FACTS DEVICES

by

**S V. JAYARAM KUMAR**



DEPARTMENT OF ELECTRICAL ENGINEERING

**INDIAN INSTITUTE OF TECHNOLOGY KANPUR**

June, 1999

# CONTROL OF SUBSYNCHRONOUS RESONANCE USING FACTS DEVICES

*A Thesis Submitted*
*in Partial Fulfilment of the Requirements*
*for the Degree of*

*DOCTOR OF PHILOSOPHY*

*by*

**S V JAYARAM KUMAR**

*to the*

DEPARTMENT OF ELECTRICAL ENGINEERING

**INDIAN INSTITUTE OF TECHNOLOGY KANPUR**

June, 1999

# CERTIFICATE

This is to certify that the work contained in the thesis entitled Control of Subsynchronous Resonance using FACTS Devices by S V Jayaram Kumar has been carried out under our supervision and this work has not been submitted elsewhere for a degree

Arindam Ghosh

Sachchidanand

Department of Electrical Engineering
Indian Institute of Technology
Kanpur India

Dedicated to

my family

# ACKNOWLEDGEMENT

It is with a deep sense of gratitude that I express my indebtedness to my supervisors Professor Arindam Ghosh and Professor Sachchidanand for their sincere, exemplary guidance throughout the course of this work

I am thankful to Dr S S Prabhu Dr S C Srivastava, Dr Avinash Joshi and Dr R K Varma for their motivation and support at various stages of the couse work

The discussions with K K Mahapatra, R K Singh, Dr Biswarup Das R P Gupta G Pillai N K Sharma and M K Misra contributed to my knowledge to a great extent The interaction with Sricharan and T S Rao and P V K Reddy made my life here more memorable I am thankful to fellow research scholars in the hostel Dr P V S N Murthy Dr Badri, Dr Srinivasan, Dr Himanshu Agrwal Dr Chandrasekhar Rao Dr Dixit Appaji P S Rao and Ravi for their valuable company and guidance throughout my stay in the campus The hospitality rendered by Dr G S Narayana and his family during my stay here is unforgettable

I would like to express my grattitude to Dr S Krishna born philosophor for guiding me to right directions throught this venture I take this oppurtunity to thank Dr Krishna's family for their hospitality and affection I would like to thank my friends M/s V V K Reddy, Dr D N Rao, kumar, Sairama, Sleeva reddy, Venkataramana, Dr P R M Rao Vennelaganti Prasad, U V S Rao for their encouragement throughout this task

It is not possible to describe adequately the support I have received from Srinivasa Murthy, Vasudha, Meghana, Gopal Lastly but of course not the least I thank my wife Girija and son Sriharsha for their forbearance throughout this venture

| | |
|---|---|
| Thesis title | CONTROL OF SUBSYNCHRONOUS RESONANCE USING FACTS DEVICES |
| Name | S V Jayaram Kumar |
| Roll number | 9420461 |
| THESIS supervisors | Dr Arindam Ghosh and Dr Sachchidanand |
| Degree for which submitted | Ph D |

## SYNOPSIS

The continuously growing demand for electric power requires the transmission of large amounts of power over long distances An economically attractive solution to increase power transfer through long transmission lines, without building new parallel circuits, is to install the series capacitors It is known that series capacitor compensation benefits power systems in many ways, such as enhancing transient stability limits, increasing power transfer capability, etc It is also known that fixed series compensation may cause sub synchronous resonance (SSR) in power systems, which can lead to the damage to machine shaft Since the discovery in 1970 that SSR was the main cause of the shaft failures at the Mohave generating station (USA) extensive research and development efforts have been devoted to the development of effective SSR mitigation measures

The definition of SSR is given by IEEE [1] Subsynchronous resonance is an electric power system condition where the electric network exchanges energy with a turbine generator at one or more of the natural frequencies of the combined system below the synchronous frequency of the system

When a series compensated power system is perturbed, its equilibrium state is disturbed, giving rise to interchange of energies between mechanical and electrical systems mutually coupled through the rotor of the synchronous generator As energies are interchanged, their frequencies of oscillations are the natural frequencies of their respective

systems The natural frequencies of oscillation of each system form their respective modes of oscillation An oscillation of generator rotor, due to disturbances, produce super syn chronous and sub synchronous components of currents (or voltages) These currents induce subsynchronous and supersynchronous torques There are many ways in which the system and the generator may interact with subsynchronous effects Couple of these interactions are (1) Torsional interaction and (2) Transient torque effect The turbine generator shaft system responds to disturbances with oscillations at its natural frequencies Oscillations of the generator rotor at its natural frequency result in modulation of generator voltage The subsynchronous frequency voltage is the complement of the natural frequency of the turbine generator shaft system When this subsynchronous frequency is close to system natural frequency, the resulting armature currents produces a subsynchronous torque which re inforces the aforementioned generator rotor oscillations This can result in sustained or growing oscillations This phenomenon is referred to as torsional interaction

System disturbances impose electromagnetic torques on generator rotor, subjecting shaft segments to torsional stresses Following a significant system disturbance in series capacitor compensated power system, the resulting electromagnetic torque oscillations at a frequency complement to the electrical system natural frequency If this frequency coincides with any of the natural modes of the turbine generator shaft, there can be large peak torques This effect is referred as transient torque effect or shaft torque amplification

Power electronic systems are finding increasing applications in power systems for both transient state and steady state operation requirements [2] STATCOM is a second gener ation FACTS device The STATCOM consists of GTO based voltage source inverter (VSI) with a dc capacitor coupling transformer and control circuit The VSI is connected to the AC bus through coupling transformer The variation in STATCOM output voltage can be achieved through the control of the firing angle [3] STATCOM with voltage controller for SSR mitigation is proposed in the literature The voltage controller along with the reactive

current controller may be considered for improving the performance of the STATCOM

Controlled series compensation (CSC) is a type of Flexible AC transmission systems (FACTS) controller which utilizes thyristor valves to control the degree of series compensation [4] CSC consists of two components, one element is a mechanically switched portion the second portion being a Thyristor Controlled series capacitor (TCSC) The TCSC consists of a fixed capacitor in parallel with a thyristor controlled reactor(TCR) The TCR reactance is varied by varying the firing angle of the thyristors, which in turn varies the effective capacitive reactance Discrete time and continuous time TCSC models were proposed in the literature to study the SSR phenomenon and to estimate the damping of torsional modes in open loop The TCSC control strategy can be utilized to study the impact of TCSC on torsional modes

It is mentioned previously that series compensated power system gives raise to subsynchronous phenomenon Various methods of counteracting subsynchronous resonance phenomenon have been considered which are great diversity in concept and methods Most of these concepts were tested with IEEE first bench mark model One of these methods is to modulate either real power or reactive power injected into the generator bus of the affected steam turbine The modulation of real power and reactive power is one of the effective means of mitigating subs nchronous resonance and this can be achieved by FACTS controllers The real power modulation can be achieved by the modulation of TCSC reactance whereas reactive power modulation can be obtained by STATCOM

The torsional interaction may be considered as small disturbance phenomenon whereas transient torque problem is due to the large disturbance The torsional interaction analysis is usually carried out utilizing linearized models The study of transient torque problem requires the detailed modeling of all system nonlinearities Digital simulation is well suited for analyzing transient torque effect [1]

Subsynchronous resonance control through FACTS controllers is gaining importance

Based on the above considerations, this thesis focussed the attention on control of subsyn chronous resonance which includes torsional interaction and transient torque effects with FACTS controllers such as STATCOM and TCSC

The objectives and scope of thesis are

1 To study the subsynchronous transient oscillation damping with the STATCOM

2 To propose a new digital control scheme for TCSC control to damp subsynchronous resonance oscillations

3 To study the control interactions between TCSC and power system stabilizer

An outline of the work reported in the thesis is given below

The first chapter gives an introduction to the various aspects of the problem presented in the thesis and reviews briefly the previously published literature

In Chapter 2 linearized model of generator system with detailed representation of stater, rotor and mechanical system along with AC network is presented The study system in this Chapter and subsequent Chapters is the celebrated IEEE First bench mark model [1] Eigenvalue analysis is carried out with the linearized overall system model The results obtained through eigenvalue analysis is validated with time domain simulation and Fourier analysis The effectiveness of NGH damping scheme [5,6] in mitigating the subsynchronous torque oscillations is studied through the detailed time domain simulation

In Chapter 3, linearized model of 12 pulse STATCOM along with voltage and reactive controller is presented [7] The control parameters are obtained through eigenvalue analysis of the linearized model The results obtained through eigenvalue analysis are validated with time domain simulation for the study of transient torque oscillations Comparative study is carried out with NGH damping scheme in mitigating subsynchronous torque oscillations

SSR analysis with TCSC in continuous time linearized domain is presented in Chapter 4 Constant angle control of TCSC is investigated The constant angle control is based on

the philosophy of maintaining the voltage drop across the compensated transmission line constant Eigenvalue analysis is carried out to predict the stability of the system and the results are validated with time domain simulation

In Chapter 5 a novel digital control scheme is proposed for TCSC control For this purpose a discrete time domain TCSC model is developed The controller is designed using state feedback approach The discrete time model along with the controller is suitably interfaced with the generator system model to obtain a homogeneous state space equation The stability of the system is analyzed through eigenvalue analysis and the results are validated with time domain simulation

The effect of excitation system that includes power system stabilizer (PSS) on tor sional modes, in the presence of TCSC controller is examined in Chapter 6 The control interaction study is carried out through eigenvalue analysis

This thesis concludes in Chapter 7 outlining the conclusions drawn from the thesis and suggest some future scope of work

## References

[1] IEEE SSR Task force Proposed terms and definitions for subsynchronous resonance in series capacitor compensated transmission lines IEEE Trans on PAS, Vol PAS 92 March/April 1980, pp 506-511

[2] N G Hingorani FACTS Flexible AC Transmission Systems, paper presented at IEE fifth international conference on AC and DC transmission, sept 1991 London, pp 1 7

[3] C Schauder et al Operation of a ± 100 MVAR TVA STATCON IEEE Trans on Power Delivery, Vol 9, No 2 1994, pp 1018 1027

[4] N Christl, R Heidin, P E Krause and S M Mckenna Advanced series compensation (ASC) with thyristor controlled impedance CIGRE regional meeting, session 1' 92, Paris

[5] N G Hingorani A new scheme for subsynchronous resonance damping of torsional

oscillations and transient torque Part 1 IEEE Trans on PAS, Vol PAS-100, No 4 1981 pp 1852 1855

[6] K B Stump R Heidin and N G Hingorani A new scheme for subsynchronous resonance damping of torsional oscillations and transient torque Part 2 IEEE Trans on PAS Vol PAS 100 No 4 1981, pp 1856-1863

[7] C Schauder and H Mehta Vector analysis and control of Advanced static var compensator IEE Proc C Vol 140, N0 4, july 1993, pp 299 306

[8] A Ghosh and G Ledwich Modeling and control of thyristor controlled series compensators IEE Proc Generation Transmission and Distribution, Vol 142 No 3 May 1995, pp 297 304

# Contents

# List of Figures

# List of Tables

# LIST OF PRINCIPAL SYMBOLS

$R$ Resistance

$L$ Inductance

$C$ Capacitance

$X$ Reactance

$D$ Damping constant

$K$ Spring constant

$M$ Inertia constant

$f$ Frequency in $Hz$

$\omega_B$ Base angular frequency in rad/sec

$\psi$ Flux

$\delta$ Rotor angle

$\theta$ Angle

$\alpha$ Firing angle

$k$ Discrete time instant

$\omega_n$ Natural frequency in rad/sec

$\zeta$ Damping ratio

$T_m, T_e$ Torques

$T_d, T_q$ Time constants

$K_P, K_I$ Controller gains

$\mathbf{x}$ State variable

$\mathbf{y}$ Output variable

$\mathbf{u}$ Input variable

Prefix $\Delta$ denotes increment

Superscript T denotes transpose

Superscript / denotes transient

Subscript N denotes network

Subscript m denotes mechanical

Subscript g denotes generator

Subscript $d, q, o$ denotes d q o axis variables

Subscript $D, Q\ O$ denotes D Q O axis variables

A dot over a symbol denotes differentiation with respect to time

The other symbols used in the text are explained as and when they are introduced

# Chapter 1

# INTRODUCTION

One of the important challenges facing the utility industry is the efficient utilization of the existing transmission network, in view of the difficulties involved in adding new transmission capacity. The increase in power flow over a given transmission network can be achieved by compensating the AC network either by series compensation of part of inductive reactance of the transmission line by series capacitors or by shunt compensation to maintain voltage at appropriate points in the network by reactive power compensators.

Series capacitors provide a direct approach to increase transmission capability which is very often the most economical solution. Unfortunately however, it can give rise to subsynchronous resonance (SSR) by interacting with the turbo-generator. Two incidents of generator shaft damage at Mohave generating station in the United States [1] prompted investigation into the nature of the problem of subsynchronous resonance and its solution. The slow nature of series capacitors control through mechanical switching restricted their usefulness which implies that faster dynamic controls are required for better utilization of AC transmission network. The advent of high voltage and high power thyristor valves and digital controllers in HVDC transmission has demonstrated the viability of fast controllers for power transmission. subsequently this has led to the concept of Flexible AC transmission systems (FACTS), which uses advanced solid state controllers to overcome the problem of underutilization of AC transmission networks.

FACTS includes host of controllers namely static var compensator (SVC), thyristor controlled series capacitor (TCSC), static compensator (STATCOM), thyristor controlled braking resistor (TCBR), thyristor controlled phase angle regulator (TCPR) unified power flow controller (UPFC), and solid state series compensator (SSSC) In this thesis an attempt has been made to apply some of the FACTS controllers to control the subsynchronous resonance caused by series capacitors Subsynchronous resonance phenomenon and the various FACTS controllers are discussed in the following sections

## 1 1 Subsynchronous Resonance

Subsynchronous resonance is a major concern for the stability of turbine generators con nected to transmission systems that employ series capacitors A disturbance in the power system can cause stimulation of turbine-generator natural torsional modes When the generator is connected to a series capacitor compensated system these oscillations can be amplified and sustained due to interaction between the electrical power system and the torsional mechanical system SSR has been defined by the IEEE SSR Task Force [2] as

*Subsynchronous resonance is an electrical power system condition where the electrical net work exchanges energy with the turbine generator at one or more of the natural frequencies of the combined system below the synchronous frequency of the system*

During the incidents of generator shaft damage at Mohave [1], it was found that the frequency of one of the torsional modes was close to the complementary frequency of subsynchronous currents present in the electrical system This resulted in large torque in the shaft section bet veen the generator and exciter which subsequently damaged the shaft

There are two pr )blems associated with SSR [3] One is steady state SSR which may be due to (a) induction generator effect and (b) torsional interaction The second problem is a

transient SSR phenomena and termed as transient torque or torque amplification problem To understand these aspects, consider a synchronous generator connected to an infinite bus through a series compensated line, as shown in Fig 1 1 The series resonant frequency of the electrical network is given by

$$f_e = f_o\sqrt{\frac{X_C}{X'' + X_L}} \tag{1 1}$$

where

$X''$ subtransient reactance of generator

$X_L$ reactance of line and transformer

$X_C$ reactance of series capacitor

$f_o$ nominal frequency

It is to be noted that since $X_C < X_L$, $f_e < f_o$

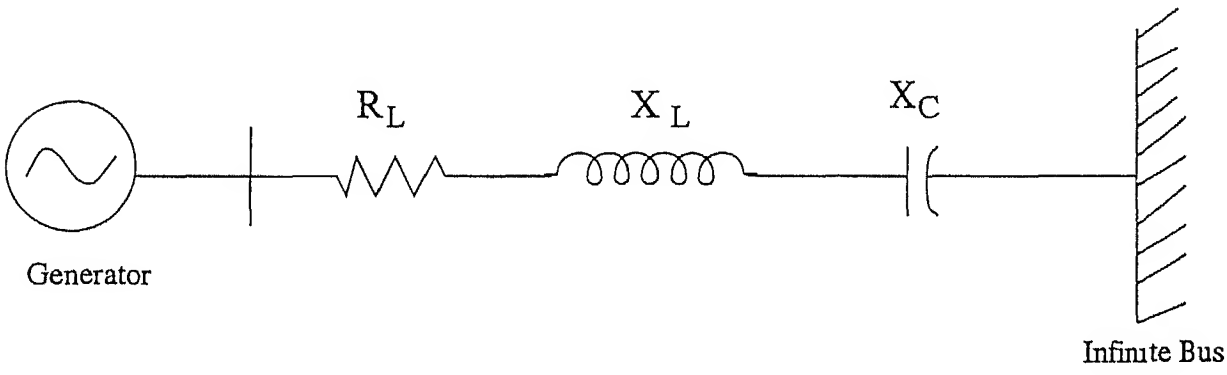


**Figure 1 1** Series compensated power system

The electrical disturbances that occur in the system cause transient currents which die away with a damping rate depending on the value of series resistance $R_L$ at frequency $f_e$ These subsynchronous currents of frequency $f_e$ flow in the armature and result in subsynchronous torques and currents in the rotor circuit at frequency $f_r$ given by

$$f_r = f_o - f_e \tag{1 2}$$

The subsynchronous rotor currents and mechanical oscillations produce subsynchronous voltage components which sustain the currents The frequency $f_r$ is defined as the complementary frequency of $f_e$

### 1 1 1 Induction Generator Effect

The induction generator effect is due to the electrical system dynamics The rotor resistance to subsynchronous currents viewed from the armature terminals is negative At the system resonant frequency $f_e$, if this negative resistance exceeds the positive resistance of network, self excitation takes place However this problem can be tackled by suitable design of amortisseur circuits [4]

### 1 1 2 Torsional Interaction

The Generator rotor oscillations at a torsional mode frequency, $f_m$ induce armature voltage components at frequencies ($f_{em}$) given by

$$f_{em} = f_o \pm f_m \tag{1 3}$$

When $f_{em}$ is close to $f_e$ (electrical resonant frequency), the subsynchronous torques produced by the subsynchronous voltage component can be sustained [4] This interplay between electrical and mechanical systems is termed as torsional interaction

### 1 1 3 Torque amplification Problem

System disturbances impose electromagnetic torques on generator rotors, subjecting shaft segments to torsional stresses Following a significant disturbance in a series capacitor compensated system, the resulting electromagnetic torque oscillates at frequency of $f_0 - f_e$ If this frequency is near to any natural frequency of shaft section, the resulting shaft torques could be much larger than those produced by a three phase fault in a system without series

capacitors This is caused by resonance between the electrical system and mechanical system natural frequencies These effects are referred to as shaft torque amplification [5]

### 1 1 4 Countermeasures for SSR

The control of SSR during transients in series compensated systems using static filters bypassing of series capacitors, excitation control etc , have been suggested in literature [6–8] A summary of the various solutions for mitigating the effect of SSR is presented in [9] Farmer et al [8] Fouad et al [7] and Li Wang [10] suggested the injection of a properly phased sinusoidal signal from the rotor motion into the excitation system Edris [11] proposed a method of counteracting SSR based on the decoupling of machine network interactions The decoupling is achieved by introducing series capacitor compensation scheme which behaves as a set of three phase asymmetrical capacitors at subsynchronous frequencies Iravani et al [12] proposed to modulate generator active power by injecting a quadrature phase voltage with thyristor controlled phase shifter Hammad et al [13] suggested thyristor phase controlled reactor utilizing its main regulator and an auxiliary speed signal to damp all torsional modes The modulation of real power and reactive power is one of the effective means of mitigating the subsynchronous resonance

Hingorani et al [14, 15] have proposed the NGH damping scheme to reduce transient machine oscillations during system disturbances The scheme involves a linear resistor in series with a pair of anti parallel thyristors connected across the capacitor When a zero voltage crossing point of the capacitor voltage is detected, the succeeding half cycle period is timed If and when the half cycle exceeds the set time, the corresponding thyristor is fired to discharge the capacitor through the resistor and bring about its current zero sooner than otherwise The thyristor stops conducting when the current through it reaches zero

The modulation of real power and reactive power is one of the e fective means of mitigating the subsynchronous resonance and this can be achieved by FACTS controllers

The real power modulation can be achieved by the modulation of TCSC reactance whereas the reactive power modulation can be obtained by STATCOM A review of various FACTS controllers is given below

## 1 2 Review of FACTS Controllers

The power flow in an AC line is dependent on three important parameters namely voltage magnitude impedance and phase angle FACTS devices control one or more of the parameters for improving the transmission capability Owing to the accuracy and fast response, FACTS devices are used to improve the dynamic performance, under steady state as well as transient state

### 1 2 1 Static Var Compensator (SVC)

SVC is the first generation FACTS device that is already in operation at various places around the world It uses a fixed capacitor (FC) or thyristor switched capacitor (TSC) in conjunction with a thyristor controlled reactor (TCR) SVC controls the magnitudes of the voltages at selected buses in the transmission network For example locating a SVC at the midpoint of a transmission line can increase power flow in the line The main feature of SVC is the voltage control by means of the reactive power compensation (obtained by varying the firing angle of the thyristors) In addition, SVC may improve transient stability by dynamically supporting the voltage at key points and steady state stability by helping to increase the swing mode damping SVC with proper control signals can be used to damp out electro mechanical oscillations Damping of power system oscillations play an important role not only in increasing the transmission capability of the line, but also for stabilization of system after critical faults in weakly coupled systems

### 1 2 2 Controlled Series Compensation (CSC)

CSC provides a way to increase the power flow on selected lines without causing the problems previously associated with series capacitors It is a second generation FACTS controller which controls the impedance between the two buses to which it is connected and hence the effective line reactance CSC consists of conventional series capacitors which are mechanically switched and a thyristor controlled series capacitor (TCSC) A single TCSC module consists of a series capacitor and a parallel path with a pair of anti parallel connected thyristor valves and a series inductor Also in parallel is a metal oxide varistor (MOV) for over voltage protection A complete compensation system may be made up of several of these modules in series

The TCSC module has three basic operating modes (i) Bypassed mode (ii) Inserted with thyristor valve blocked (iii) Inserted with vernier control In the bypassed mode thyristors are gated for full conduction ($180^0$) and the current flow in the reactor is continuous and sinusoidal The net reactance is slightly inductive because the susceptance of the reactor is larger than that of the capacitor This mode is used mainly for protecting the capacitor against the over voltages (during transient over currents in the line) This mode is also termed as thyristor reactor mode In the inserted mode no current flows through the valves with the blocking of gate pulses In this case TCSC reactance is same as that of the fixed capacitor and there is no difference in the performance of TCSC in this mode with that of a fixed capacitor This mode is also termed as waiting mode In the inserted mode with vernier control, the thyristor valves are gated such that they conduct for a part of a cycle ($\alpha_{min} < \alpha < 180^0$) The effective TCSC reactance (in the capacitive region) increases as $\alpha$ is reduced below $180^0$ and the TCSC reactance is maximum when $\alpha = \alpha_{min}$ which may be three times of fixed capacitive reactance This angle ($\alpha_{min}$) is above the value of $\alpha$ corresponding to the parallel resonance of thyristor controlled reactor and the fixed capacitor (at fundamental frequency)

### Control of TCSC

The TCSC control system arrangement is shown in Fig 1 2 [16] It can be observed from this figure that the TCSC control functions are partitioned into two levels i e, common level and module level The control commands flow from common level to module level while the status information is sent back from each module level The module controller executes the ordered change in reactance level The common control level receives signals of line current and TCSC voltage to generate feedback signals for closed loop control functions It also receives commands from energy management center for setting power order The major control functions are usually power scheduling control power swing damping control and transient stability control

## 1 2 3 Static Compensator (STATCOM)

A STATCOM is a second generation FACTS controller used for reactive power control and incorporates Voltage Source Converters (VSC) A six pulse VSC consists of six Gate Turn-Off (GTO) thyristors with inverse connected diodes connected as a Graetz bridge with a capacitor connected on the DC side The STATCOM is connected to high voltage AC bus through a coupling transformer Essentially a STATCOM produces a set of three phase output voltages each of which is in phase with and coupled to the respective AC system bus voltage through a small reactance that is generally provided by the leakage reactance of the coupling transformer Ideally as the STATCOM output voltage is in phase with the AC system voltage, the reactive power exchange between the AC system and the STATCOM can be regulated by controlling the magnitude of the STATCOM output voltage That is, if the amplitude of the output voltage is increased above that of the AC system voltage, then the current flows through the reactance to the AC system which is tantamount to the STATCOM supplying reactive (capacitive) power to the AC system On the other hand, if the magnitude of the output voltage of the STATCOM is reduced below that of

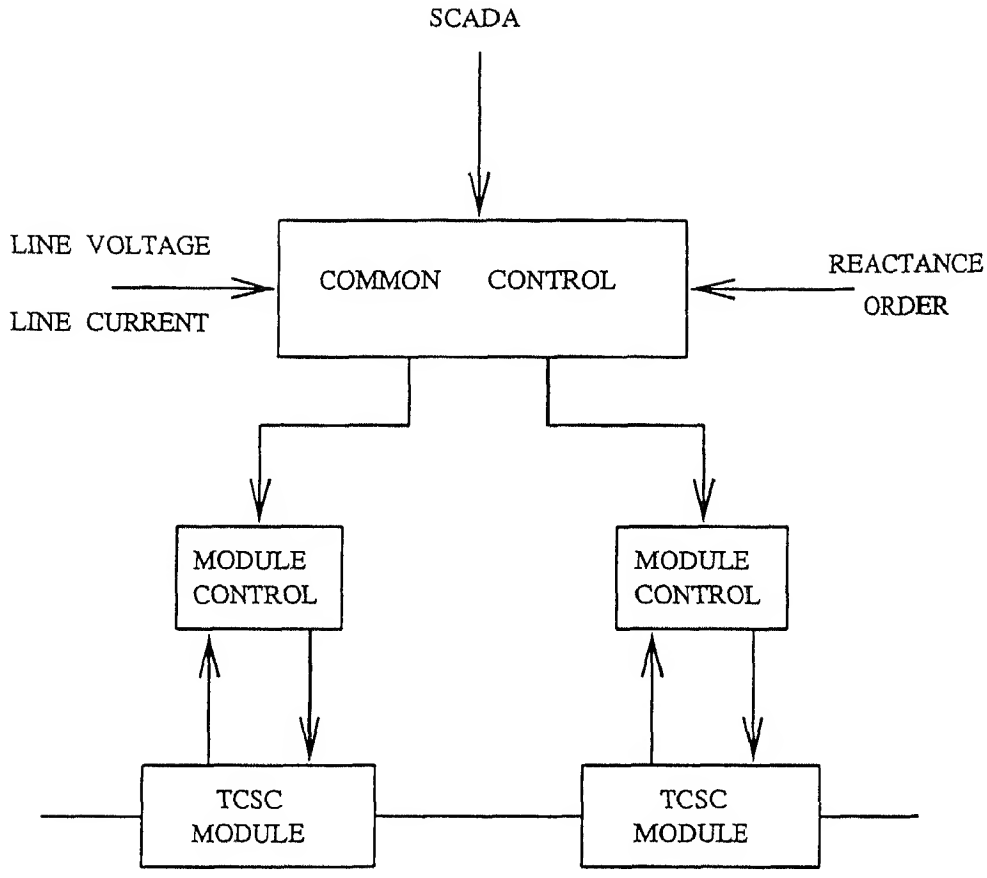


**Figure 1 2** TCSC Control System

the AC system voltage then the current flows from the AC system to the STATCOM and as a result the STATCOM absorbs reactive (inductive) power from the AC bus If the magnitude of the output voltage is equal to the AC system voltage magnitude, the reactive power exchange is zero The converter terminal voltage can be made to lead or lag the AC system voltage by controlling the firing angle [17] Multi pulse converters are usually used to reduce harmonics

### 1 2 4 Static Synchronous Series Compensator (SSSC)

A SSSC is a solid state voltage source inverter, which injects an almost sinusoidal voltage of variable magnitude in series with a transmission line This has the same structure as that of a STATCOM except that the coupling transformer is connected in series with the transmission line The injected voltage is almost in quadrature with the line current A small part of the injected voltage, which is in phase with the line current, provides the losses in the inverter Most of the injected voltage which is in quadrature with the line current emulates inductive or a capacitive reactance in series with the transmission line This emulated variable reactance, inserted by the injected voltage source influences the electric power flow in the transmission line [18]

Although subsynchronous resonance phenomena in series compensated system has been analyzed in detail and countermeasures suggested for overcoming the phenomenon it is necessary to analyze the phenomenon in the presence of FACTS devices and their controls, as the developments of FACTS devices are quite recent

## 1 3 Review of Literature

### 1 3 1 TCSC Modeling

Most of the TCSC models were developed utilizing sampled data approach Ghosh et al [19] proposed a discrete time domain TCSC model based on the linearized behavior of

the state transition equations that can predict the shift in zero-crossings of the line current (or capacitor voltage ) very accurately This model captures the system transient behavior accurately Rajaraman et al [20] presented a method for computing the eigenvalues of the system in discrete time domain The model development in [20] does not present a stand alone TCSC model The total system equations were developed with and without conducting of thyristors through Poincare map which is obtained by integrating the total system equations and taking into account the changes in equations when the switching occurs This approach requires sampling of full state at every sampling instant which is impractical for large power systems

Othman et al described the TCSC dynamics alone at the switching instants and then converted them into a continuous time model This model assumes that line current is forcing function to the TCSC equations and therefore is an independent quantity This is the major drawback of the model as change in TCSC firing angle will cause change in line current Verghese et al [21] presented a quasi steady state TCSC model based on phasor dynamics approach This model assumes line current is sinusoidal This model will be discussed in Chapter 4 Christ et al [22] presented an approach to calculate the fundamental frequency impedance of a TCSC This approach will be utilized later in the thesis

### 1 3 2 SSR mitigation with TCSC

A method for computing the eigenvalues and damping of SSR modes based on discrete time domain model for the IEEE first benchmark model is presented in [20] The dampings associated with subsynchronous modes of oscillation of a TCSC compensated network are computed by linearizing the Poincare map associated with the steady state operation The TCSC is operated with constant firing angle The analysis is confined to torsional modes and impact of TCSC dynamics on network modes is not mentioned Sampled data

model [23] of TCSC along with the higher level controllers utilized to stabilize the unstable torsional modes of IEEE first bench mark model

The design installation and basic control modes of the Slatt TCSC is described in [24] The Slatt TCSC is comprised of six identical TCSC modules that are connected in series A number of field tests were performed to demonstrate the effect of the TCSC in mitigating SSR [25] All tests were for radial case and focus on the particular torsional mode (mode 4) which may be destabilized The field test plots show that while conventional series capacitors can cause subsynchronous oscillations the response when inserting the same capacitor with thyristor switch performing vernier control shows no subsynchronous oscillations To evaluate the ability of TCSC in mitigating SSR caused by a conventional series capacitor a small TCSC operating in vernier control was added to a large series capacitor bank Without the TCSC, mode 4 was negatively damped However, the addition of TCSC resulted in significant improvement in damping of mode 4 The results of field tests were identical to the simulation results obtained using EMTP and TNA measurements

The analogue simulator based TCSC studies are presented in [16] The study examines numerous aspects of TCSC performance including response to faults, power swing damping and SSR The effectiveness of TCSC was evaluated by measuring the electrical damping torque as a function of frequency Comparison of damping torque plots of the system with no series capacitor to the system with TCSC operating in vernier mode showed that the plots are identical i e , the TCSC vernier control resulted in the electrical system look like an uncompensated system Comparison of damping torque plots with conventional series capacitors to that with TCSC operating in vernier mode showed that the TCSC significantly reduced the negative electrical damping in the rotor oscillation frequency range

An EMTP study of SSR mitigation of the Slatt TCSC is presented in [26] A dis turbance is applied by switching in the series compensation (either fixed compensation

or TCSC operating in vernier mode) and the speed deviations of the various masses are observed For the case with TCSC torsional modes (1,2 and 4) are significantly smaller compared to the case of fixed compensation Frequency domain analysis to compute the equivalent TCSC impedance is also presented The TCSC impedance study showed that the vernier operation of the TCSC provides equivalent resistive damping

The Steady state and transient characteristics of the ASC circuit installed at the Kayenta substation are discussed by Krause et al [27] The ASC control mode provides controlled firing of the thyristors to maintain either a fixed capacitive ASC impedance (constant reactance control) or to regulate the transmission line current The controller utilizes a TCSC fundamental frequency impedance verses firing angle look up table for converting controller output to thyristor firing angle For reactance control the ASC con troller determines the proper firing angle to provide the desired reactance In the current control mode, a control system is used to determine the impedance required to maintain the desired line current The electrical damping torque plots (obtained by using a simu lator) for cases of a conventional capacitor and an equivalent ASC with reactance control showed that while the damping is negative with conventional capacitors the ASC provides positive damping at SSR frequencies

Bowler et al [28] have described the constant reactance control of TCSC as well as modulated reactance control In modulated reactance control, the reactance order is mod ulated using an input signal that is synthesized from the voltage and current measurements of the capacitor The effectiveness of TCSC in damping power swings and providing higher power transfer by permitting higher levels of compensation by mitigating SSR effects is pre-sented Damping torque analysis of the system showed that for an unstable SSR condition, by adding a small TCSC with constant reactance control reduces the negative damping at torsional mode frequencies Modulated reactance control of TCSC resulted in positive damping torque throughout the range of torsional mode frequencies thereby eliminating

the destabilizing influence of SSR A root locus plot of the torsional modes as a function of controller gain illustrated that the damping of torsional modes is increased with increase in controller gain In this study the TCSC has been represented by linear transfer functions obtained from the time domain simulations

Heiden et al [29] presented SSR characteristics of different types of series compensation schemes The performance of NGH scheme and advanced series compensation scheme (ASC) is analyzed from transient torque and torsional interaction view point It is shown that ASC scheme provides better performance during major disturbances The conclusions are drawn based on time domain simulations In the torsional interaction studies it is shown that the behavior of ASC is inductive in the subsynchronous frequency range

### 1 3 3 STATCOM and its Characteristics

The majority of the STATCOM papers published are related to voltage control and power flow control Edwards et al [30] describe a ±1 MVAR prototype Advanced Static VAR Generator (ASVG) The purpose of the prototype development was to verify performance under practical operating conditions This ASVG is based on a 12 pulse voltage source inverter The prototype could regulate the line voltage and the reactive power in both the leading and lagging directions The mathematical model for the Advanced Static VAR Compensator or STATCOM is derived in [31] and frequency domain analysis is used to obtain the relevant transfer functions for control system synthesis The results are illustrated with measured waveforms obtained from a scaled analogue model Schauder et al [32] presented the development and installation of a ±100 MVAR STATCOM at the Sullivan substation of the TVA power system The operation of the same STATCOM is presented in [17] The effectiveness of voltage control and reactive current control of STATCOM is demonstrated Two Advanced Sta ic Var Compensator (ASVC) configurations are presented in [33] for power transmissior applications The study concludes that

the best performance can be achieved by ASVC employing PWM switching techniques Low frequency oscillation damping with STATCOM is presented in [34] The STATCOM controller in this case is designed using state feedback approach Time simulations are car ried out with 12 pulse STATCOM to verify the interactions between the STATCOM and AC transmission system The application of STATCOM in damping torsional oscillations has not been reported in many papers In [35] an attempt has been made in which the the STATCOM is connected at the generator terminals It has been shown that in this configuration the STATCOM cannot stabilize the torsional modes when operated in the voltage control mode The unstable torsional modes are damped with generator speed as auxilary signal along with the voltage controller

## 1 4 Objectives and scope of the Thesis

It is mentioned previously that series compensated power system gives raise to subsyn chronous phenomenon Various methods of counteracting subsynchronous resonance phe nomenon have been considered that have great diversity in concept and methods Most of these concepts were tested with IEEE first bench mark model One of these methods is to modulate either real power or reactive power injected into the generator bus of the affected steam turbine The use of reactive power modulation is used in [13] to damp sub synchronous resonance oscillations The real power and reactive power modulation can be achieved with FACTS devices such as TCSC and STATCOM Excitation system and PSS also interact with the torsional modes Combined with control system theory, eigenvalue studies can be used to design controllers of SSR countermeasures Digital time domain simulation is most useful tool for the study of transient torque problem In view of the above, the objectives and scope of thesis are

1 To study the subsynchronous transient oscillation damping with the STATCOM

2 To propose a new digital control scheme for TCSC control to damp subsynchronous resonance oscillations

3 To study the control interactions between TCSC and power system stabilizer

## 1 5 Outline of the Thesis

In Chapter 2 the linearized model of generator system with detailed representation of stater rotor and mechanical system along with AC network is presented The study system is IEEE First bench mark (IEEE FBM) model Eigenvalue analysis is carried out with the linearized overall system model The results obtained through eigenvalue analysis is validated with time domain simulation and Fourier analysis The effectiveness of NGH damping scheme in mitigating the subsynchronous torque oscillations is studied through the detailed time domain simulation using PSCAD/EMTDC

In Chapter 3 the linearized model of a 12 pulse STATCOM along with voltage and reactive current controller is presented The control parameters are obtained through eigenvalue analysis of the linearized model The studies are carried out on IEEE FBM The results obtained through eigenvalue analysis are validated with time domain simulation for the study of transient torque oscillations Comparative study is carried out with NGH damping scheme in mitigating subsynchronous torque oscillations

SSR analysis with TCSC in continuous time linearized domain is presented in Chapter 4 Constant angle control of TCSC is investigated The constant angle control is based on the philosophy of maintaining the voltage drop across the compensated transmission line constant Eigenvalue analysis is carried out to predict the stability of the system and the results are validated with time domain simulation

In Chapter 5, a novel digital control scheme is proposed for TCSC control For this purpose a discrete time domain TCSC model is developed The controller is designed using

state feedback approach The discrete time model along with the controller is suitably interfaced with the generator system model to obtain a homogeneous state space equation The stability of the system is analyzed through eigenvalue analysis and the results are validated with time domain simulation

The effect of excitation system that includes power system stabilizer (PSS) on torsional modes, in the presence of TCSC controller is examined in Chapter 6 The control interaction study is carried out through eigenvalue analysis

Chapter 7 outlines the conclusions drawn from the thesis and suggests some future scope of work

# Chapter 2

# SSR ANALYSIS OF A SERIES COMPENSATED POWER SYSTEM

The study of subsynchronous resonance (SSR) phenomena requires detailed time domain simulation of the system considering all relevant nonlinearities However, the first step towards assessing the possibility of occurance of subsynchronous resonance phenomena is generally through the study of the system in a linearized domain The linearized domain analysis is supplemented by time domain analysis for detailed investigation This approach is also convenient while designing control for any controllable device in power system This however requires development of a system model in the linearized domain For this purpose the general practice is to adopt a modular approach in formulating the system model with each component being modeled separately to any desired degree of detail The various individual component models are then suitably interfaced to derive the complete system model The development of power system model, following the above mentioned approach is described in this chapter Study of subsynchronous resonance phenomena in IEEE first benchmark system is carried out using this linearized system model The results are validated with detailed t me domain simulation using EMTDC/PSCAD software Also, the efficacy of NGH damping scheme [14] in controlling SSR has been studied through

digital simulation

# 2 1 Power System Component Models

A single machine infinite bus (SMIB) power system includes generator system and a trans mission system The representation of generator system comprising the synchronous ma chine and the associated mechanical system is described here along with the transmission network These component models are developed in the linearized domain

## 2 1 1 Synchronous Machine Model

The synchronous machine has three armature windings ($a$ $b$ $c$) on the stator a field winding ($f$), a damper winding ($h$) along the direct axis and two damper windings ($g$ and $k$) along the quadrature axis Fig 2 1 shows the layout of the windings of the synchronous machine In the following analysis, saturation is neglected The model consists of equations for stator and rotor windings

Stator Equations

The stator is represented by the two axis equivalent of the three phase windings, a $d$-axis winding on the direct axis and a $q$ axis winding on the quadrature axis The flux linkages associated with the $d$ and $q$ axis windings are given by [4]

$$\begin{aligned} -\frac{1}{\omega_B}\Psi_d - (1+s_g)\,\Psi_q - R_a i_d &= v_{gd} \\ -\frac{1}{\omega_B}\Psi_q + (1+s_g)\,\Psi_d - R_a i_q &= v_{gq} \end{aligned} \tag{2 1}$$

where $\omega_B$ is the base rotor speed in rad/sec, $s_g$ is the slip, $R_a$ is the armature resistance, $i_d$ and $i_q$ are respectively the $d$ and $q$ axis components of machine current, and $v_{gd}$ and $v_{gq}$ represent the d and q axis components of the machine terminal voltages $\Psi$ denotes the rate of change of the flux linkage $\Psi$ In eq (2 1), all the quantities are expressed in per unit

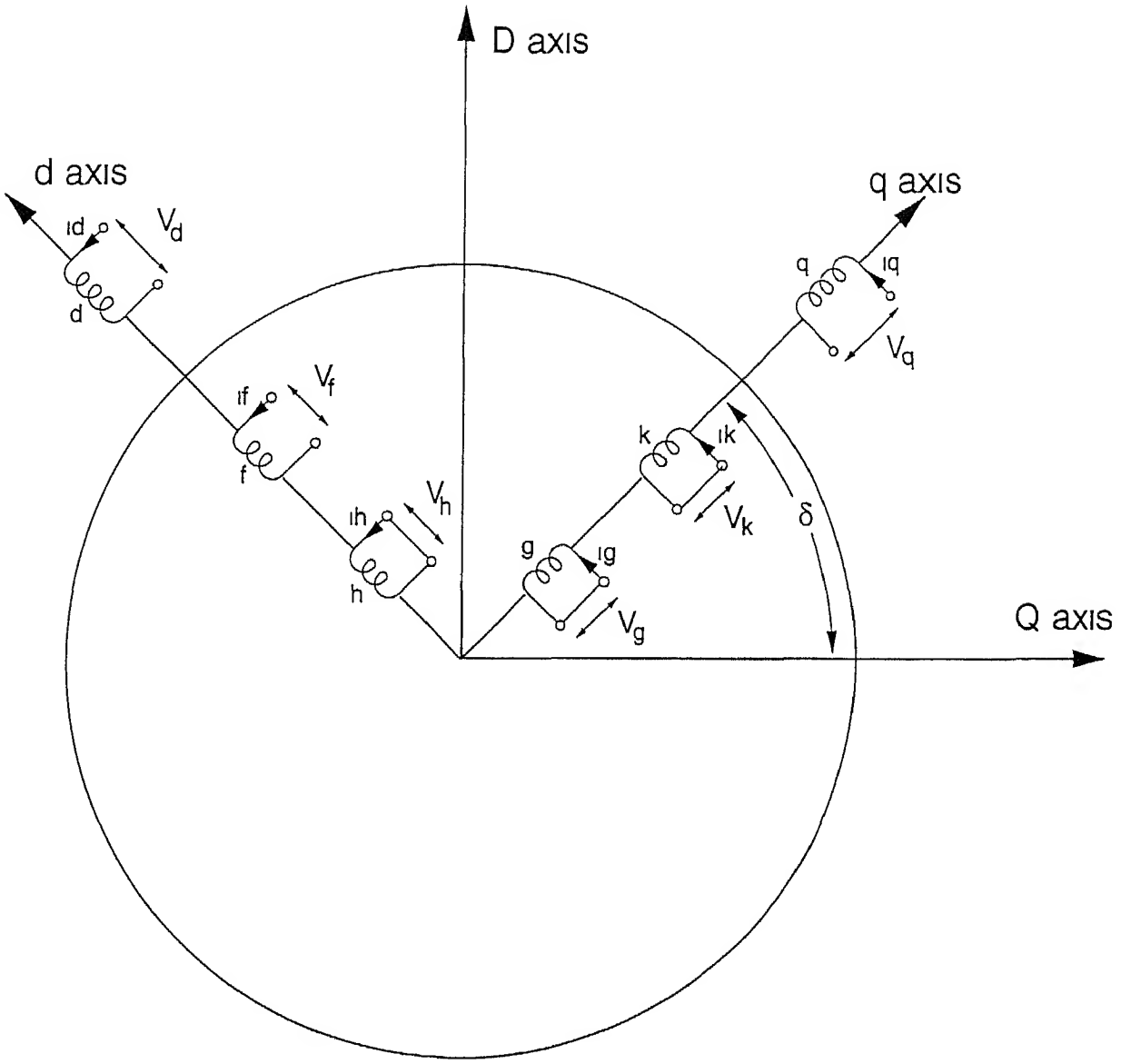


Figure 2 1 Layout of the windings of the sy ichronous machine

To have a common axis of reference with the transmission network, the voltages $v_{gd}$ and $v_{gq}$ are transformed to synchronously rotating reference frame (D Q reference frame) using the following transformation [4]

$$\begin{bmatrix} v_{gd} \\ v_{gq} \end{bmatrix} = \begin{bmatrix} cos\delta & -sin\delta \\ sin\delta & cos\delta \end{bmatrix} \begin{bmatrix} v_{gD} \\ v_{gQ} \end{bmatrix} \tag{2 2}$$

where $v_{gD}$ and $v_{gQ}$ are the components of voltage along D and Q axis $\delta$ is the angle by which $d$ axis leads $D$ axis

Rotor Equations

The rotor which has the field winding ($f$) and a damper winding ($g$) is represented as [4]

$$\begin{aligned} E'_d &= \frac{1}{T'_{qo}} \left[ -E'_d - \left( Y_q - X'_q \right) i_q \right] \\ E'_q &= \frac{1}{T'_{do}} \left[ -E'_q + \left( Y_d - X'_d \right) i_d + E_{FD} \right] \end{aligned} \tag{2 3}$$

where $E'_d$ and $E'_q$ are d and q axis rotor voltages, $T'_{do}$ and $T'_{qo}$ are the open circuit transient time constants $Y_d$ and $X_q$ are the synchronous reactances, $X'_d$ and $X'_q$ are the transient reactances and $E_{FD}$ is the field voltage referred to the stator side

The currents $i_d$ and $i_q$ are related to the flux linkages and voltage sources by

$$\begin{aligned} \Psi_d &= Y'_d i_d + E'_q \\ \Psi_q &= Y'_q i_q - E'_d \end{aligned} \tag{2 4}$$

Substituting $i_d$ and $i_q$ from eq (2 4) into eq (2 1) and eliminating $v_{gd}$ and $v_{gq}$ using eq (2 2), the following equations are obtained after linearizing the resulting equations

$$\begin{aligned} \triangle\Psi_d = &-\frac{R_a\omega_B}{Y_d}\triangle\Psi_d - \omega_B\triangle\Psi_q + \frac{R_a\omega_B}{Y_d}\triangle E'_q - \omega_B\Psi_q\triangle s_g \\ &+\omega_B v_{gq}\triangle\delta - \omega_B cos\delta_0\triangle v_{gD} + \omega_B sin\delta_0\triangle v_{gQ} \\ \triangle\Psi_q = &\ \omega_B\triangle\Psi_d - \frac{R_a\omega_B}{Y_q}\triangle\Psi_q - \frac{R_a\omega_B}{x_q}\triangle E'_d + \omega_B\Psi_d\triangle s_g \\ &-\omega_B v_{gd}\triangle\delta - \omega_B sin\delta_0\triangle v_{gD} - \omega_B cos\delta_0\triangle v_{gQ} \end{aligned} \tag{2 5}$$

whe e, the subscript 0' indicates nominal (operating point) values Similarly combining

eqs (2 3) and (2 4) and linearizing we get

$$\begin{aligned}\Delta E'_d &= \frac{1}{T'_{qo}}\left[-\frac{X_q}{X'_q}\Delta E'_d - \left(\frac{X_q}{X_q}-1\right)\Delta\Psi_q\right] \\ \Delta E'_q &= \frac{1}{T'_{do}}\left[\left(\frac{X_d}{X'_d}-1\right)\Delta\Psi_d - \frac{X_d}{X'_d}\Delta E_q + \Delta E_{FD}\right]\end{aligned} \tag{2 6}$$

Defining a state vector as $\Delta \mathbf{x}_{s1} = \left[\Delta\Psi_d \;\; \Delta\Psi_q \;\; \Delta E'_d \;\; \Delta E'_q\right]^T$ we can write eqs (2 5) and (2 6) in the following state space form

$$\Delta \mathbf{x}_{s1} = [\mathbf{A}_{s1}]\,\Delta \mathbf{x}_{s1} + [\mathbf{B}_{s11}]\,\Delta \mathbf{u}_{s11} + [\mathbf{B}_{s12}]\,\Delta \mathbf{u}_{s12} + [\mathbf{B}_{s13}]\,\Delta \mathbf{u}_G \tag{2 7}$$

where the input vectors are $\Delta \mathbf{u}_{s11} = [\Delta\delta \;\; \Delta s_g]^T \;\; \Delta \mathbf{u}_{s12} = \Delta E_{FD} \;\; \Delta \mathbf{u}_G = [\Delta v_{gD} \;\; \Delta v_{gQ}]^T$ The output equation for stator and rotor variables can be written as

$$\Delta \mathbf{y}_{s1} = [\mathbf{C}_{s1}]\,\Delta \mathbf{x}_{s1} \tag{2 8}$$

where $[\mathbf{C}_{s1}]$ is an identity matrix such that $\Delta \mathbf{y}_{s1} = \Delta \mathbf{x}_{s1}$ The matrices $[\mathbf{A}_{s1}]$, $[\mathbf{B}_{s11}]$ $[\mathbf{B}_{s12}]$ and $[\mathbf{B}_{s13}]$ are defined in Appendix A

## 2 1 2 Mechanical System Representation

The mechanical system comprises generator, shaft and turbines The shaft can be viewed as a mass spring damper system as shown in Fig 2 2 Each major rotating element of the mechanical system is modeled as a mass represented by its inertia The shaft by a spring with its stiffness represented by its spring constant The damping of each mass and shaft section is represented by dash pot damping The equation for $i^{th}$ mass connected by elastic shaft sections to mass $(i-1)$ and mass $(i+1)$ is given by [4]

$$\begin{aligned}&M_i\frac{d^2\delta_i}{dt^2} + D_i\frac{d\delta_i}{dt} + D_{i\,i-1}\left(\frac{d\delta_i}{dt} - \frac{d\delta_{i-1}}{dt}\right) + \\ &D_{i\,i+1}\left(\frac{d\delta}{dt} - \frac{d\delta_{i+1}}{dt}\right) + K_{i\,i-1}\left(\delta_i - \delta_{i-1}\right) + K_{i\,i+1}\left(\delta_i - \delta_{i+1}\right) = T_{mi} - T_e\end{aligned} \tag{2 9}$$

where

$M_i$ is the moment of inertia of $i^{th}$ mass

$\delta_i$ is the angle of rotation of $i^{th}$ mass with respect to synchronously rotating reference frame

$D_i$ is the self damping co efficient of $i^{th}$ mass

$D_{i\,i-1}$ is the mutual damping coefficient between $i^{th}$ and $i-1^{th}$ masses

$K_{i\,i-1}$ is the spring constant of the shaft connecting $i^{th}$ and $i-1^{th}$ masses

$T_{mi}$ is the mechanical torque applied on $i^{th}$ mass

$T_e$ is the electromagnetic torque on $i^{th}$ mass

The inertia $M_i$ is given by

$$M_i = \frac{2H_i}{\omega_B} \tag{2 10}$$

where $H_i$ is the inertia constant of $i^{th}$ mass Also,

$$\delta_i = \omega_B s_i \tag{2 11}$$

where $s_i$ is the slip of $i^{th}$ mass For a $N$ mass system, there are $N$ such second order

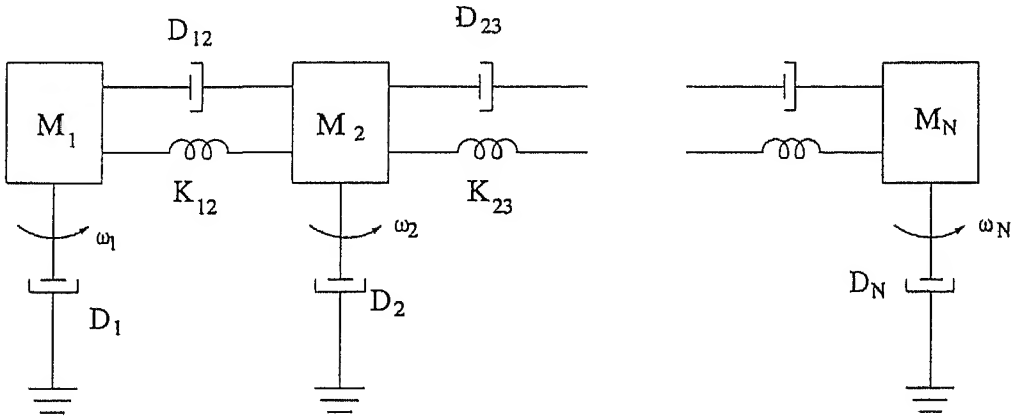


Figure 2 2 Spring mass model of a turbine generator shaft

differential equations of type of eq (2 9), which an be stacked in the form

$$[\mathrm{M}]\ \delta + [\mathrm{D}]\ \delta + [\mathrm{K}]\ \delta = [\mathrm{T_m}] - [\mathrm{T_e}] \tag{2 12}$$

where, [M] is the matrix of mass inertia, [D] is the matrix of damping coefficients and [K] is the spring constant matrix $\mathbf{T_m}$ and $\mathbf{T_e}$ are the vectors of mechanical and electromagnetic torques respectively and $\delta$ is vector of angles of rotation Note that $\mathbf{T}_e$ has only one non zero element corresponding to the generator rotor Combining eq (2 11) with eq (2 12) and then linearizing we get the following state space equation for the mechanical system associated with a synchronous machine

$$\Delta \mathbf{x}_m = [\mathbf{A}_m]\, \Delta \mathbf{x}_m + [\mathbf{B}_m]\, \Delta \mathbf{u}_m \tag{2 13}$$

$$\Delta \mathbf{y}_m = [\mathbf{C}_m]\, \Delta \mathbf{u}_m \tag{2 14}$$

where the state vector $\mathbf{x}_m$ represents the perturbed values of rotor slips (of different rotors), shaft torques and generator rotor angle The input vector $\mathbf{u}_m$ represents the perturbed value of generator electromagnetic torque applied at the generator rotor mass The output vector $\mathbf{y}_m$ consists of perturbed values of generator rotor angle and slip In deriving the above equations it is assumed that the mechanical torque input to the turbine is constant

To illustrate the illustration of derivation of mechanical system equations, let us consider the electrical equivalent circuit of a two mass mechanical system shown in Fig 2 3 Mass 1 is assumed to be a turbine and mass 2 to be a generator In this circuit mass is analogous to capacitance, torque is analogous to current and the spring constant is analogous to inverse of inductance Following the above procedure the linearized equations for the two mass system can be written as

$$\begin{aligned} 2H_1 \Delta s_1 &= \Delta T_1 - \Delta T_{12} - (D_1 + D_{12})\, \Delta s_1 + D_{12} \Delta s_2 \\ 2H_2 \Delta s_2 &= -\Delta T_2 + \Delta T_{12} - (D_2 + D_{12})\, \Delta s_2 + D_{12} \Delta s_1 \end{aligned} \tag{2 15}$$

Also, the shaft torque (i e current flowing through the inductance connected between node 1 and node 2) can be expressed as

$$\begin{aligned} \Delta T_{12} &= K_{12}\, (\Delta s_1 - \Delta s_2) \\ \Delta \delta &= \omega_B\, \Delta s_2 \end{aligned} \tag{2 16}$$

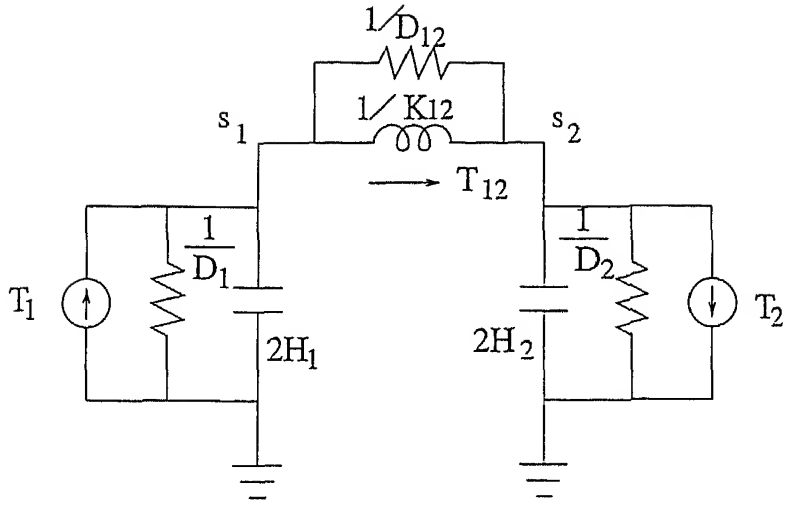


Figure 2 3 Electrical equivalent of two mass model

where $s_1$ is the slip of the mass 1 $s_2$ is the generator rotor slip $T_1$ is the mechanical torque input to the mass 1 and $T_2$ is the generator electrical torque For the two mass system shown in Fig 2 3 the state space model is given by

$$\begin{aligned} \Delta \mathbf{x}_m &= [\mathbf{A}_m]\,\Delta \mathbf{x}_m + [\mathbf{B}_m]\,\Delta \mathbf{u}_m \\ \Delta \mathbf{y}_m &= [\mathbf{C}_m]\,\Delta \mathbf{u}_m \end{aligned}$$

where, $\Delta \mathbf{x}_m = [\ \Delta s_1\ \Delta s_2\ \Delta T_{12}\ \Delta \delta]^T$, $\Delta \mathbf{y}_m = [\Delta \delta\ \Delta s_2]^T$ and $\Delta \mathbf{u}_m = \Delta T_2$

The turbine generator shaft of generating system can be represented as a six mass system [36] It is possible to adopt the above modeling approach to represent the six mass mechanical system which consists of a high pressure turbine(HP), an intermediate pressure turbine(IP), two low pressure turbines(LPA LPB), a generator(GEN) and an exciter(EXC)

For the six mass mechanical system the state vector can be written as $\Delta \mathbf{x}_m = [\Delta \mathbf{x}_{m1} \Delta \mathbf{x}_{m2}]^T$ where

$\Delta \mathbf{x}_{m1} = [\Delta s_e\ \Delta s_g\ \Delta s_{LPB}\ \Delta s_{LPA}\ \Delta s_{IP}\ \Delta s_{HP}]^T$ *and*

$\Delta x_{m2} = [\Delta T_{GEN-EXC}\ \Delta T_{LPB-GEN}\ \Delta T_{LPA-LPB}\ \Delta T_{IP-LPA}\ \Delta T_{HP-IP}\ \Delta\delta]^T$

The input vector $\Delta u_m = \Delta T_e$ and the output vector $\Delta y_m = [\Delta\delta\ \Delta s_g]^T$ The expression for electrical torque $\Delta T_e$ is given by

$$T_e = \Psi_d i_q - \Psi_q i_d \tag{2 17}$$

Substituting for $i_d$ $i_q$ from eq (2 4) and linearizing eq (2 17) we get the following expression

$$\Delta T_e = \left(\frac{v_q + E'_d}{x'_q} - \frac{\psi_q}{x'_d}\right)\Delta\Psi_d + \left(-\frac{\psi_d + E'_q}{x'_d} + \frac{v_d}{x'_q}\right)\Delta\Psi_q + \frac{\psi_d}{x'_q}\Delta E'_d + \frac{\psi_q}{x'_d}\Delta E'_q$$

This expression can be rewritten as

$$\Delta T_e = [C_{mel}]\,\Delta x_{sl} \tag{2 18}$$

where $[C_{mel}] = \left[\left(\frac{\psi_q + E_d}{x_q} - \frac{\psi_q}{x_d}\right)\ \left(-\frac{v_d + E_q}{x_d} + \frac{\psi_d}{x_q}\right)\ \frac{\psi_d}{x_q}\ \frac{v_q}{x'_d}\right]$ and as defined earlier $\Delta x_{sl} = [\Delta\Psi_d\ \Delta\Psi_q\ \Delta E'_d\ \Delta E'_q]^T$

### 2 1 3 Combined Synchronous Machine - Mechanical System Model

Defining state vector as $\Delta x_G^T = [\Delta x_{sl}^T\ \Delta x_m^T]$ eqs (2 7) and (2 13) can be combined as

$$\Delta x_G = \begin{bmatrix} A_{sl} & \\ & A_m \end{bmatrix}\Delta x_G + \begin{bmatrix} B_{sl1} \\ 0 \end{bmatrix}\Delta u_{sl1} + \begin{bmatrix} B_{sl3} \\ 0 \end{bmatrix}\Delta u_G + \begin{bmatrix} 0 \\ B_m \end{bmatrix}\Delta u_m \tag{2 19}$$

From eqs (2 18) and (2 14), the following is evident $\Delta u_m = \Delta T_e = C_{mel}\Delta x_{sl}$ $\Delta u_{sl1}$ $= \Delta y_m = C_m\Delta x_m$, Using the above expressions, eq 2 19 can be rewritten as

$$\Delta x_G = \begin{bmatrix} A_{sl} & B_{sl1}C_m \\ B_M C_{mel} & A_m \end{bmatrix}\Delta x_G + \begin{bmatrix} B_{sl3} \\ 0 \end{bmatrix}\Delta u_G$$

$$\Delta x_G = [\ A_G\ ]\,\Delta x_G + [\ B_G\ ]\,\Delta u_G \tag{2 20}$$

The output of the generating system model is the currents of the synchronous machine defined as $\Delta y_G = \left[\Delta i_D \; \Delta i_Q \;\; \Delta i_D \; \Delta i_Q\right]^T$ The currents $i_D$ and $i_Q$ are obtained from the relationship [4]

$$\begin{bmatrix} i_D \\ i_Q \end{bmatrix} = \begin{bmatrix} cos\delta & sin\delta \\ -sin\delta & cos\delta \end{bmatrix} \begin{bmatrix} i_d \\ i_q \end{bmatrix} \tag{2 21}$$

Substituting for $i_d$ and $i_q$ from eq (2 4) in eq (2 21) and linearizing we get

$$\begin{bmatrix} \Delta i_D \\ \Delta i_Q \end{bmatrix} = [C_{G1}]\, \Delta x_G \tag{2 22}$$

The matrix $[C_{G1}]$ is defined in Appendix A Combining eqs (2 20) and (2 22), we get the output equation for the generating system as

$$\Delta y_G = [C_G]\, \Delta x_G + [D_G]\, \Delta u_G \tag{2 23}$$

The matrices $[C_G]$ and $[D_G]$ are defined in Appendix A

### 2 1 4 Transmission Network

The transmission network comprises transmission lines, transformers and capacitors It is a general practice to neglect transmission line dynamics in low frequency ($0\ 1-2\ 0Hz$) electro mechanical oscillation studies In contrast the eigenvalue analysis in the subsynchronous frequency range ($10-40Hz$) requires dynamic representation of the transmission network based on linearized differential equations In developing the network model, it is assumed that the three phases are uncoupled This makes the voltage drops in each phase a function of only the current in that phase This assumption simplifies the transmission network equations in the a b c reference frame which are transformed to synchronously rotating reference frame ($D$ $Q$ reference frame) The relationship between $D-Q$ reference frame and $d-q$ reference frame is given in eq (2 2) A typical series compensated AC network is shown in Fig 2 4 This can be represented in $D-Q$ reference frame as

$$\Delta x_N = [A_N]\, \Delta x_N + [B_N]\, \Delta u_N \tag{2 24}$$

$$\Delta y_N = [C_N]\, \Delta x_N \tag{2 25}$$

where $\Delta x_N = [\Delta v_{CD}\ \Delta v_{CQ}]^T$ $\Delta u_N = [\Delta i_{GD}\ \Delta i_{GQ}]^T$ $\Delta y_N = [\Delta v_{CD}\ \Delta v_{CQ}]^T$

$$A_N = \begin{bmatrix} 0 & -\omega_B \\ \omega_B & 0 \end{bmatrix} \text{ and } B_N = \begin{bmatrix} \frac{1}{C} & 0 \\ 0 & \frac{1}{C} \end{bmatrix}$$

It can be noticed that the input to the transmission network model are the current injections obtained as the output of the generator system model Also, the output of the transmission network model are the voltages which are the input to the generator system model

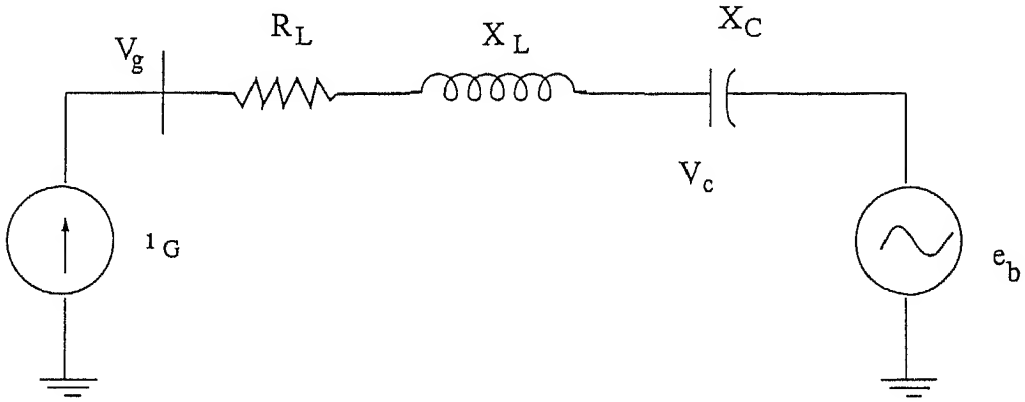


Figure 2 4 AC network model

## 2 2 Combined Generator-Network System Model

The state and output equations of the total system can be expressed in the following form

$$\Delta x = [A]\,\Delta x + [B]\,\Delta u \tag{2 26}$$

$$\Delta y = [C]\,\Delta x + [D]\,\Delta u \tag{2 27}$$

where $\Delta x^T = [\Delta x_G^T\ \Delta x_N^T]$ $\Delta u^T = [\Delta u_G^T\ \Delta u_N^T]$ and $\Delta y^T = [\Delta y_G^T\ \Delta y_N^T]$ As the input of one subsystem is related to the output of the other subsystem, the overall input vector

can be related to the overall system output vector as

$$\Delta \mathrm{u} = [\mathrm{F}]\, \Delta \mathrm{y} \tag{2 28}$$

The elements of the [F] matrix can be derived from the knowledge of the interconnection amongst the various subsystems Now utilizing eq (2 28), eqs (2 26) and (2 27) can be combined as

$$\Delta \mathrm{x} = \left[\mathrm{A} + \mathrm{BF}(I - \mathrm{DF})^{-1}\mathrm{C}\right] \Delta \mathrm{x} = [\mathrm{A}_T]\, \Delta \mathrm{x} \tag{2 29}$$

where

$$[\ \mathrm{A}\ ] = \begin{bmatrix} \mathrm{A}_G & \\ & \mathrm{A}_N \end{bmatrix} \quad [\ \mathrm{B}\ ] = \begin{bmatrix} \mathrm{B}_G & \\ & \mathrm{B}_N \end{bmatrix}$$

$$[\ \mathrm{C}\ ] = \begin{bmatrix} \mathrm{C}_G & \\ & \mathrm{C}_N \end{bmatrix} \textit{and} \ [\ \mathrm{D}\ ] = \begin{bmatrix} \mathrm{D}_G & \\ & 0 \end{bmatrix}$$

## 2 3 Eigenvalue Analysis of IEEE - FBM

The system modeling approach described in the previous sections is utilized to study the SSR behavior of the IEEE First Benchmark Model [IEEE-FBM] based on eigenvalue analysis The system details of the IEEE FBM [36] is given in Appendix B The initial conditions calculation is given in Appendix C It is assumed that the series capacitor compensates 70% of the transmission line reactance, i e, $X_C = 0\ 7X_L$ Mechanical damping is neglected in this study The generator delivers 0 9 per unit power at a power factor of 0 9 lag Table 2 1 gives the eigenvalues of the study system From this it can be observed that supersynchronous and subsynchronous network mode eigenvalues are stable There are four unstable torsional modes The low frequency mode or mode 0 is damped The resonant frequency of

Table 2 1 System Eigenvalues

| Series Capacitance = 0 35 per unit, $X_C = 0\ 7\ X_L$ | comments |
|---|---|
| 4 419 ± j612 43 | Supersyn Net Mode |
| 3 434 ± j141 175 | Subsyn Net Mode |
| 0 0000003 ± j298 176 | Mode 5 |
| 0 0019 ± j202 81 | Mode 4 |
| 0 0461 ± j160 27 | Mode 3 |
| 0 0373 ± j127 164 | Mode 2 |
| 0 055 ± j99 704 | Mode 1 |
| 0 49 ± j10 56 | Mode 0 |
| 3 922 | |
| 0 19 | |

the series compensated transmission system is obtained from the relationship $f_{er} = \sqrt{\frac{1}{LC}}$ where $L$ and $C$ are transmission line inductance and capacitance respectively With 70% compensation the transmission line resonant frequency is 266 57 rad/s(42 42$Hz$) and the complimentary frequencies are 643 564 rad/s (102 42$Hz$) and 110 418 rad/s (17 58$Hz$) From the Table 2 1, it is evident that two of the unstable eigenvalues have frequency close to the resonant frequency of 110 418 rad/s (17 58$Hz$) one at 99 704 rad/s (15 868$Hz$) and another at 127 164 rad/s (20 238$Hz$) This situation may lead to resonance with turbine generator shaft To further validate this observation, obtained through eigenvalue analysis a detailed digital simulation of IEEE FBM is carried out

## 2 4 Simulation Studies

The time domain simulation of IEEE FBM is performed using PSCAD/EMTDC software package (version 3 0) to study the response of various shaft torques to a small disturbance All system nonlinearities are represented The field excitation is assumed to be constant The system operating condition is same as that taken for eigenvalue analysis A disturbance of 0 1 per unit torque is applied at the HP turbine input for a period of 0 1 sec The

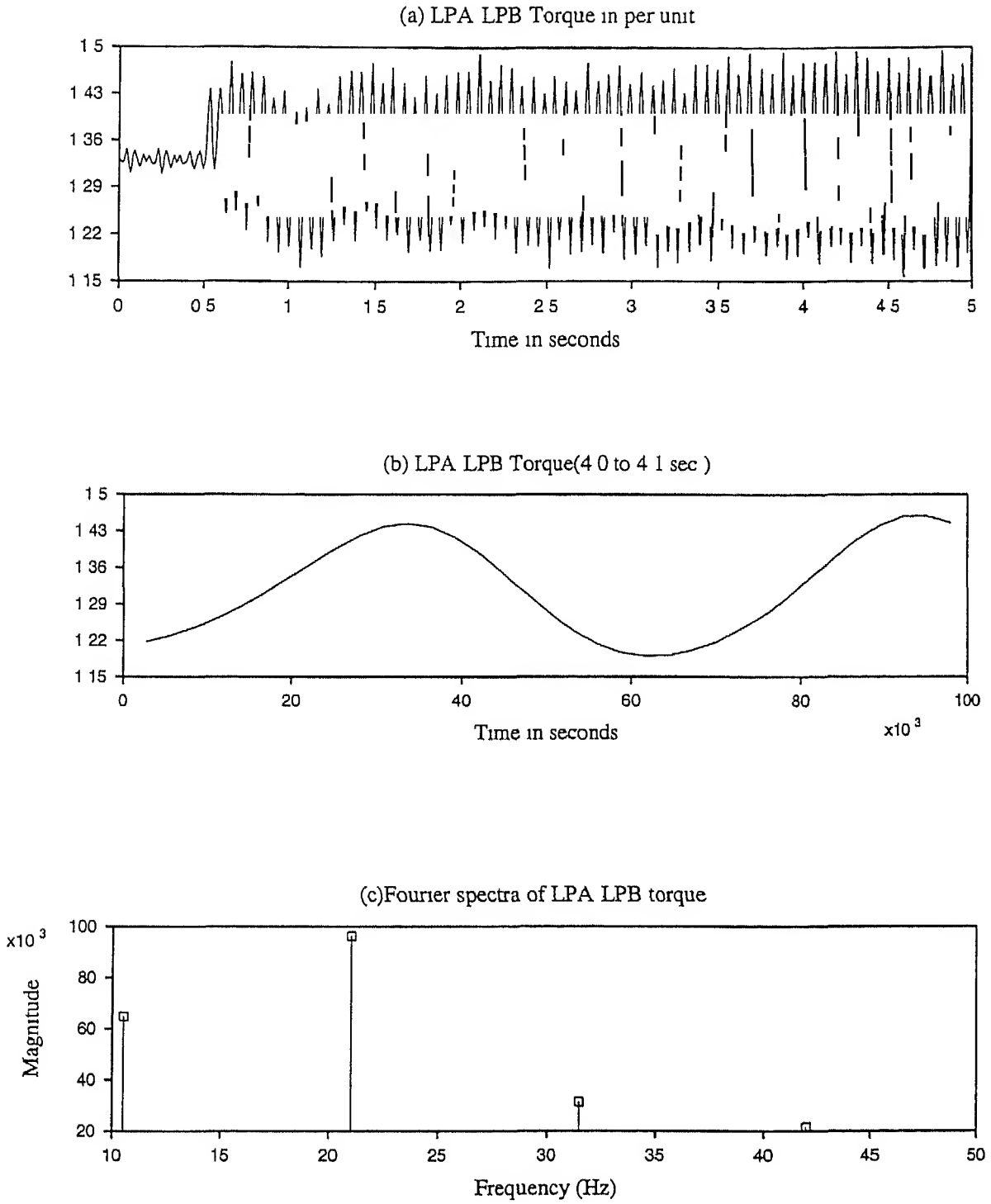


Figure 2 5 Fourier spectra of LPA LPB torque as a result of small disturbance

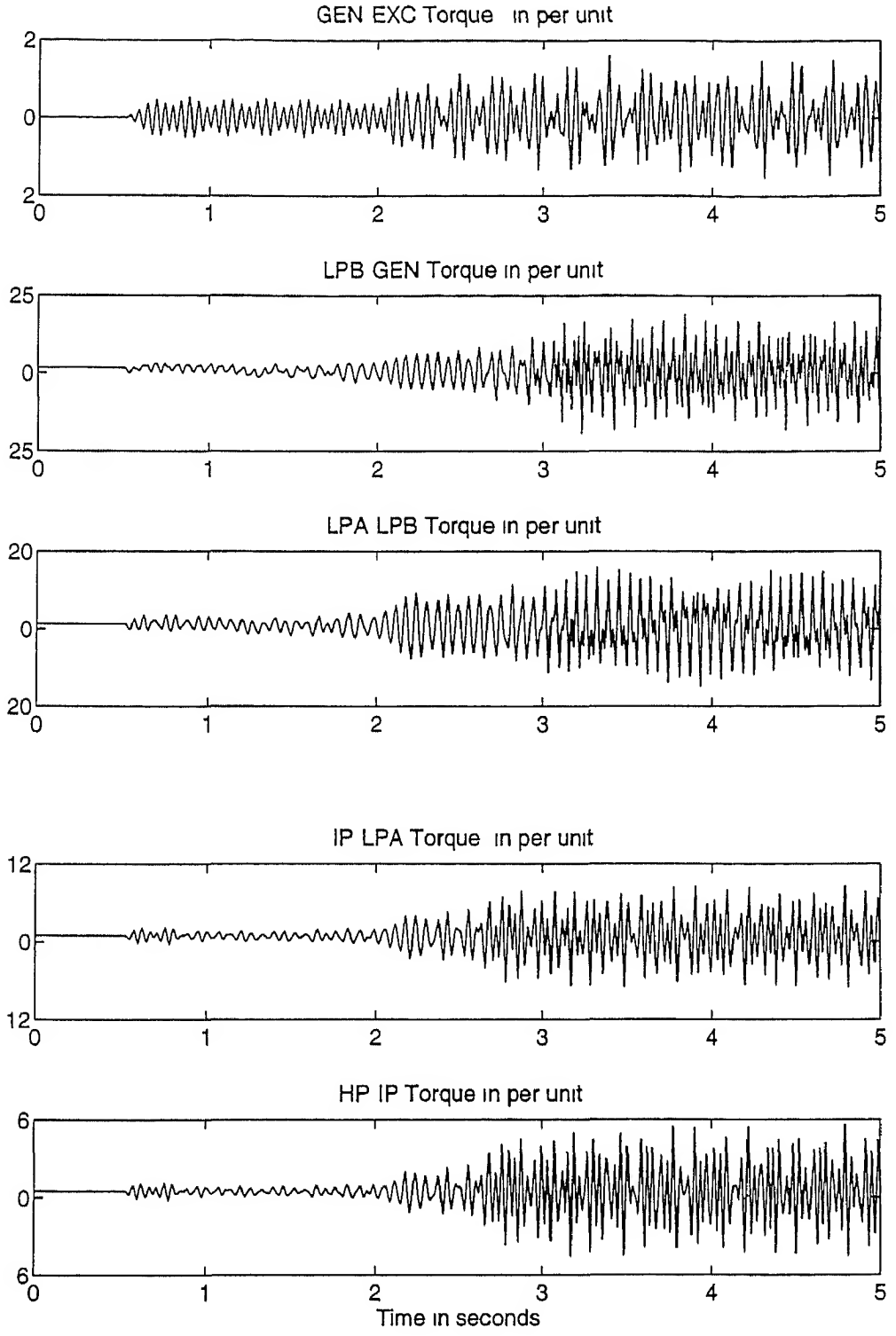


**Figure 2 6** Transient torque response for a 3 phase to ground fault with fault impedance

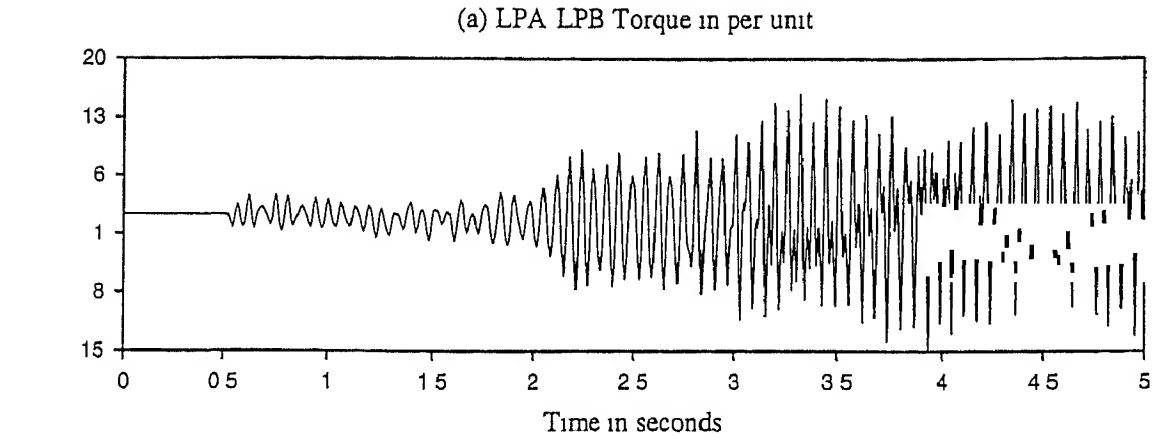


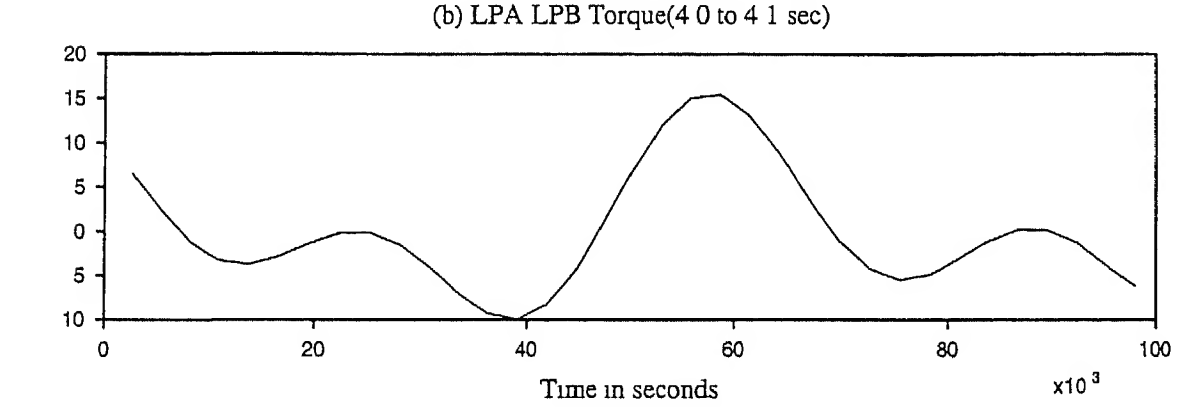


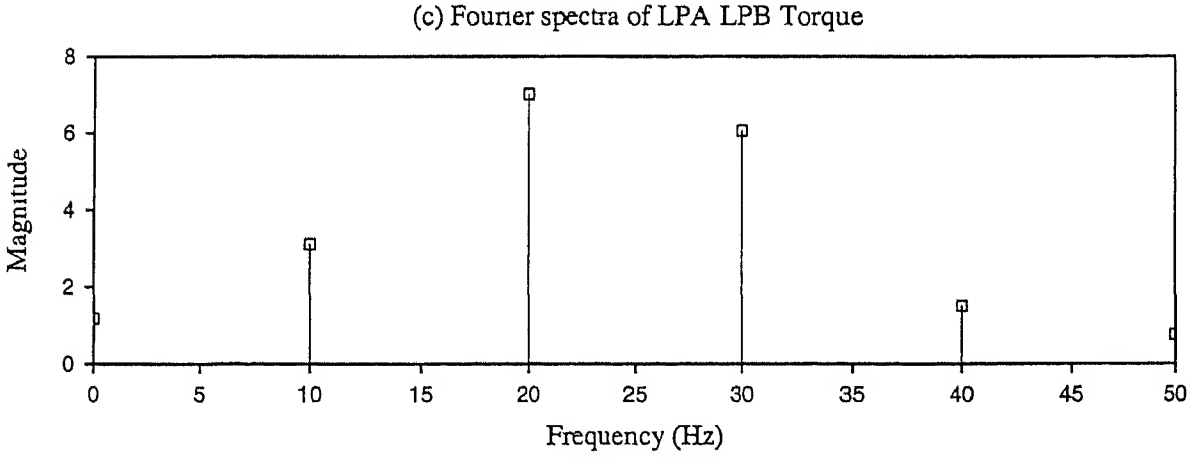


Figure 2 7 Fourier spectra of LPA LPB torque

disturbance is applied at a time t = 0 5 sec Fig 2 5(a) shows the LPA LPB torque as a result of this disturbance The LPA LPB torque in the interval 4 0 sec to 4 1 sec is shown in Fig 2 5 (b) The Fourier spectra of the LPA LPB shaft torque shown in Fig 2 5 (c) This indicates a predominant presence of 20 62$Hz$ component which is close to the mode 2 frequency obtained in eigenvalue analysis

To study the system behavior under large disturbance the study system is subjected to a three phase to ground fault through a fault impedance of 0 04 per unit at infinite bus end The fault is applied at 0 5 secs and is cleared after 4 5 cycles The shaft torques are shown Fig 2 6

From the plots given Fig 2 6 it can be observed that the shaft torques increase with time as a result of torque amplification This behavior is indicative of the unstable system operation due to the onset of SSR phenomenon A similar observation regarding unstable system behavior is evident from the eigenvalue results given in Table 2 1 The LPA-LPB torque of Fig 2 6 is reproduced in Fig 2 7(a) Its variation over the interval 4 0 sec to 4 1 sec is shown in Fig 2 7 (b) The Fourier spectra of LPA LPB torque is shown in Fig 2 7 (c) This plot also shows the presence of 20$Hz$ component, a frequency which is close to mode 2 frequency obtained in eigenvalue analysis

From the time domain simulation, it is evident that the amplitude of shaft torques increase which may result in the turbine generator shaft damage Many generator based counter measures are suggested in the literature to deal with transient torque problem [4, 11, 14, 37, 38] One of the capacitor based counter countermeasure to suppress transient oscillations due to subsynchronous resonance is NGH damping scheme [14, 15] In the following section the application of NGH damping scheme to IEEE first benchmark model is discussed

## 2 5 Study of IEEE-FBM with NGH Damping Scheme

The basic NGH scheme for one phase includes a linear resistor in series with anti parallel thyristors connected across the capacitor as shown in Fig 2 8 The anti parallel thyristor

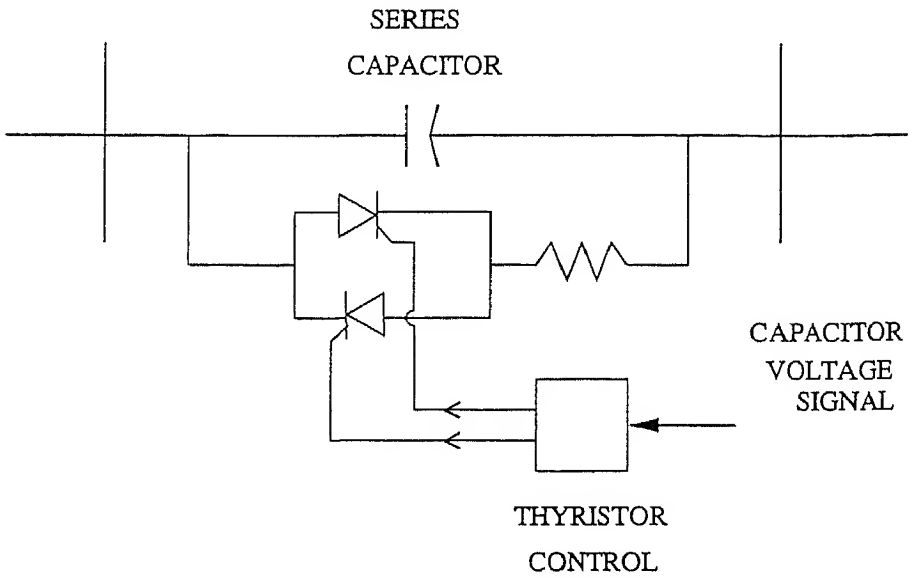


Figure 2 8 Basic NGH scheme

pair in the NGH damper functions as a bidirectional switch The gating of the pair is so controlled that the current can flow in either direction depending on the direction of the line current For normal operating condition, successive zero crossing points of the capacitor voltage are timed In the steady state this time will be equal to half cycle period of the system frequency ($\frac{T}{2}$, where T is the time period of the voltage) If and when half cycle period deviates from the set time of $\frac{T}{2}$, the thyristor switches are closed to discharge the capacitor energy through the linear resistor

The system under study is IEEE FBM with a series capacitor of (0 35 per unit) reac tance which compensates 70 % of the transmission line reactance The series capacito is assumed to be made up of two banks, one having 0 301 per unit capacitance and the other

0 049 per unit capacitance The NGH scheme is applied to 0 049 per unit capacitor bank In the study all nonlinearities are represented and the field voltage is assumed constant Self damping of 0 2 per unit and mutual damping of 0 3 per unit is added to the haft To study the effectiveness of NGH damping scheme in mitigating SSR, the following studies are carried out

(i) Capacitor insertion test

(ii) Three phase short circuit test

(iii) High speed reclosure test

(i)Capacitor insertion

During capacitor insertion operations, subsynchronous frequency oscillations are present due to the interaction between the line inductance and series capacitors and these oscillations mav excite the torsional modes A capacitor insertion study is carried out without NGH device In this study, the generator is delivering 0 9 per unit power Initially the capacitor segment of 0 301 per unit is in service and the other capacitor segment of 0 049 per unit is inserted at time $t = 0\ 5$ secs Fig 2 9 shows the transient torque response with the fixed capacitor insertion It can be seen that during the fixed capacitor insertion the GEN E\C torque is excited and the oscillations are growing as a result of subsynchronous resonance phenomenon The NGH device is expected to suppress these oscillations Consequentlv the capacitor segment of 0 049 per unit is inserted with NGH device at t = 0 5 sec, while the fixed capacitor segment of 0 301 per unit is considered to be in service The GEN E\C torque and LPA LPB torque responses are shown in Fig 2 10 From the Fig 2 10 it is evident that the NGH device is effective in stabilizing the shaft torques during capacitor insertion by damping the subsynchronous oscillations

(ii) Three-Phase short circuit fault

In this study the generator is delivering 0 9 per unit power Three phase to ground faults,

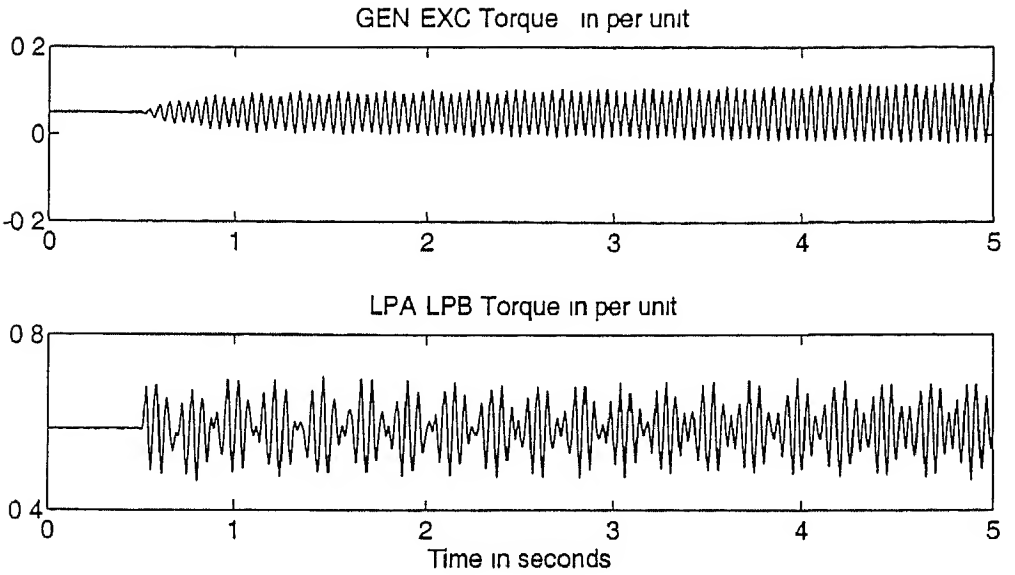


**Figure 2 9** Transient torque response with fixed capacitor insertion

with duration of one cycle (0 01666 sec) and 4 5 cycles (0 075 sec) are applied at the infinite bus end through a fault impedance of 0 04 per unit The fault is applied at time t = 0 5 sec The shaft torques response is shown in Fig 2 11 and Fig 2 12 From the responses shown in Figs 2 6, 2 11 and 2 12, it can be observed that with the NGH damper the transient oscillations do not grow and on the contrary have gradually decreasing amplitude This is indicative of stable system operation The Gen Exc torque oscillations are reduced faster compared to the other shaft torques The peak values of the different shaft torques for the two different fault durations are given in Table 2 2

**Table 2 2** Peak shaft torques for different fault clearing times

| Fault clearing time in seconds | peak value of torques in per unit | | | | |
|---|---|---|---|---|---|
| | Gen Exc torque | LPB Gen torque | LPA-LPB torque | IP-LPA torque | HP IP torque |
| 0 016 | 0 456 | 2 751 | 2 846 | 1 838 | 1 054 |
| 0 075 | 0 4248 | 2 465 | 2 50 | 1 52 | 0 819 |

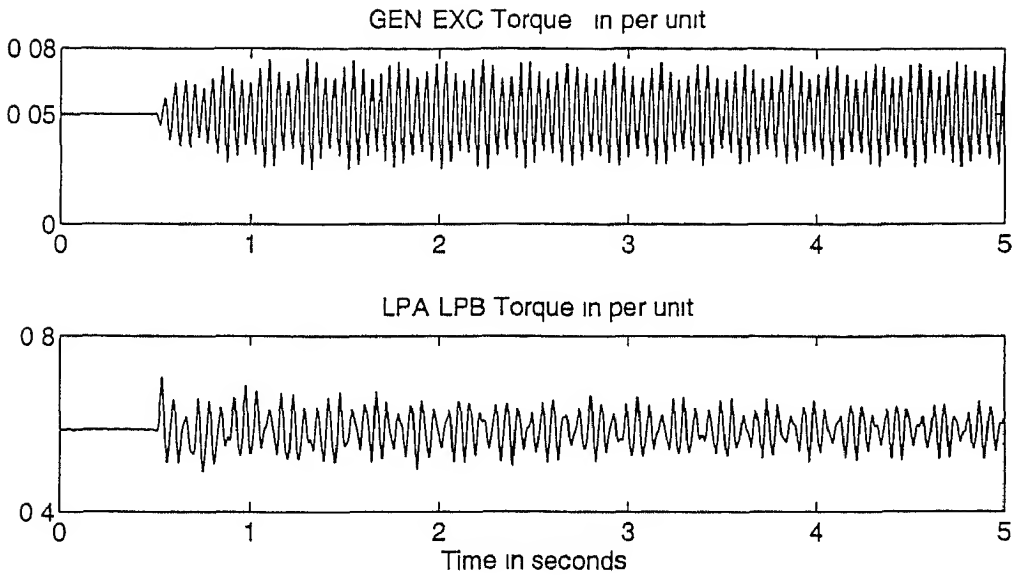


**Figure 2 10** Transient torque response with insertion of capacitor having NGH damping scheme

(iii) High speed reclosure

When a generator is connected to multiple lines and a fault occurs close to the generator on one line, the system voltage drops and the generator is no longer able to deliver the prefault power to the network Consequently the rotor angle increases The restoration of the voltage at the instant of line tripping at increased load angle causes stress on the shaft segments The reclosure of the line has most significant effect on the shaft transient torques A successful reclosure results in high transient torques due to the sudden return of load An unsuccessful reclosure subjects the system to another fault In the case of a single tied generator, the load angle increases after fault occurance, during short circuit and the reclosing time intervals A successful reclosure with a high magnitude of phase difference between the generator and the system causes severe stress on shaft segments Thus the reclosing action for a single tied generator results in higher shaft torques in series compensated systems In the present study, the generator is delivering 0 5 per unit power to the infinite bus A three phase to ground fault is applied at t = 0 5 sec The fault is

cleared after 3 cycles by the breakers at both ends of the line The breakers are closed successfully in 15 cycles after fault clearance Fig 2 13 shows the dynamic response of shaft torques to a 3 15 cycle successful reclosure test and it can be observed that, even at a reduced power level high speed reclosure test is producing peak torques greater than those encountered during the three phase fault case shown in Fig 2 11 The NGH scheme is able to render the damping effect on shaft torque oscillations

## 2 6 Conclusions

In this chapter the torsional mode stability information obtained through eigenvalue analysis using linearized system model is verified with detailed time domain simulation The control of transient torques with NGH damping scheme is illustrated with time domain simulation The simulation results pertaining to capacitor insertion case reveal that the NGH damping scheme is able to stabilize the transient torque oscillations, but the damping effect is inadequate For the case of three phase fault disturbance the damping effect is found to be more pronounced on Gen Exc torque compared to the other shaft torques The rate of damping of oscillations of LPA LPB and LPB Gen torques is moderate This may be due to the chosen value of capacitance Though NGH damping scheme arrests the growth of transient oscillations but its effect on peak torque reduction is not significant The NGH device do not have the capability of increasing the power transfer and its function is limited to damping the transient torques

Modulation of real power and reactive power are the effective means of damping the power system oscillations and this modulation can be obtained by incorporating FACTS devices such as TCSC and STATCOM In the next chapter, the control of subsynchronous resonance phenomena with the STATCOM is discussed

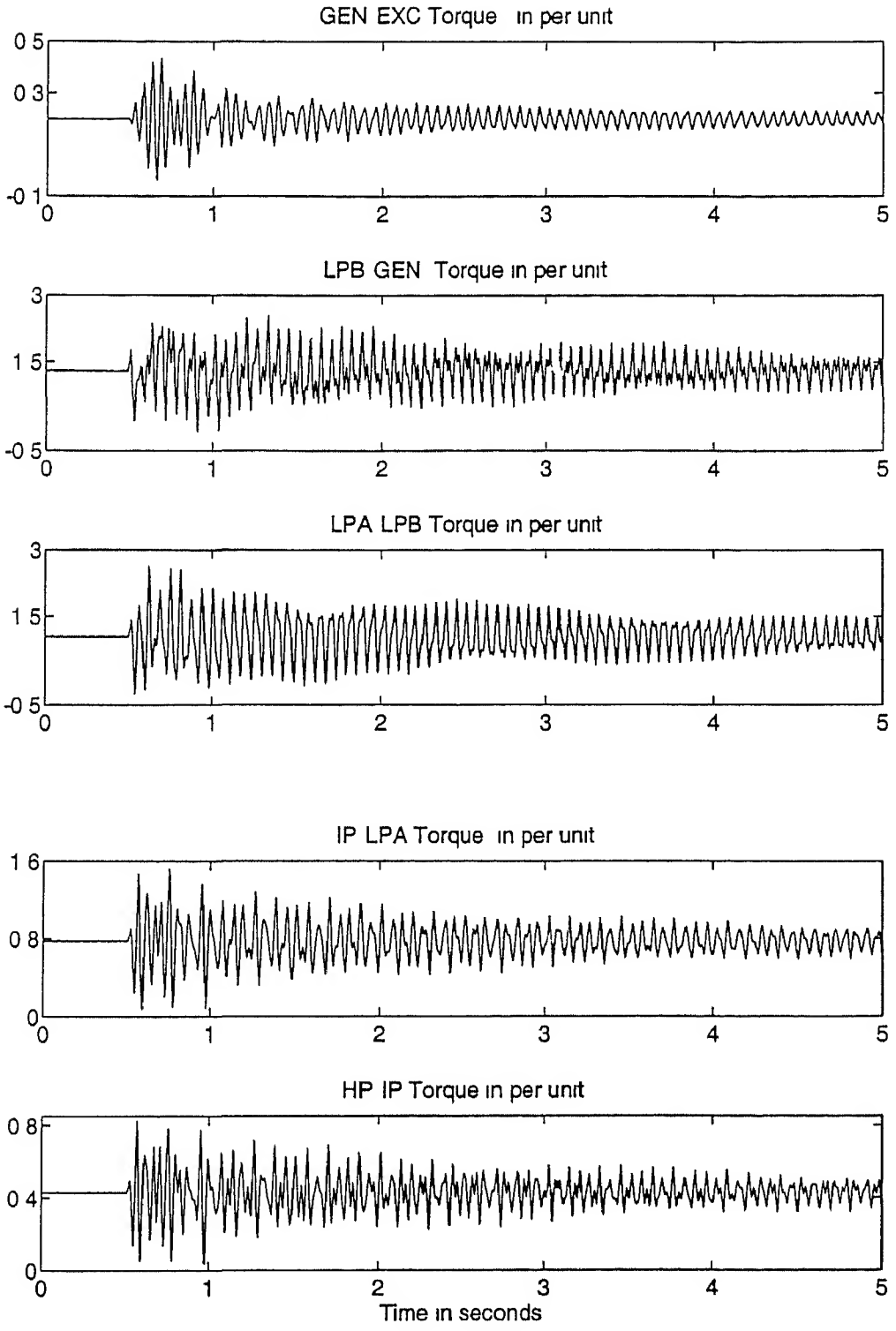


Figure 2 11 Transient torque response for a 3 phase fault (4 5 cycles) with NGH scheme

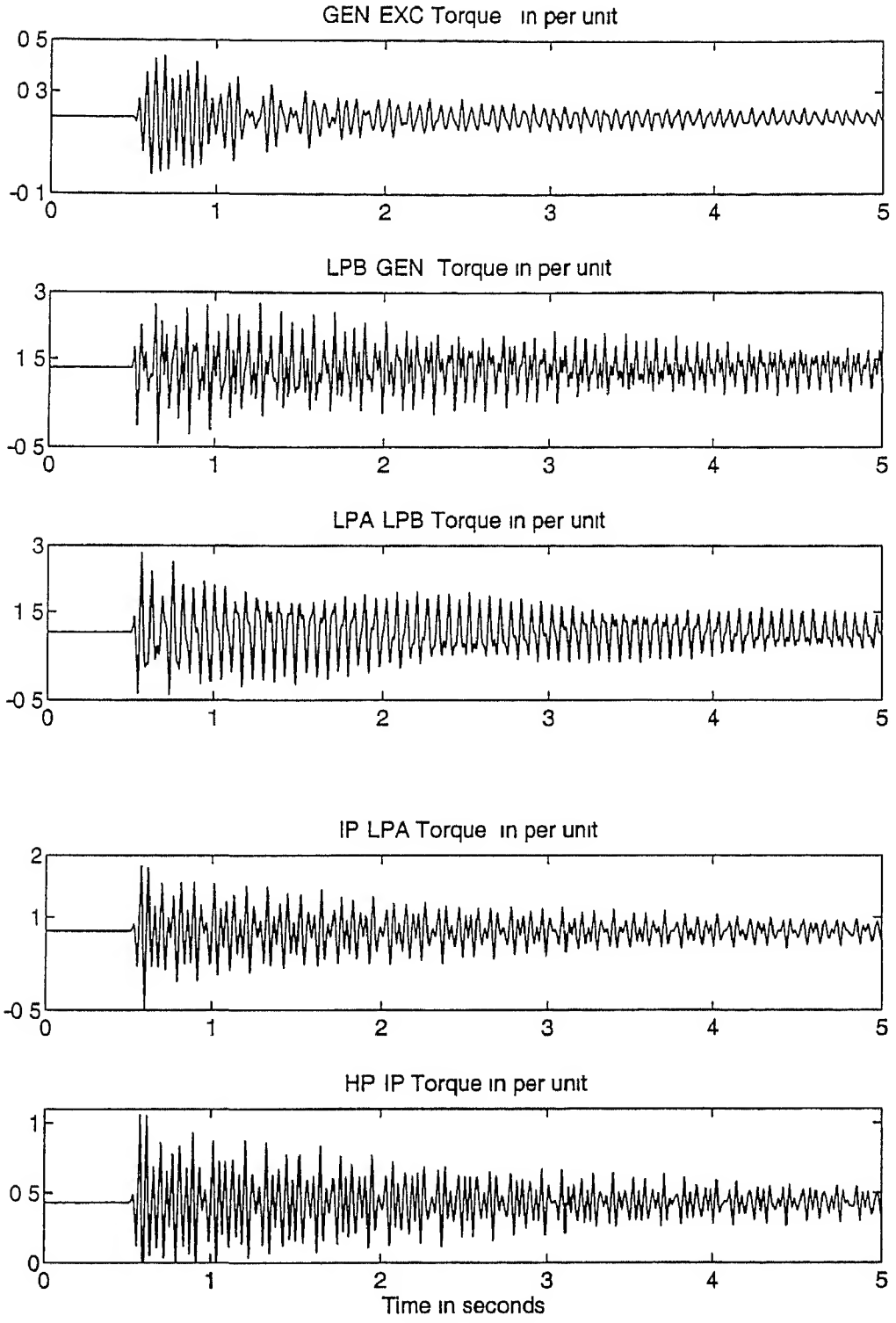


Figure 2 12 Transient torque response for a 3 phase fault (1 cycle) with NGH scheme

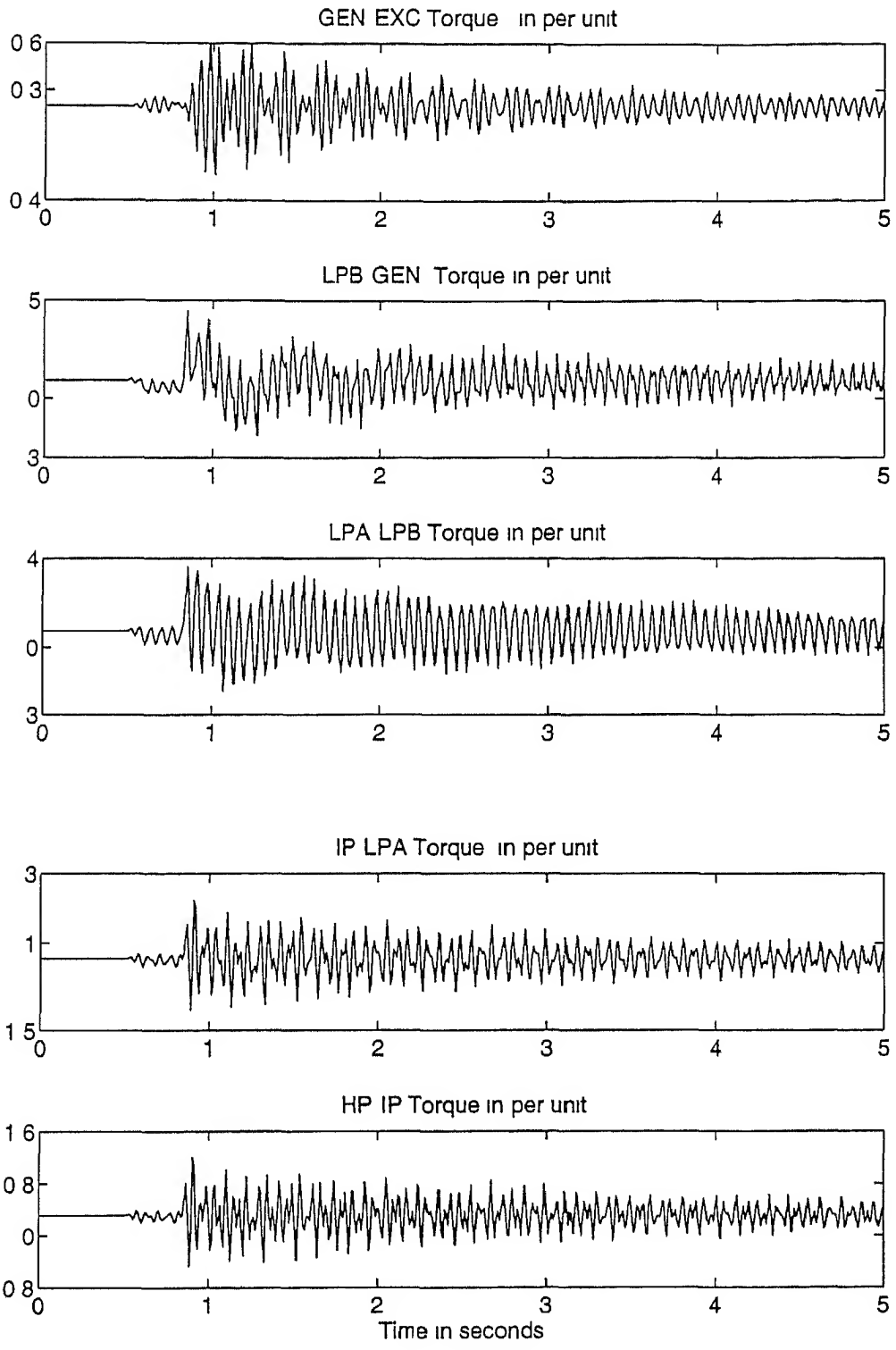


Figure 2 13 Transient torque response with High speed reclosure

# Chapter 3

# SSR ANALYSIS WITH STATCOM

The Flexible AC Transmission System devices will need to be used along with the conventional series capacitors to achieve the objective of improvements in the loadability of the system and extended performance The availability of high power gate turnoff thyristors (GTO) have recently led to the development of a new equipment called Static Compensator (STATCOM), which is a second generation FACTS device based on voltage source inverters STATCOM uses self commutating devices like GTOs and is an advanced form of SVC The operating and functional characteristics of STATCOM are, however different from those of SVC The STATCOM does not use capacitor or reactor banks to produce reactive power It operates as a controllable electronic synchronous voltage source connected to the line through the leakage inductance of a coupling transformer and draws reactive current from the line in essentially the same way as a rotating Synchronous Condenser (without the mechanical inertia and long excitation time constant) The controlled synchronous voltage is maintained in phase with the line voltage It can, thus, draw either inductive or capacitive current by varying the magnitude of this voltage Furthermore, the DC capacitor bank, to which the voltage source inverter is connected, does not play an active role in the VAR generation

The subsynchronous resonance oscillations can be damped by modulating the real and reactive power The reactive power modulation based countermeasure is considered in this

chapter, where we consider the STATCOM as a reactive power source The STATCOM is connected at the generator terminal and operated in voltage control mode

## 3 1 System Modeling

The system under study is the IEEE-FBM with fixed series compensation The configuration of the study system which is shown in Fig 3 1 consists of a generator feeding power to an infinite bus through a series compensated transmission line The STATCOM is connected at the generator terminals The system can be divided into the following subsystems

(i) Generator System

(ii) AC Network

(iii) STATCOM

The generator system model and the network model are the same as given in Chapter 2 For the sake of completeness the models are reproduced below

Generator System

The state space model of the generator system is given by

$$\Delta \mathbf{x_G} = [\mathbf{A}_G]\,\Delta \mathbf{x}_G + [\mathbf{B}_G]\,\Delta \mathbf{u}_G \tag{3 1}$$

where $\Delta \mathbf{x}_G^T = \left[\Delta \mathbf{x}_{s1}^T \; \Delta \mathbf{x}_m^T\right]$, $\Delta \mathbf{x}_{s1}$ and $\Delta \mathbf{x}_m$ are the state vectors of stator and mechanical system, $\Delta \mathbf{u}_G = [\Delta v_{gD} \; \Delta v_{gQ}]^T$ The output equation is given by

$$\Delta \mathbf{y}_G = [\mathbf{C}_G]\,\Delta \mathbf{x}_G + [\mathbf{D}_G]\,\Delta \mathbf{u}_G \tag{3 2}$$

where $\Delta \mathbf{y}_G = \left[\Delta i_D \; \Delta i_Q \; \Delta i_D \; \Delta \; i_Q\right]^T$ The matrices $[\mathbf{A}_G]$, $[\mathbf{B}_G]$, $[\mathbf{C}_G]$ and $[\mathbf{D}_G]$ are defined in Chapter 2

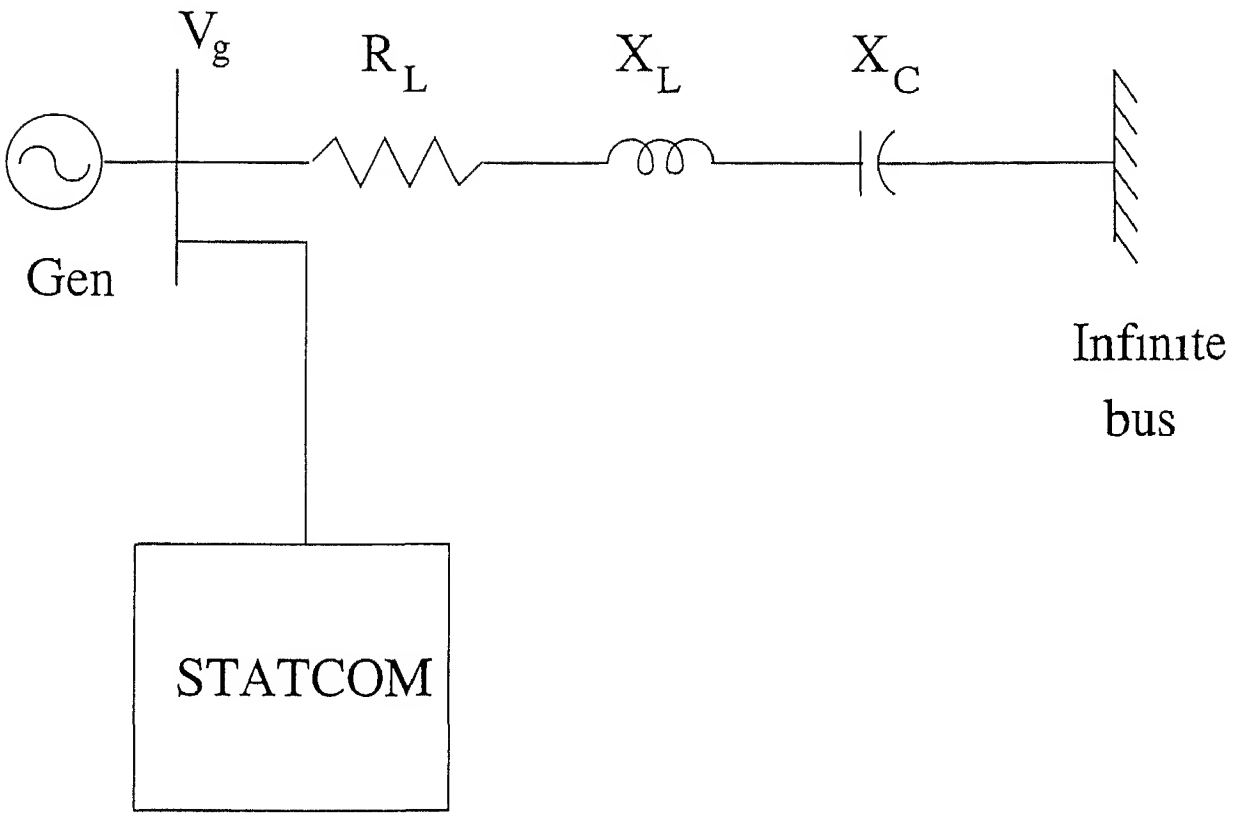


Figure 3 1 Schematic diagram of the system under study

AC Network

The state and output equations of the AC network are given by

$$\Delta \mathbf{x}_N = [\mathbf{A}_N]\,\Delta \mathbf{x}_N + [\mathbf{B}_N]\,\Delta \mathbf{u}_N \quad (3.3)$$

$$\Delta \mathbf{y}_N = [\mathbf{C}_N]\,\Delta \mathbf{x}_N \quad (3.4)$$

where state vector contains D Q axes capacitor voltages i e $\Delta \mathbf{x}_N = [\Delta v_{CD}\ \Delta v_{CQ}]^T$ The input vector contains D Q axes line currents and D Q axes STATCOM currents i e $\Delta \mathbf{u}_N = [\Delta i_{GD}\ \Delta i_{GQ}\ \Delta i_{sD}\ \Delta i_{sQ}]^T$ The output vector is given as $\Delta \mathbf{y}_N = [\Delta v_{CD}\ \Delta v_{CQ}]^T$

### 3 1 1 STATCOM Representation

The STATCOM is based on the voltage source inverter (VSI) using Gate Turn Off (GTO) thyristor valves A basic 6 pulse VSI circuit is shown in Fig 3 2 This consists of six GTO thyristors each having an anti parallel diode and a capacitor connected on the DC side The VSI is connected to the system bus through a small reactance which is the leakage reactance of the coupling transformer

The magnitude of the VSI output voltage can be controlled to produce a fundamental output voltage in phase with the AC system voltage If the VSI output voltage is greater than the AC system voltage, capacitive current is drawn from the power system and conversely, if the VSI output voltage is lower than the AC system voltage, inductive current is drawn By varying the phase angle of the inverter output voltage relative to the AC system voltage the output voltage of the STATCOM is varied thereby varying the reactive power supplied or drawn Also, the STATCOM can negotiate the exchange of real power with the AC system by varying the phase angle of the inverter output voltage That is, the STATCOM supplies real power to the AC system from its DC capacitor if the STATCOM output vol age is made to lead the AC system voltage By the same token, the STATCOM absorbs re il power from the AC system, if the STATCOM output voltage is made to lag

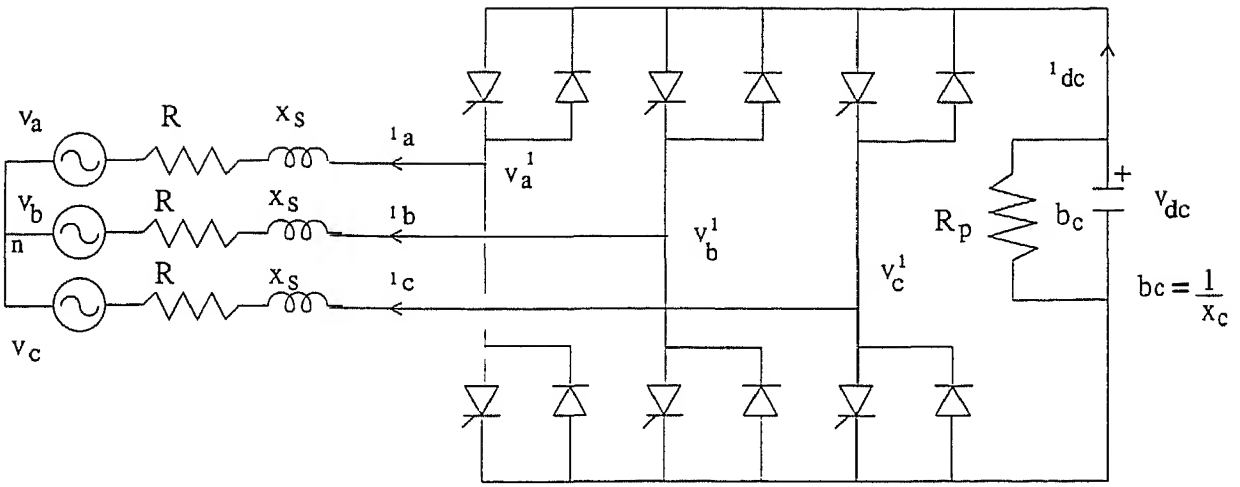


**Figure 3 2** A basic 6 pulse voltage source inverter

the AC system voltage This particular property is used to maintain the capacitor voltage at the desired level

## 3 1 2 Modeling Of STATCOM

Consider the circuit of Fig 3 2 A set of three phase voltage is produced from the input DC voltage The GTOs are assumed to have negligible turn off and turn on time For the discussion presented below, we shall neglect both AC and DC side harmonics and consider only the fundamental frequency components The dynamics of a six pulse STATCOM can be described by the following equations

$$
\begin{aligned}
v_{dc} &= -\frac{\omega_B}{b_c}\left(\frac{v_{dc}}{R_p} + i_{dc}\right) \\
i_a &= -\frac{\omega_B}{X_s}\left(Ri_a - \left(v_a^1 - v_a\right)\right) \\
i_b &= -\frac{\omega_B}{X_s}\left(Ri_b - \left(v_b^1 - v_b\right)\right) \\
i_c &= -\frac{\omega_B}{X_s}\left(Ri_c - \left(v_c^1 - v_c\right)\right)
\end{aligned}
\tag{3 5}
$$

where $v_a^1$ $v_b^1$ and $v_c^1$ are the three phase instantaneous voltages at the inverter AC side terminals $R$ and $X_s$ are the resistance and leakage reactance of the transformer, $R_p$ rep resents the switching losses in the inverter $v_{dc}$ and $i_{dc}$ are the voltage across and current through the capacitor $i_a$ $i_b$ and $i_c$ are the instantaneous currents on the AC side and $v_a$ $v_b$ and $v_c$ are the instantaneous voltages of the AC bus The instantaneous three phase AC bus phase voltages are given by

$$\begin{aligned} v_a &= v_m sin\left(\omega_B t + \theta\right) \\ v_b &= v_m sin\left(\omega_B t + \theta - 120^0\right) \\ v_c &= v_m sin\left(\omega_B t + \theta + 120^0\right) \end{aligned} \tag{3 6}$$

where where $\theta$ is the AC bus voltage angle defined with respect to the infinite bus voltage of Fig 3 1 and $v_m = \sqrt{2}v_{ph}$

For a six pulse inverter with pulse duration of $60^0$ the peak value of the fundamen tal component of the phase voltage is $\frac{2}{\pi}v_{dc}$ consequently, the three phase instantaneous voltages at the inverter AC terminals can be expressed as

$$\begin{aligned} v_a^1 &= v_{dc}\frac{2}{\pi}sin\left(\omega_B t + \beta + \theta\right) \\ v_b^1 &= v_{dc}\frac{2}{\pi}sin\left(\omega_B t + \beta + \theta - 120^o\right) \\ v_c &= v_{dc}\frac{2}{\pi}sin\left(\omega_B t + \beta + \theta + 120^o\right) \end{aligned} \tag{3 7}$$

where $\beta$ is the angle between the inverter output voltage and AC bus voltage and $\omega_B$ is the base frequency

Assuming power balance between the AC and DC sides, the following equation can be written inverter [31]

$$v_{dc}i_{dc} = v_a^1 i_a + v_b^1 i_b + v_c^1 i_c \tag{3 8}$$

Defining $\gamma = (\omega_B t + \beta + \theta)$ we write the dc current expression using eq (3 8)

$$i_{dc} = \frac{2}{\pi}\left[i_a sin\left(\gamma\right) + i_b sin\left(\gamma - 120^o\right) + i_c sin\left(\gamma + 120^o\right)\right] \tag{3 9}$$

Substituting eqs (3 6) and (3 7) in eq (3 5) we get

$$\begin{aligned} i_a &= -\frac{\omega_B}{X_s}\left[Ri_a - \frac{2}{\pi}v_{dc} sin\left(\gamma\right) - v_m sin\left(\omega_B t + \theta\right)\right] \\ i_b &= -\frac{\omega_B}{X_s}\left[Ri_b - \frac{2}{\pi}v_{dc} sin\left(\gamma - 120^o\right) - v_m sin\left(\omega_B t + \theta - 120^o\right)\right] \\ i_c &= -\frac{\omega_B}{X_s}\left[Ri_c - \frac{2}{\pi}v_{dc} sin\left(\gamma + 120^o\right) - v_m sin\left(\omega_B t + \theta + 120^o\right)\right] \end{aligned} \tag{3 10}$$

The above equation can be written in the following state space form

$$\mathbf{x}_{abc} = [\mathbf{A}]\,\mathbf{x}_{abc} + [\mathbf{B}_1]\,\mathbf{v}_{dc} + [\mathbf{B}_2]\,\mathbf{u}_{abc} \tag{3 11}$$

where $\mathbf{x}_{abc}^T = [i_a \;\; i_b \;\; i_c]$, $\mathbf{u}_{abc}^T = [v_a \;\; v_b \;\; v_c]$

Substituting eq (3 9) in eq (3 5), the $DC$ capacitor voltage can be written as

$$v_{dc} = -\frac{\omega_B}{b_c}\left[\frac{v_{dc}}{R_p} + \frac{2}{\pi}(i_a sin(\gamma) + i_b sin(\gamma - 120^o) + i_c sin(\gamma + 120^o))\right] \tag{3 12}$$

The quantities in the $abc$ reference frame can be expressed in $DQO$ reference frame using the following transformation

$$\begin{bmatrix} i_a \\ i_b \\ i_c \end{bmatrix} = \sqrt{\tfrac{2}{3}}\begin{bmatrix} cos(\omega_{Bt}) & sin(\omega_{Bt}) & \frac{1}{\sqrt{2}} \\ cos(\omega_{Bt} - 120^0) & sin(\omega_{Bt} - 120^0) & \frac{1}{\sqrt{2}} \\ cos(\omega_{Bt} + 120^0) & sin(\omega_{Bt} + 120^0) & \frac{1}{\sqrt{2}} \end{bmatrix}\begin{bmatrix} i_D \\ i_Q \\ i_O \end{bmatrix} = [T]\,[i_{DQO}] \tag{3 13}$$

Premultiplying both sides of eq (3 11) by $\mathbf{T}^{-1}$, the following expression is obtained

$$[\mathrm{T}^{-1}]\mathrm{x}_{abc} = [\mathrm{T}^{-1}][A]\mathrm{x}_{abc} + [\mathrm{T}^{-1}][B_1]\mathrm{v}_{dc} + [\mathrm{T}^{-1}][B_2]\mathrm{u}_{abc} \tag{3 14}$$

Equation(3 14) can be rewritten as

$$[\mathrm{T}^{-1}]\mathrm{x}_{abc} = [\mathrm{T}^{-1}][A][\mathrm{T}][\mathrm{T}^{-1}]\mathrm{x}_{abc} + [\mathrm{T}^{-1}][B_1]\mathrm{v}_{dc} + [\mathrm{T}^{-1}][B_2]\mathrm{u}_{abc} \tag{3 15}$$

Using eq (3 13) the following expression is written

$$\mathrm{T}^{-1}\mathrm{x}_{abc} = \mathrm{x}_{DQO} + \mathrm{T}^{-1}\mathrm{x}_{abc} = \mathrm{x}_{DQO} + \mathrm{T}^{-1}\mathrm{T}\mathrm{x}_{DQO} \tag{3 16}$$

Substituting eq (3 16) in eq (3 15) gives

$$\mathrm{x}_{DQO} = [A]\,\mathrm{x}_{DQO} - \left[\mathrm{T}^{-1}\mathrm{T}\right]\mathrm{x}_{DQO} + [B_1]\,\mathrm{v}_{dc} + \mathrm{T}^{-1}\,[B_2]\,\mathrm{u}_{DQO} \tag{3 17}$$

where $\mathrm{x}_{DQO}^T = [\imath_{sD}\ \imath_{sQ}\ \imath_{sO}]$, $\mathrm{u}_{DQO}^T = [v_{sD}\ v_{sQ}\ v_{sO}]$ the quantities $\imath_{sD}, \imath_{sQ}, \imath_{sO}$ and $v_{sD}\ v_{sQ}\ v_{sO}$ are the STATCOM currents and voltages in DQO reference frame

From eq (3 17) the $DQ$ components of STATCOM currents can be obtained as

$$\imath_{sD} = -\frac{R\omega_B}{X_s}\imath_{sD} - \omega_B\imath_{sQ} + \omega_B k v_{dc}\frac{sin(\beta+\theta)}{X_s} - \frac{\omega_B}{X_s}v_{sD}$$

$$\imath_{sQ} = \omega_B\imath_{sD} - \frac{R\omega_B}{X_s}\imath_{sQ} + \omega_B k v_{dc}\frac{cos(\beta+\theta)}{X_s} - \frac{\omega_B}{X_s}v_{sQ}$$

Similarly, using the quantities expressed in $DQO$ reference frame eq (3 12) can be written as

$$v_{dc} = -\omega_B k\frac{sin(\beta+\theta)}{b_c}\imath_{sD} - \omega_B k\frac{cos(\beta+\theta)}{b_c}\imath_{sQ} - \frac{\omega_B}{b_c R_p}v_{dc}$$

where $k = \frac{\sqrt{6}}{\pi}$ for six pulse converter and $k = \frac{2\sqrt{6}}{\pi}$ for a 12 pulse converter

The above expressions for $\imath_{sD}, \imath_{sQ}$ and $v_{dc}$ can be combined as

$$\mathrm{x}_{SE} = [\mathrm{A}_0]\,\mathrm{x}_{SE} + [\mathrm{B}_0]\,\mathrm{u}_S \tag{3 18}$$

where $\mathrm{x}_{SE} = [\imath_{sD}\ \imath_{sQ}\ v_{dc}]^T$, $\mathrm{u}_S = [v_{sD}v_{sQ}]^T$ and $[\mathrm{A}_0] = [\mathrm{J}]$ The elements of the [J] matrix is given below

$$J_{11} = -\frac{R\omega_B}{X_s},\quad J_{12} = -\omega_B,\quad J_{13} = \omega_B k\frac{sin(\beta+\theta)}{X_s}$$

$$J_{21} = \omega_B,\quad J_{22} = -\frac{R\omega_B}{X_s},\quad J_{23} = \omega_B k\frac{cos(\beta+\theta)}{X_s}$$

$$J_{31} = -\omega_B k\frac{sin(\beta+\theta)}{b_c}\quad J_{32} = -\omega_B k\frac{cos(\beta+\theta)}{b_c}\quad J_{33} = -\frac{\omega_B}{b_c R_p}$$

The matrix $[\mathbf{B}_0]$ is given by

$$[\ \mathbf{B}_0\ ] = \begin{bmatrix} -\frac{\omega_B}{X} & 0 \\ 0 & -\frac{\omega_B}{Y} \\ 0 & 0 \end{bmatrix} \begin{bmatrix} v_{sD} \\ v_{sQ} \end{bmatrix}$$

It may be noted that STATCOM voltage $v_s$ is same as the generator voltage $v_g$ since both STATCOM and the generator are connected to the same bus as shown in Fig 3 1 The angle $\theta$ can be expressed as

$$\theta = tan^{-1}\left(\frac{v_{sD}}{v_{sQ}}\right) \tag{3 19}$$

Linearizing the eq (3 19) about an operating point, we get

$$\triangle\theta = \frac{v_{sQ0}}{{v_{s0}}^2}\triangle v_{sD} - \frac{v_{sD0}}{{v_{s0}}^2}\triangle v_{sQ} \tag{3 20}$$

where $v_{s0}$ is the STATCOM bus voltage at the nominal operating point Linearizing eq (3 18) and utilize eq (3 20) the following state space equation is obtained

$$\triangle \mathbf{x}_{SE} = [\mathbf{A}_{SE}]\,\triangle \mathbf{x}_{SE} + [\mathbf{B}_{SE1}]\,\triangle \mathbf{u}_S + [\mathbf{B}_{SE2}]\,\triangle\beta \tag{3 21}$$

where $\mathbf{A}_{SE} = \mathbf{A}_0$, $\mathbf{B}_{SE1} = \mathbf{G}$, and $\mathbf{B}_{SE2} = \mathbf{H}$ The elements of the [G] matrix are given below

$$G_{11} = -\frac{\omega_B}{X_s}\left[1 - \frac{k\ v_{dc0}\ cos(\beta_0+\theta_0)\ v_{sQ0}}{v_{s0}^2}\right],\ \ G_{12} = -\frac{\omega_B}{X_s}\frac{v_{sD0}}{{v_{s0}}^2} k\ v_{dc0}\ cos(\beta_0+\theta_0),$$

$$G_{21} = -\frac{\omega_B}{X_s}\frac{v_{sQ0}}{{v_{s0}}^2} k\ v_{dc0}\ sin(\beta_0+\theta_0),\ \ G_{22} = -\frac{\omega_B}{X_s}\left[1 - \frac{k\ v_{dc0}\ sin(\beta_0+\theta_0)\ v_{sD0}}{v_{s0}^2}\right],$$

$G_{31} = kc_1\ \frac{\omega_B\ v_{Q0}}{b\ v_0^2}$, $G_{32} = -kc_1\ \frac{\omega_B\ v_{sD0}}{b\ v_0^2}$ and $c_1 = -i_{sD0}\ cos(\beta_0+\theta_0) + i_{sQ0}\ sin(\beta_0+\theta_0)$

The elements of the [H] matrix are given below

$H_{11} = \omega_B\ k\ v_{dc0}\ \frac{cos(\beta_0+\theta_0)}{X}$ $H_{21} = \omega_B\ k\ v_{dc0}\ \frac{sin(\beta_0+\theta_0)}{X}$ and

$H_{31} = -\frac{\omega_B k}{b}\ (i_{sD0}\ cos(\beta_0+\theta_0) - i_{sQ0}\ sin(\beta_0+\theta_0))$

The output equation is given by

$$\triangle \mathbf{y}_{SE} = \begin{bmatrix} \triangle i_{sD} \\ \triangle i_{sQ} \end{bmatrix} = \begin{bmatrix} 0 & 0 \\ 0 & 1 & 0 \end{bmatrix} \triangle \mathbf{x}_{SE} = [\mathbf{C}_{SE}]\,\triangle \mathbf{x}_{SE} \tag{3 22}$$

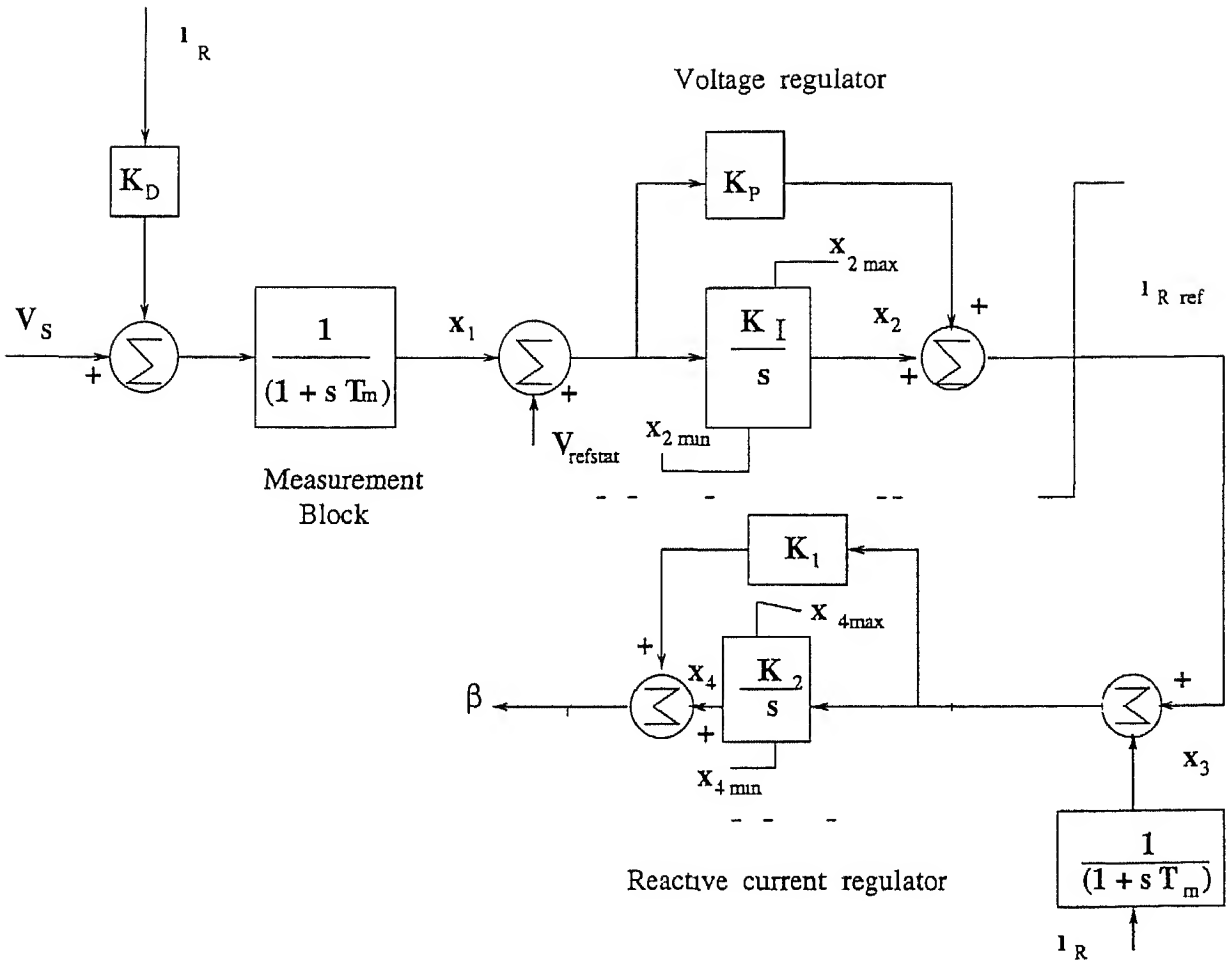


Figure 3 3 Block diagram of the STATCOM controller

The STATCOM controller dynamics can be expressed through the following equations

$$\begin{aligned} \dot{x}_1 &= -\frac{1}{T_m}x_1 + \frac{1}{T_m}\left(v_s - K_D i_R\right) \\ \dot{x}_2 &= K_I\left(V_{refstat} - x_1\right) \\ \dot{x}_3 &= \frac{1}{T_m}\left(-x_3 + i_R\right) \\ \dot{x}_4 &= K_2\left(x_2 + K_p\left(V_{refstat} - x_1\right) - x_3\right) \end{aligned} \tag{3 23}$$

The reactive power $Q_s$ of the STATCOM is expressed in terms of $D-Q$ components of voltage and current as

$$Q_s = v_{sQ} i_{sD} - v_{sD} i_{sQ}$$

From the above equation we can write the expression for STATCOM current as

$$i_R = \frac{v_{sQ} i_{sD} - v_{sD} i_{sQ}}{v_s} \tag{3 24}$$

In the linearized domain eq (3 25) can be written as

$$\begin{aligned} \Delta i_R = \tfrac{1}{v\,0}\left[v_{sQ0}\Delta i_{sD} - v_{sD0}\Delta i_{sQ}\right] + \left[-\tfrac{i\,Q0}{v\,0} - \tfrac{i_{R0}}{v_0^2}\,v_{sD0}\right]\Delta v_{sD} \\ + \left[\tfrac{i_{sD0}}{i\,0} - \tfrac{i_{R0}}{v_0^2}\,v_{sQ0}\right]\Delta v_{sQ} \end{aligned} \tag{3 25}$$

and the STATCOM bus voltage can be expressed in its $D-Q$ components as

$$v_s^2 = v_{sD}^2 + v_{sQ}^2$$

It may be noted that $v_s$ is same as $V_g$ shown in Fig 3 1 Linearizing the above equation we get

$$\left(v_{s0} + \Delta v_s\right)^2 = \left(v_{sD0} + \Delta v_{sD}\right)^2 + \left(v_{sQ0} + \Delta v_{sQ}\right)^2$$

Neglecting the higher order terms, the above equation can be approximated as

$$\Delta v_s = \frac{v_{sD0}}{v_s 0}\Delta v_{sD} + \frac{v_{sQ0}}{v_s 0}\Delta v_{sQ} \tag{3 26}$$

Combining eq (3 23) with eqs (3 25) and (3 26), we get

$$\Delta \mathbf{x}_{SC} = \left[\mathbf{A}_{SC}\right]\Delta \mathbf{x}_{SC} + \left[\mathbf{B}_{SC1}\right]\Delta \mathbf{u}_{SC1} + \left[\mathbf{B}_{SC2}\right]\Delta \mathbf{u}_{SC2} \tag{3 27}$$

where $\Delta \mathbf{x}_{SC}^T = [\Delta x_1\ \Delta x_2\ \Delta x_3\ \Delta x_4]$ $\Delta \mathbf{u}_{SC1}^T = [\Delta \imath_{sD}\ \Delta \imath_{sQ}]$ and $\Delta \mathbf{u}_{SC2}^T = [\Delta v_{sD}\ \Delta v_{sQ}]$ The output equation is given by

$$\Delta \mathbf{y}_{SC} = \Delta\beta = [\mathbf{C}_{SC}]\,\Delta \mathbf{x}_{SC} \tag{3 28}$$

The matrices $[\mathbf{A}_{SC}]$ $[\mathbf{B}_{SC1}]$ $[\mathbf{B}_{SC2}]$ and $[\mathbf{C}_{SC}]$ are defined in Appendix D

The input to the STATCOM controller state space model is the $D-Q$ components of STATCOM current which is obtained as the output of the STATCOM model The output of the STATCOM controller is $\Delta\beta$ which is the which is one of the input in the STATCOM model Based on this inter component relationship, the STATCOM controller and the STATCOM models can be combined using eqs (3 21), (3 22), (3 27) and (3 28) as

$$\Delta \mathbf{x_S} = [\mathbf{A}_S]\,\Delta \mathbf{x}_S + [\mathbf{B}_S]\,\Delta \mathbf{u}_S \tag{3 29}$$

where,

$$\left[\ \Delta \mathbf{A}_S\ \right] = \begin{bmatrix} \mathbf{A}_{SE} & \mathbf{B}_{SE2}\mathbf{C}_{SC} \\ \mathbf{B}_{SC1}\mathbf{C}_{SE} & \mathbf{A}_{SC} \end{bmatrix} \quad \left[\ B_S\ \right] = \begin{bmatrix} \mathbf{B}_{SE1} \\ \mathbf{B}_{SC2} \end{bmatrix}$$

and $\Delta \mathbf{u}_S = \Delta \mathbf{u}_{SC2}$ Also,

$$\Delta \mathbf{y}_S = \begin{bmatrix} \Delta \imath_{sD} \\ \Delta \imath_{sQ} \\ \Delta \imath_{sD} \\ \Delta \imath_{sQ} \end{bmatrix} = [\mathbf{C}_S]\,\Delta \mathbf{x}_S + [\mathbf{D}_S]\,\Delta \mathbf{u}_S \tag{3 30}$$

The matrices $[\mathbf{C}_S]$ and $[\mathbf{D}_S]$ are defined in Appendix D Equations (3 29) and (3 30) give the state space model of the STATCOM including its controller

## 3 2 Combined Generator-Network-STATCOM Model

The various subsystem models given by eqs (3 1) to (3 4), (3 29) and (3 30) can be combined to get the overall system model The interconnection diagram is shown in Fig 3 4 From the diagram it can be seen that the input variable of STATCOM model are related to the output variables of the network model The network input variables are obtained from

the generator system and the STATCOM models The various subsystem models can be interconnected in the manner

$$\Delta \mathbf{u} = [\mathbf{F}]\ \Delta \mathbf{y} \tag{3 31}$$

where $\Delta \mathbf{u} = \left[\Delta \mathbf{u}_G^T\ \Delta \mathbf{u}_S^T\ \Delta \mathbf{u}_N^T\right]^T$, $\Delta \mathbf{y} = \left[\Delta \mathbf{y}_G^T\ \Delta \mathbf{y}_S^T\ \Delta \mathbf{y}_N^T\right]^T$ and $\Delta \mathbf{x} = \left[\Delta \mathbf{x}_G^T\ \Delta \mathbf{x}_S^T\ \Delta \mathbf{x}_N^T\right]^T$ The elements of matrix $[F]$ provide the interfacing between various component models as shown in Fig 3 4

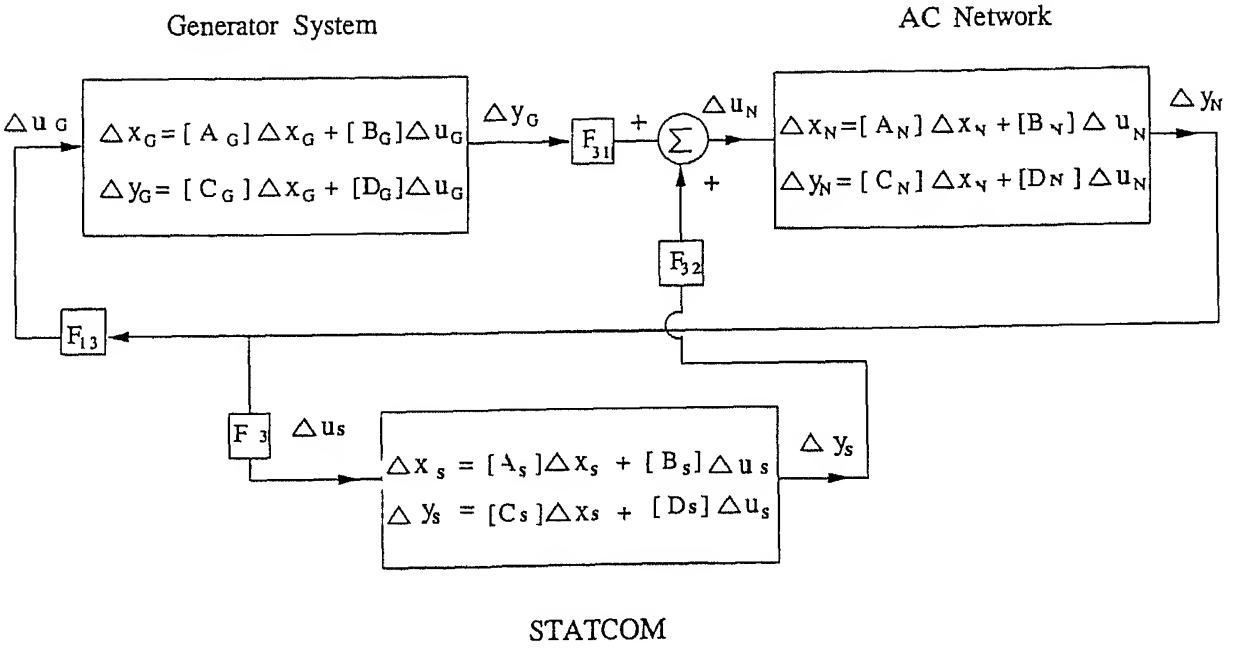


**Figure 3 4** Interconnection pattern

For the AC network the injected current is the algebraic sum of generator current and STATCOM current Hence the input vector in the network model will change to accommodate the STA COM output variables The input and output vectors of individual subsystems are given below

For the generator

$$\Delta \mathbf{u}_G = [\Delta v_{gD}\ \Delta v_{gQ}]^T \text{ and } \Delta \mathbf{y}_G = \left[\Delta i_D\ \Delta i_Q\ \Delta i_D\ \Delta i_Q\right]^T$$

For the AC network

$$\Delta \mathbf{u}_N = [\Delta i_{GD}\ \Delta i_{GQ}\ \Delta i_{sD}\ \Delta\ i_{sQ}]^T \text{ and } \Delta \mathbf{y}_N = [\Delta v_{CD}\ \Delta v_{CQ}]^T$$

For STATCOM

$$\Delta \mathbf{u}_S = [\Delta v_{sD}\ \Delta v_{sQ}]^T \text{ and } \Delta \mathbf{y}_S = \left[\Delta i_{sD}\ \Delta i_{sQ}\ \Delta i_{sD}\ \Delta i_{sQ}\right]^T$$

The state and output equations of the component models are combined to obtain the state and output equation of the entire system in the form

$$\Delta \mathbf{x} = [\mathbf{A}]\,\Delta \mathbf{x} + [\mathbf{B}]\,\Delta \mathbf{u} \tag{3 32}$$

$$\Delta \mathbf{y} = [\mathbf{C}]\,\Delta \mathbf{x} + [\mathbf{D}]\,\Delta \mathbf{u} \tag{3 33}$$

where

$$[\mathbf{A}] = diag\,[\mathbf{A}_G\ \mathbf{A}_S\ \mathbf{A}_N] \quad [\mathbf{B}] = diag\,[\mathbf{B}_G\ \mathbf{B}_S\ \mathbf{B}_N],$$

$$[\mathbf{C}] = diag\,[\mathbf{C}_G\ \mathbf{C}_S\ \mathbf{C}_N] \text{ and } [\mathbf{D}] = diag\,[\mathbf{D}_G\ \mathbf{D}_S\ \mathbf{D}_N]$$

Substituting eq (3 33) in eq (3 31) to eliminate $\Delta \mathbf{y}$ and incorporating the resulting ex pression for $\Delta \mathbf{u}$ in eq (3 32) gives

$$\Delta \mathbf{x} = \left[\mathbf{A} + \mathbf{BF}(\mathbf{I} - \mathbf{DF})^{-1}\mathbf{C}\right] \Delta \mathbf{x} = [\mathbf{A}_T]\,\Delta \mathbf{x} \tag{3 34}$$

The details of F matrix are given in Appendix D

## 3 3 Eigenvalue Analysis

To illustrate the development of the system model the eigenvalue analysis of IEEE FBM is under taken In the IEEE FBM the generator is delivering 0 9 per unit power to transmission system at 0 9 power factor lag The generator excitation is assumed to be constant Self damping of 0 2 per unit and mutual damping of 0 3 per unit is added to the shaft to account for steam damping [13] The value of series capacitor is chosen to compensate 70% of the transmission line reactance(i e $X_C = 0\ 3o$ per unit) STATCOM data is given in Appendix D A 12 pulse STATCOM is assumed to be supplying reactive power of 0 14 per unit The initial condition calculation of STATCOM is given in Appendix D The overall system eigenvalues are given in Table 3 1

The study is initially carried out considering that the STATCOM controller has a voltage regulator only The voltage controller gains are taken as $K_P = 0\ 74$ and $K_I = 10$ To neglect the effect of the reactive current controller the gains $K_1$ and $K_2$ are set to zero From the system eigenvalues given in Table 3 1, it can be seen that without the STATCOM the mode 2 is unstable Introduction of the STATCOM with only the voltage results in the stabilization of mode 2, while at the same time it destabilizes the mode 4 The damping of mode 3 and mode 1 is increased The networks mode damping is also improved

In a subsequent study, both the voltage and the reactive current regulators are con sidered The reactive current controller gains are chosen as $K_1 = 0\ 13$ and $K_2 = 0\ 01$ From the eigenvalue results it can be observed that STATCOM increases the damping of all the torsional modes when both the controllers are active The damping of the network modes is greatly enhanced Compared to the previous case, the damping of mode 2 is increased, whereas the damping of mode 1 and mode 3 is decreases The subsynchronous network mode damping is marginally decreased, whereas the supersynchronous network mode damping s increased The frequency of oscillation of subsynchronous network mode

is decreased compared to that in the earlier case The effect of the STATCOM in improving the damping of torsional modes as observed from the eigenvalue analysis is further validated through dynamic digital simulation

**Table 3 1** Eigenvalues for different control strategies of STATCOM

| Without STATCOM | With STATCOM voltage control alone | With STATCOM voltage control and reactive current control | comments |
|---|---|---|---|
| 4 42± j612 43 | 10 17±63ɔ 19 | 13 09±637 92 | Supsvn Net Mode |
| 3 45± j141 11 | 28 93± j169 79 | 28 04± j134 69 | Subsvn Net Mode |
| 1 38 ± j298 16 | 2 05±j298 15 | 2 05±j298 15 | Mode ɔ |
| 0 28 ± j203 03 | 0 65 ± j204 88 | 0 534 ± j204 24 | Mode 4 |
| 0 89 ± j159 12 | 1 56 ± j160 72 | 1 27 ± j160 11 | Mode 3 |
| 0 03±j129 14 | 0 217±j129 19 | 0 218±j129 128 | Mode 2 |
| 0 11±j98 6ɔ1 | 0 158±j100 159 | 0 88±j99 64 | Mode 1 |
| 0 43±j10 56 | 0 71±j26 78 | 2 24±j18 44 | Mode 0 |
| | 278 94l±4189 75 | 285 34±4192 48 | |
| | | 156 13±253 33 | |
| | | 0 32±0 35 | |
| | 250 | 250 | |
| | 250 | | |
| 3 91 | -3 695 | 3 5 | |
| 0 20 | 0 168 | 0 079 | |
| | 83 47 | | |

## 3 4 Time Domain Simulation

Time domain simulation is carried out to observe the shaft torque response during major disturbance using PSCAD/EMTDC package version 3 0 It may be mentioned here that the torque amplification is severe at higher compensation levels [36] The chosen capacitive compensation provides suitable test case for torque amplification All system nonlineari ties are incorporated in detail Dynamics of the excitatio n system is neglected Governor action is not considered The STATCOM is considered to be equipped with both voltage

and reactive current controllers The generator is delivering 0 9 per unit power A three phase to ground fault of 4 5 cycle duration with 0 04 per unit fault impedance is applied at the infinite bus at time t = 0 5 sec The plots of the shaft torques are shown in Fig 3 5 It can be observed from the results that the STATCOM is effective in damping the torsional oscillations For the same level of transmission line compensation the peak shaft torques associated with NGH damping scheme and STATCOM are tabulated in Table 3 2 It can be seen that there is a significant reduction in the peak values of GEN EXC and LPA LPB torques with STATCOM The reduction in peak values is marginal in the case of IP LPA and HP IP torques Though there is marginal increase in peak value of LPB-Gen torque, the amplitude of oscillations are progressively decreasing It can be seen from Fig 3 6 that the STATCOM is also able to regulate the generator terminal voltage effectively It may be mentioned that no attempt has been made here to optimize the controller parameters of STATCOM

**Table 3 2** Peak shaft torques with different devices

| Name of the Device | peak value of torques in per unit | | | | |
|---|---|---|---|---|---|
| | Gen Exc torque | LPB Gen torque | LPA LPB torque | IP LPA torque | HP IP torque |
| NGH damper | 0 4248 | 2 465 | 2 50 | 1 52 | 0 819 |
| STATCOM | 0 3085 | 2 5 | 2 16 | 1 47 | 0 8 |

## 3 5 Conclusions

In this chapter the effectiveness of the reactive power modulation feature of STATCOM in damping the subsynchronous torsional oscillations is studied A linearized model of

the STATCOM along with the IEEE FBM is derived to study the transient torque problem The effect of both the voltage and reactive current controllers of STATCOM is investigated The voltage control scheme alone is not able to provide entire damping to torsional oscillations The voltage control along with the reactive current control is able to damp the torsional oscillations The control scheme is implemented using local measurements alone

The Shunt compensators provide an indirect approach to increase the power transfer over a transmission line to certain extent The series capacitors provide direct approach to increase the power transmission capability which is very often the most economical solution In the above discussion the damping of SSR oscillations is demonstrated using reactive power modulation The real power modulation can also be used for damping SSR oscillations The TCSC is one of the FACTS devices that can be used for real power mod ulation In the next chapter the damping of SSR phenomenon using TCSC is presented

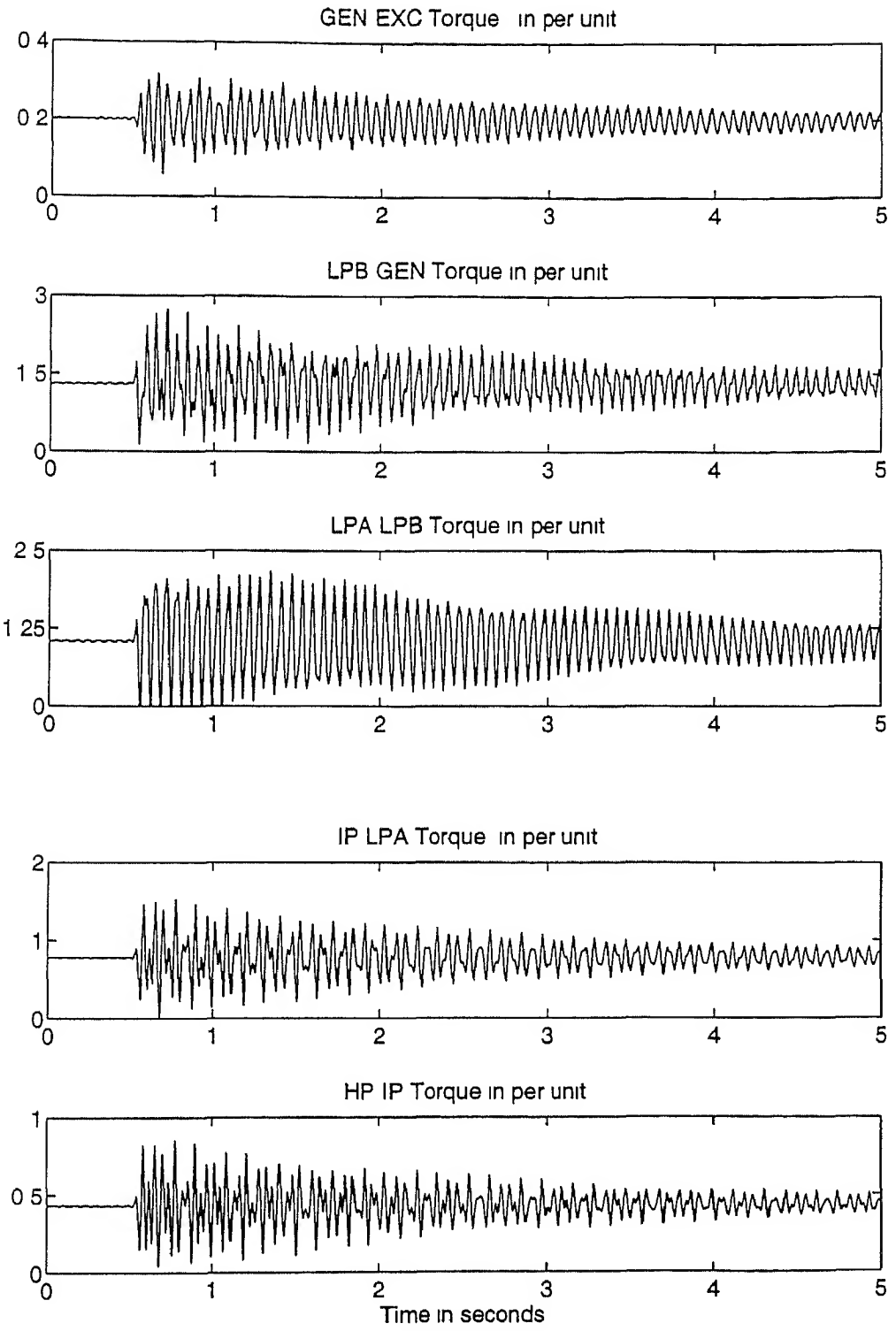


**Figure 3 5** System response with STATCOM for a three phase fault

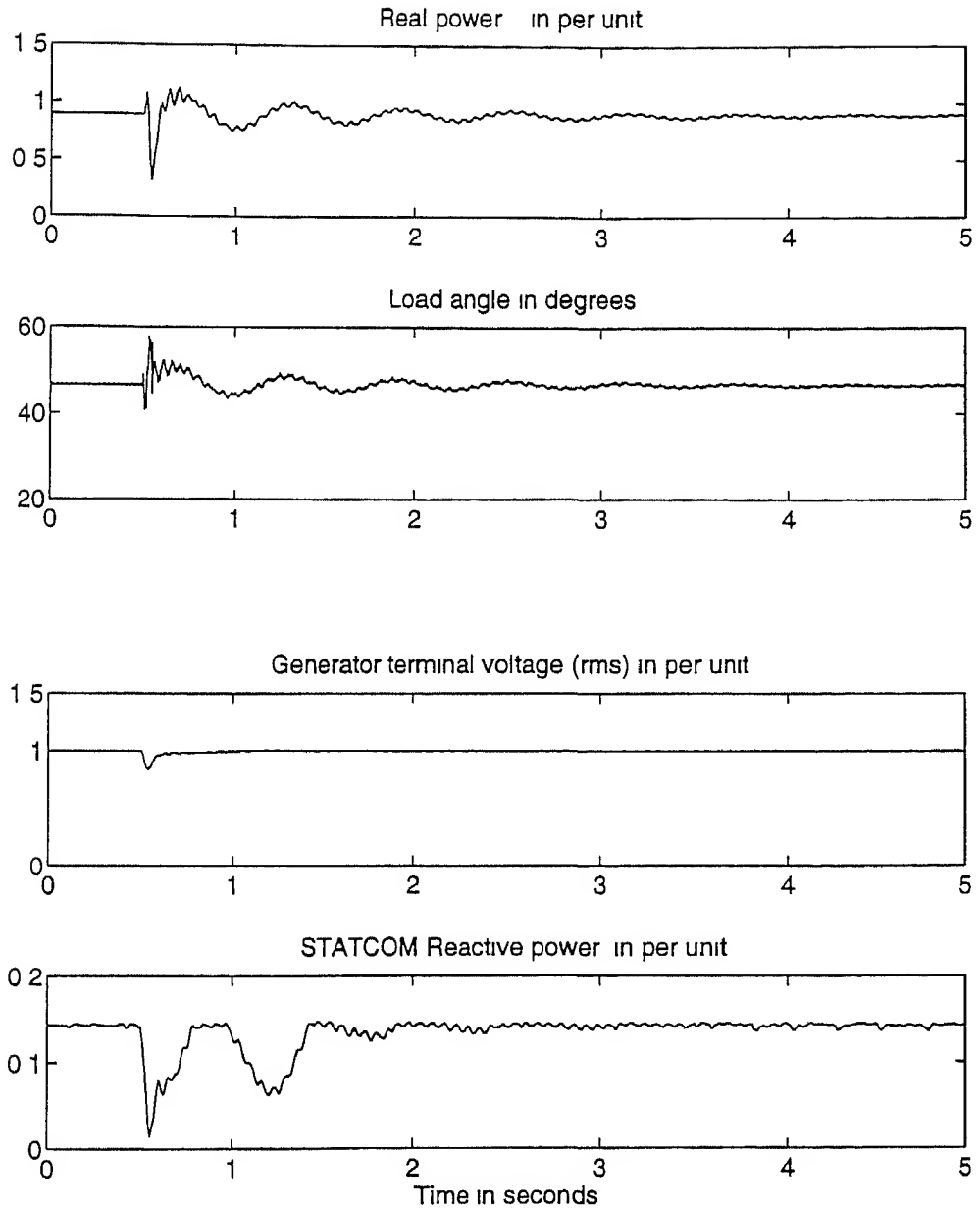


**Figure 3 6** System response with STATCOM for a three phase fault

# Chapter 4

# SSR ANALYSIS WITH TCSC

In the previous chapter SSR analysis with the STATCOM is discussed The thyristor controlled series capacitor (TCSC) is one of the FACTS device considered for control of power flow over the transmission line In this chapter, SSR analysis with TCSC is presented A simple proportional integral control is used for TCSC control The TCSC model is same as that given in [21] The study is carried out using eigenvalue analysis and the results are validated through PSCAD/EMTDC simulation

## 4 1 System Modeling

The system under study is the IEEE FBM with a controlled series compensation as shown in Fig 4 1 The variable reactance $X_C$ shown in Fig 4 1 comprises of fixed capacitor and a TCSC It can be seen that the study system is the same as that given in Fig 2 4 except for variable $X_C$ Hence the eigenvalue analysis technique given in Chapter 2 is directly applicable here However, to facilitate the inclusion of the continuous time TCSC model and its associated PI controller, the AC network equations will be different from those given in Chapter 2 The turbine generator model is also the same as given in Chapter 2 For the sake of completeness, the turbine generator model is reproduced here

$$\Delta \mathbf{x}_G = [\mathbf{A}_G]\, \Delta \mathbf{x}_G + [\mathbf{B}_G]\, \Delta \mathbf{u}_G \tag{4 1}$$

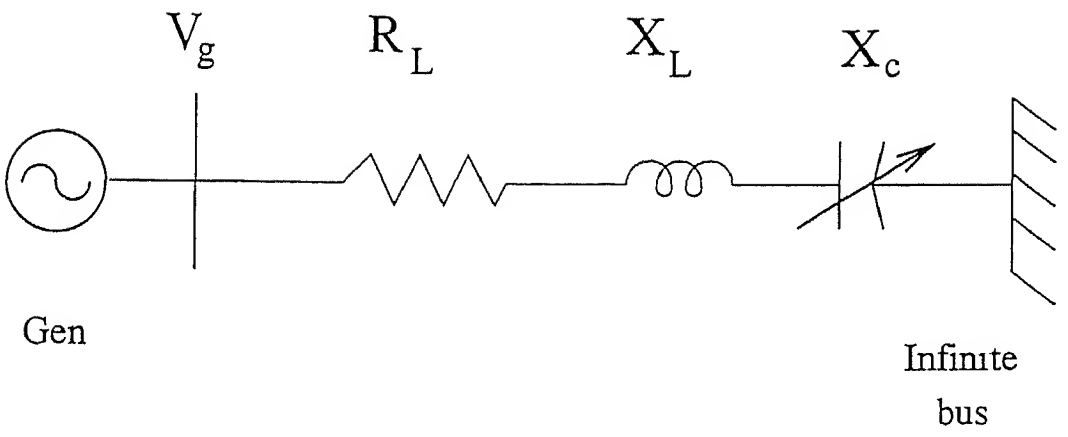


Figure 4 1 IEEE FBM with Controlled Series Compensation

where $\Delta \mathbf{x}_G^T = [\Delta \mathbf{x}_{s1}^T \ \Delta \mathbf{x}_m^T]$, $\Delta \mathbf{u}_G = [\Delta v_{gD} \ \Delta v_{gQ}]^T$, $\Delta \mathbf{x}_{s1}$ and $\Delta \mathbf{x}_m$ are the state vectors associated with the synchronous machine and the mechanical system The output equation of the generator system is given by

$$\Delta \mathbf{y}_G = [\mathbf{C}_G] \Delta \mathbf{x}_G + [\mathbf{D}_G] \Delta \mathbf{u}_G \tag{4 2}$$

where $\Delta \mathbf{y}_G = [\Delta i_D \ \Delta i_Q \ \Delta i_D \ \Delta i_Q]^T$ The matrices $[\mathbf{A}_G]$ $[\mathbf{B}_G]$ $[\mathbf{C}_G]$ and $[\mathbf{D}_G]$ are defined in Chapter 2

### 4 1 1 AC Network Representation

The AC network consists of transformers, transmission line a fixed capacitor and a TCSC and it can be represented as a two port network with the generator current entering into one port and the other port being connected to the infinite bus This is shown in Fig 4 2, where, $i_G$ represents the current through the line, $e_b$ represents the infinite bus voltage and $v_{CF}$ represents the voltage across the fixed capacitor $C_F$ It is assumed that machine output currents $i_D$ and $i_Q$ are equal to the network injection currents, i e , $i_{GD}$ and $i_{GQ}$ respectively

The TCSC model given in [21] is developed based on the representation of voltages

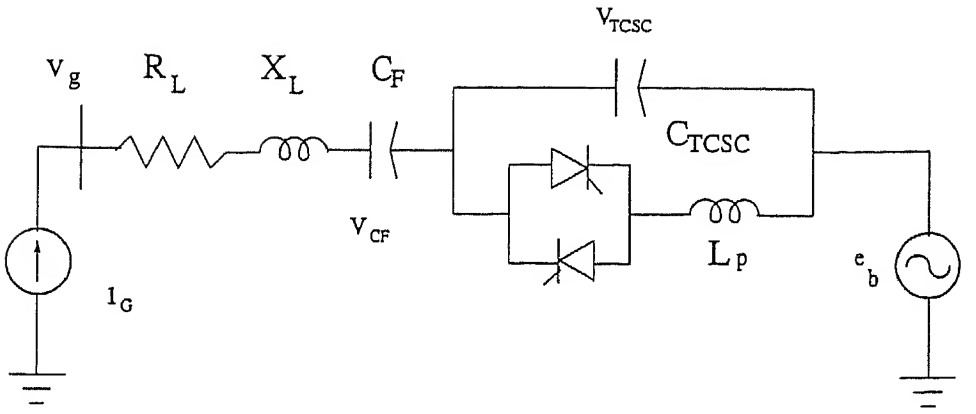


**Figure 4 2** AC Network

and currents as time varying Fourier series quantities and utilizing the short term Fourier coefficients The Fourier series is truncated to get the fundamental components of voltages and currents in a quasi static phasor representation The voltage and current phasors are used to describe TCSC dynamics with the assumption that line current is essentially sinusoidal The quasi steadv state model of the TCSC is mentioned below and the details are given in Appendix E

$$C_{TCSC}\, v_{TCSC} = i_G + \frac{v_{TCSC}}{X_{TCSCeff}(\sigma)}$$

where, $X_{TCSCeff}(\sigma)$ is the effective TCSC reactance and $\sigma$ is the conduction angle The conduction angle is related to firing angle by the relation $\sigma = \pi - 2\alpha$ The network dynamic equations are

$$C_F\, v_{CF} = i_G \tag{4 3}$$

$$C_{TCSC}\, v_{TCSC} = i_G + \frac{v_{TCSC}}{X_{TCSCeff}(\sigma)} \tag{4 4}$$

The network equations in $D-Q$ domain are given by

$$\begin{aligned}
v_{CFD} &= \frac{\imath_{GD}}{C_F} - \omega_B\, v_{CFQ} \\
v_{CFQ} &= \frac{\imath_{GQ}}{C_F} + \omega_B\, v_{CFD} \\
v_{TCSCD} &= \frac{\imath_{GD}}{C_{TCSC}} - \omega_B\, v_{TCSCQ} + \frac{v_{TCSCD}}{C_{TCSC}\, X_{TCSC}(\sigma)} \\
v_{TCSCQ} &= \frac{\imath_{GO}}{C_{TCSC}} + \omega_B\, v_{TCSCD} + \frac{v_{TCSCQ}}{C_{TCSC}\, X_{TCSC}(\sigma)}
\end{aligned}$$

These equations are linearized to get the following state space form

$$\Delta \mathbf{x}_N = [\mathbf{A}_N]\, \Delta \mathbf{x}_N + [\mathbf{B}_N]\, \Delta \mathbf{u}_N \tag{4 5}$$

where $\Delta \mathbf{x}_N = \left[\Delta v_{CFD}\ \Delta v_{CFQ}\ \Delta v_{TCSCD}\ \Delta v_{TCSCQ}\right]^T$ $\Delta \mathbf{u}_N = \left[\Delta \imath_{GD}\ \Delta \imath_{GQ}\ \Delta \sigma\ \Delta \imath_{GD}\ \Delta \imath_{GQ}\right]^T$
The generator terminal voltage is given by

$$v_g = e_b + \imath_{CF} + v_{TCSC} + R_L\, \imath_G + L_L\, \imath_G$$

The above equation is transformed into D Q reference frame as

$$v_{gD} = e_{bD} + v_{CFD} + \imath_{TCSCD} + R_L\, \imath_{GD} + L_L\, \imath_{GD} + \omega_B\, L_L\, \imath_{GQ}$$

$$v_{gQ} = e_{bQ} + v_{CFQ} + \imath_{TCSCQ} + R_L\, \imath_{GQ} + L_L\, \imath_{GQ} - \omega_B\, L_L\, \imath_{GD}$$

where $R_L$ and $L_L$ are the resistance and inductance of the transmission line respectively Linearizing the above equations and combining with eq (4 5) we can write the output equation in the following form

$$\Delta \mathbf{y}_N = [\mathbf{C}_N]\, \Delta \mathbf{x}_N + [\mathbf{D}_N]\, \Delta \mathbf{u}_N \tag{4 6}$$

where $\Delta \mathbf{y}_N = \left[\Delta v_{gD}\ \Delta v_{gQ}\ \Delta v_{TCSCD}\ \Delta v_{TCSCQ}\right]^T$ The matrices $[\mathbf{A}_N]$, $[\mathbf{B}_N]$ $[\mathbf{C}_N]$ and $[\mathbf{D}_N]$ are defined in Appendix E

### 4 1 2 TCSC Controller

The TCSC is represented as a variable capacitive reactance in series with the transmis sion line By changing the series compensation level using automatic controller (affected through the use of thyristors) the power flow through the line can be controlled to improve both steady state and transient stability and to damp out the oscillations The purpose of the controller is to maintain the TCSC reactance at the desired value specified by $\alpha$ the firing angle of thyristors The TCSC reactance remains constant in steadv state and is modulated during transient conditions in response to the control signal The objective of the control here is to maintain the machine angle constant Assuming that both infinite bus and generator voltage being regulated, this amounts to keeping the voltage across the line constant Let this voltage across the line be denoted by $V$, and the current flowing through the line by $I_G$, line inductive reactance by $X_L$ and fixed capacitive reactance by $X_{CF}$ we, thus, have the following requirement

$$|V| = |I_G(X_L - X_{CF}) - V_{TCSC}| = constant \equiv K_1 \tag{4 7}$$

In the above equation, the line resistance is neglected and the line current and the TCSC voltage are represented bv their rms values For the study system the increased power flow through the compensated line is associated with the increase in the current $I_G$ through the line In order to maintain the voltage drop $V$ across the line at a constant value the above equation implies that $X_{TCSC}$ should increase Thus, in this case, the series compensation must increase with the total power dispatch so that a higher power is transferred at a given angle This is called constant angle strategy

The TCSC control system is shown in Fig 4 3 [22] The TCSC voltage is passed through a gain $K_v = \frac{1}{X_L - X_{CF}}$ and is connected to line current reference junction The line current $i_G$ is monitored and compared to a desired reference current The algebr ic sum of the reference current, line current and the signal proportional to TCSC voltage is an error

signal that is fed to proportional integral (PI) controller The output of the PI controller is a signal equal to the change in conduction angle proportional to the desired change in TCSC reactance to maintain zero error input The TCSC controller equation is given by

$$x_1 = K_I K_v v_{TCSC} - K_I i_G + K_I I_{ref}$$

The TCSC voltage can be expressed by its $D - Q$ components as

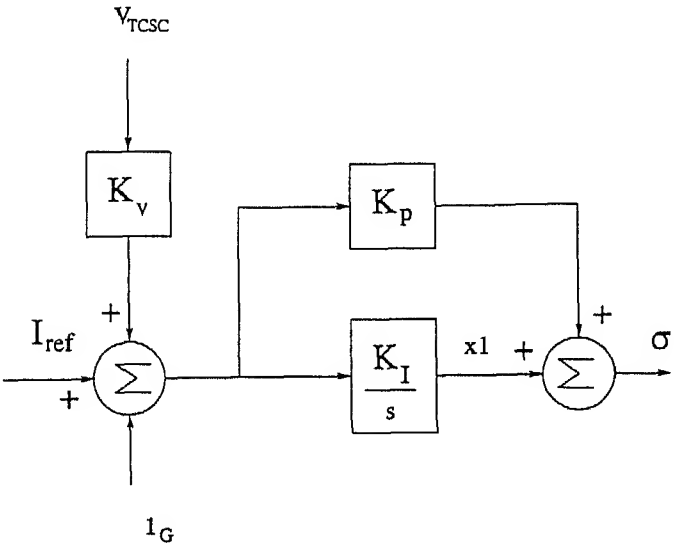


**Figure 4 3** TCSC Controller

$$v_{TCSC}^2 = v_{TCSCD}^2 + v_{TCSCQ}^2$$

Linearizing the above equation we get

$$(v_{TCSC0} + \Delta v_{TCSC})^2 = (v_{TCSCD0} + \Delta v_{TCSCD})^2 + (v_{TCSCQ0} + \Delta v_{TCSCQ})^2$$

neglecting the higher order terms we can write

$$\Delta v_{TCSC} = \frac{v_{TCSCD0}}{v_{TCSC0}} \Delta v_{TCSCD} + \frac{v_{TCSCQ0}}{v_{TCSC0}} \Delta v_{TCSCQ}$$

Similarly we can obtain the incremental relationship for line current The linearized equation for the line current is given by

$$\Delta i_G = \frac{i_{GD0}}{i_{G0}} \Delta i_{GD} + \frac{i_{GQ0}}{i_{G0}} \Delta i_{GQ}$$

Now we can write the linearized TCSC control system dynamic equations in the state space form as

$$\Delta \mathbf{x}_C = [\mathbf{A}_C] \Delta \mathbf{x}_C + [\mathbf{B}_C] \Delta \mathbf{u}_C \tag{4 8}$$

where,

$$[\ A_C\ ] = [0] \ \ and \ \ [\ B_C\ ] = \left[ \frac{K_I K\ v_{TCSCD}}{v_{TCSC0}} \quad \frac{K_I K\ v_{TCSCQ}}{v_{TCSC0}} \quad -\frac{K_I i_{GD}}{i_{G0}} \quad -\frac{K_I i_{GQ}}{i_{G0}} \right]$$

$\Delta \mathbf{x}_C = [\Delta x_1]$ and $\Delta \mathbf{u}_C = \left[\Delta v_{TCSCD}\ \Delta v_{TCSCQ}\ \Delta i_{GD}\ \Delta i_{GQ}\right]^T$ The output equation is given by

$$\Delta \mathbf{y}_C = [\mathbf{C}_C] \Delta \mathbf{x}_C + [\mathbf{D}_C] \Delta \mathbf{u}_C \tag{4 9}$$

where $\Delta \mathbf{y}_C = \Delta \sigma$ The matrices $[\mathbf{C}_C]$ and $[\mathbf{D}_C]$ are given by $[\mathbf{C}_C] = [1]$ and

$$[\ D_C\ ] = \left[ \frac{K_P K\ v_{TCSCD0}}{v_{TCSC0}} \quad \frac{K_P K\ v_{TCSCQ0}}{v_{TCSC0}} \quad -\frac{K_P i_{GD0}}{G0} \quad -\frac{K_P i_{GQ0}}{i_{G0}} \right]$$

### 4 1 3 Combined Generator - Network System Model

The overall system includes subsystems of generator, network and TCSC controller The interconnection pattern of these subsystems is shown in Fig 4 4 The generator system input quantities are obtained from the network output variables, and the network input quantities are obtained from the generator system output variables and the TCSC controller output variables The TCSC controller inputs are related to generator and network outputs These subsystems are interconnected as shown in Fig 4 4 to obtain overall system

model The state and output equations of the total system can be written in the following state space form

$$\Delta \mathbf{x} = [\mathbf{A}]\,\Delta \mathbf{x} + [\mathbf{B}]\,\Delta \mathbf{u} \tag{4 10}$$

$$\Delta \mathbf{y} = [\mathbf{C}]\,\Delta \mathbf{x} + [\mathbf{D}]\,\Delta \mathbf{u} \tag{4 11}$$

where $\Delta \mathbf{x} = \left[\Delta \mathbf{x}_G^T\ \Delta \mathbf{x}_N^T\ \Delta \mathbf{x}_C^T\right]^T$, $\Delta \mathbf{u} = \left[\Delta \mathbf{u}_G^T\ \Delta \mathbf{u}_N^T\ \Delta \mathbf{u}_C^T\right]^T$ $\Delta \mathbf{y} = \left[\Delta \mathbf{y}_G^T\ \Delta \mathbf{y}_N^T\ \Delta \mathbf{y}_C^T\right]^T$ and the matrices

$$[\ \mathrm{A}\ ] = \begin{bmatrix} \mathrm{A}_G & & \\ & \mathrm{A}_N & \\ & & \mathrm{A}_C \end{bmatrix} \quad [\ \mathrm{B}\ ] = \begin{bmatrix} \mathrm{B}_G & & \\ & \mathrm{B}_N & \\ & & \mathrm{B}_C \end{bmatrix}$$

$$[\ \mathrm{C}\ ] = \begin{bmatrix} \mathrm{C}_G & & \\ & \mathrm{C}_N & \\ & & \mathrm{C}_C \end{bmatrix} \textit{and} \ [\ \mathrm{D}\ ] = \begin{bmatrix} \mathrm{D}_G & & \\ & \mathrm{D}_N & \\ & & \mathrm{D}_C \end{bmatrix}$$

For the study system the input and output vectors of each subsystem are given by

$$\Delta \mathbf{u}_G = [\Delta v_{gD}\ \Delta v_{gQ}]^T \quad \Delta \mathbf{y}_G = \left[\Delta i_{GD}\ \Delta i_{GQ}\ \Delta i_{GD}\ \Delta i_{GQ}\ \right]^T,$$

$$\Delta \mathbf{u}_N = \left[\Delta i_{GD}\ \Delta i_{GQ}\ \Delta \sigma\ \Delta i_{GD}\ \Delta i_{GQ}\right]^T, \Delta \mathbf{y}_N = [\Delta v_{gD}\ \Delta v_{gQ}\ \Delta v_{ccD}\ \Delta v_{ccQ}]^T,$$

$$\Delta \mathbf{u}_C = [\Delta v_{ccD}\ \Delta v_{ccQ}\ \Delta i_{CD}\ \Delta i_{CQ}]^T \textit{ and } \Delta \mathbf{y}_C = \Delta \sigma$$

The input to each subsystem is related to the output variables of the other subsystems The equations for various subsystem inputs can be combined to give the overall system input vector The relationship between the overall system input vector and the output vector is expressed through interface matrix as

$$\Delta \mathbf{u} = [\mathbf{F}]\,\Delta \mathbf{y} \tag{4 12}$$

Now utilizing eq (4 12) and then combining eqs (4 10) and (4 11) with the interface matrix [F] we get the overall system model as

$$\Delta \mathbf{x} = \left[\mathbf{A} + \mathbf{BF}(\mathbf{I} - \mathbf{DF})^{-1}\mathbf{C}\right]\Delta \mathbf{x} = [\mathbf{A}_T]\,\Delta \mathbf{x} \tag{4 13}$$

The details of the [F] matrix are given in Appendix E

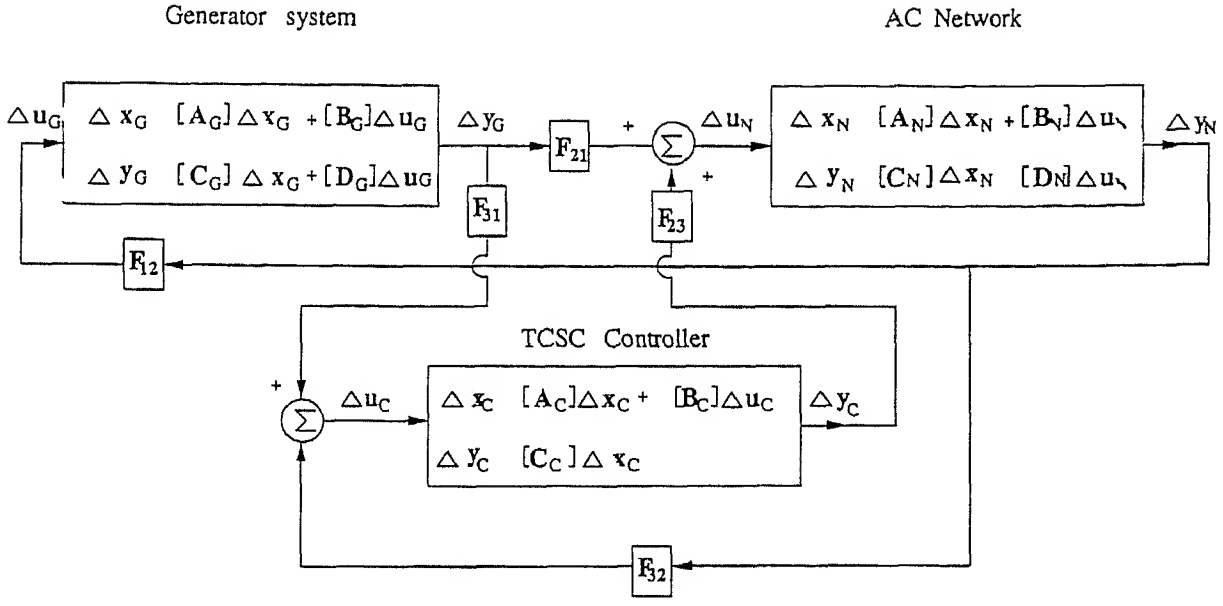


**Figure 4 4** Interconnection Diagram

## 4 2 Eigenvalue Analysis

The study of IEEE-FBM is carried out to examine the performance of the controller in damping SSR oscillations through real power modulation The study system configuration is shown in Fig 4 1 and the data is given in Appendix B The generator is delivering 0 9 per unit power to transmission system at 0 9 power factor lag The field voltage is assumed to be constant and governor action is not considered Self damping of 0 2 per unit and mutual damping of 0 3 per unit is added to the shaft [13] The target compensation of the line is assumed to be 70% (0 35 per unit) This is achieved through a fixed series compensation ($C_F$ as shown in Fig 4 2) which is assumed to be of 0 2546 per unit ( 72 74% of target compensation) and the b lance can be (0 0954 per unit) achieved through TCSC which has vernier control (enabled through a combination of fixed capacitor and a inductor

connected in series with anti parallel thyristors) The ratio of fixed capacitor reactance and inductor reactance of TCSC module is chosen as 4 [39]

The overall system eigenvalues are listed in Table 4 1 In this table two different sets of eigenvalues are given One with the entire compensation of 70 % being provided with the fixed capacitor and the other partly through fixed compensation and the balance through the TCSC as shown in Fig 4 2 The proportional gain $K_P = 0\,01$ and integral gain $K_I = 10$ are selected for the study It can be observed from the Table 4 1 that mode 2 is negatively damped for with entire fixed capacitance With the introduction of TCSC mode 2 is positively damped Thus TCSC contributes towards the damping of mode 2 There is slight improvement in the mode 3 damping The damping of mode 1 is increased, whereas the mode 0 damping is decreased The subsynchronous network mode frequency is increased, whereas the supersynchronous network mode frequency is decreased The damping of subsynchronous network mode is increased

**Table 4 1** Eigenvalues of TCSC with continuous time control

| With Fixed Capacitance | With TCSC Const Angle control ($K_P = 0\,01$ $K_I = 10$) | Comments |
|---|---|---|
| 4 41 ± j612 432 | 4 71 ± j497 92 | Supsyn Net Mode |
| 3 44 ± j141 11 | 3 29 ± j255 93 | Subsyn Net Mode |
| 1 38 ± j298 158 | 1 38 ± j298 16 | Mode 5 |
| 0 27 ± j203 03 | 0 27 ± j203 24 | Mode 4 |
| 0 8860 ± j159 11 | 0 92 ± j159 48 | Mode 3 |
| 0 03 ± j129 142 | 0 042 ± j128 88 | Mode 2 |
| 0 10 ± j98 64 | 0 151 ± j98 04 | Mode 1 |
| 0 431 ± j10 55 | 0 21 ± j7 58 | Mode 0 |
| | 0 ± j377 | |
| | 3 18 +j 0 010 | |
| | 0 04 + j 0 30 | |
| | 0 08 j 0 30 | |
| 3 91 | | |
| 0 19 | | |

The effect of controller gains on torsional modes is shown in Fig 4 5 From the Fig 4 5, it can be observed that the controller gain $K_I$ (with $K_P$ fixed at 0 01) has minimum influence on torsional mode damping, whereas, the network mode damping is significantly influenced by the gain The damping of the network mode is decreased with the increase in controller gain $K_I$ With $K_I$ fixed at 10, the variation in controller gain $K_P$ also has only minimal influence on the torsional modes However the network mode gets destabilized at a value of $K_P = 0\ 095$

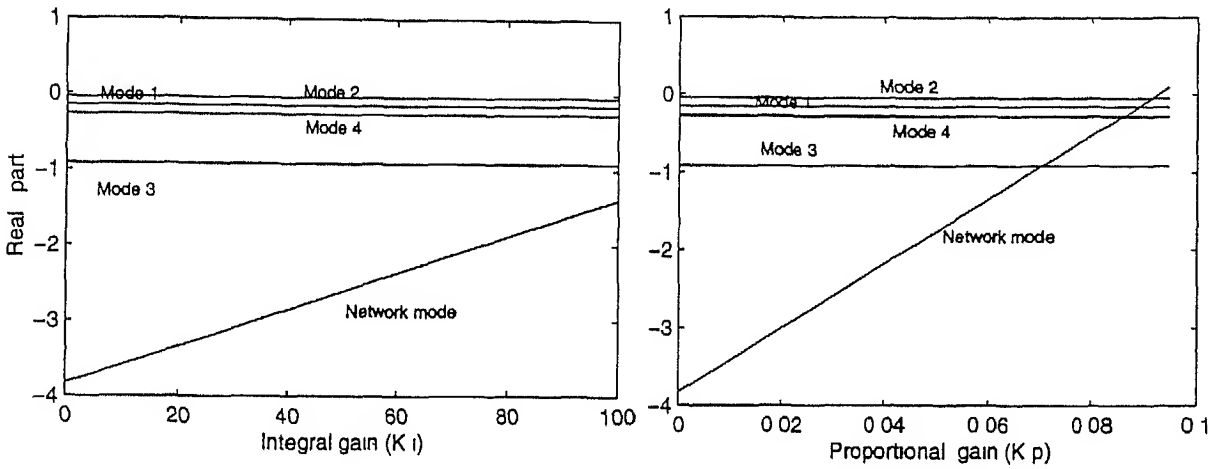


Figure 4 5 Variation of real part of system modes with Controller gains

The effect of variation in TCSC reactance, which leads to variation in power flow over the line, is shown in Table 4 2 with $K_I = 10$ and $K_P = 0\ 01$ The damping of the subsynchronous network mode is increased with the increase in the value of TCSC reactance, whereas, the damping of supersynchronous network mode is decreased Also the damping of the zeroth mode is increased with the increase in the TCSC reactance

From the eigenvalue analysis study, it can be observed that the TCSC with the constant angle control as suggested through the control of line voltage drop having more influence on the network mode damping This is due to the fact that the feedback signal considered

is the electrical system quantity and it is expected that it influences the electrical modes compared to the mechanical system modes [13]

Table 4 2 Eigenvalues for different TCSC reactances

| $X_{TCSC} = 0\ 0932p\ u$ P=0 8 p u | $X_{TCSC} = 0\ 0954p\ u$ P = 0 9 p u | $X_{TCSC} = 0\ 1004p\ u$ P=1 0 p u | Comments |
|---|---|---|---|
| 4 79 ± j497 94 | 4 71 ± j497 92 | 4 67± j497 89 | Supsyn Net Mode |
| 3 18 ± j255 85 | 3 29 ± j255 93 | 3 55± j255 99 | Subsyn Net Mode |
| 1 38 ± j298 168 | 1 38 ± j298 16 | 1 38± j298 16 | Mode 5 |
| 0 27 ± j203 24 | 0 27 ± j203 24 | 0 27± j203 23 | Mode 4 |
| 0 92 ± j159 47 | 0 92 ± j159 48 | 0 92 ± j 159 47 | Mode 3 |
| 0 042 ± j128 88 | 0 042 ± j128 88 | 0 042 ± j 128 88 | Mode 2 |
| 0 15 ± j98 04 | 0 151 ± j98 04 | 0 15 ± j 98 04 | Mode 1 |
| 0 201 ± j7 58 | 0 21 ± j7 58 | 0 23 ± j 7 58 | Mode 0 |
| 0± j377 | 0 ± j377 | 0 ± j377 | |

## 4 3 Time Domain Simulation

To validate the observations made through the results shown in Fig 4 5 that the controller gains have minimal influence on the torsional modes, a time domain simulation of the study system has been carried out for two different sets of controller parameters A disturbance of 0 1 per unit is applied at the HP turbine input for a period of 0 1 sec The variation in shaft torque and line power is shown in Figs 4 6 and 4 7 As expected the same real power flow on the line is achieved with two different sets of controller parameters The various shaft torques are almost identical with the two sets of controller parameters, thus,confirming the results shown in Fig 4 5

The performance of the TCSC with the constant angle control which is achieved by maintaining the voltage drop across the line considered, is further examined with the syste n subjected to a major disturbance The disturbance considered is a three phase to ground fault of 4 5 cycle duration at infinite bus end with a fault impedance of 0 04 per

unit The plots of the shaft torques are shown in Fig 4 8 It can be noticed from the Fig 4 8 that the response curves have decreasing amplitudes The same behavior can be observed from the generator real power response and the load angle response shown in Fig 4 9

The above results indicates that in the event of large disturbance the study system is stable with the TCSC and that the system behavior is not adversely affected by SSR From the response curves it can be observed that the peak values of Gen Exc torque LPB Gen torque and LPA-LPB torque are 0 315 per unit 2 25 per unit and 2 012 per unit respectively

## 4 4 Conclusions

In this chapter, the effect of TCSC on subsynchronous resonance phenomenon has been investigated The control of TCSC based on constant angle control strategy has been considered This control is achieved by maintaining the voltage drop across the line is constant It has been shown that the TCSC has a beneficial influence on the SSR response of the system while the TCSC controller parameters influence the network modes They have minimal influence on mechanical system modes The study results obtained through eigenvalue analysis are validated through detailed digital simulation

For the purpose of eigenvalue analysis the TCSC compensated study system has been modeled in the continuous time linearized domain and however, does not consider the discrete nature of TCSC operation The current trend seems to be exploring the possibility of application of digital control schemes for power transmission systems and this will be discussed in the next chapter

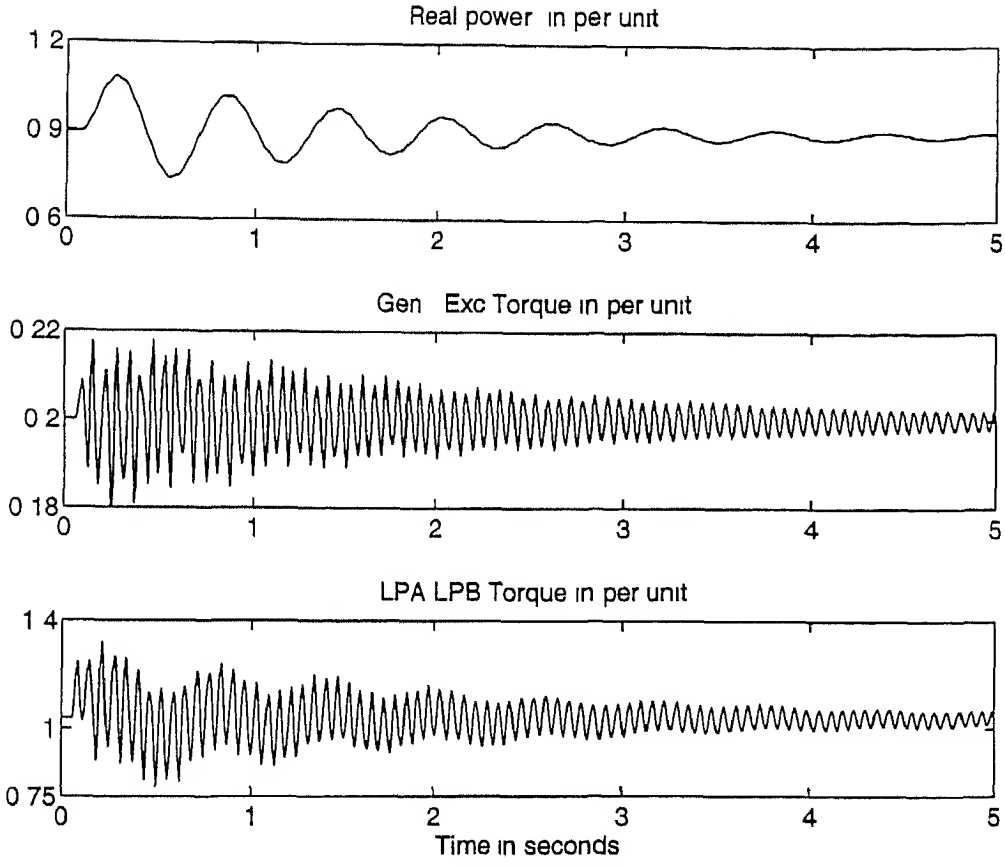


**Figure 4 6** System response with $K_I$ =20 and $K_P$=0 001

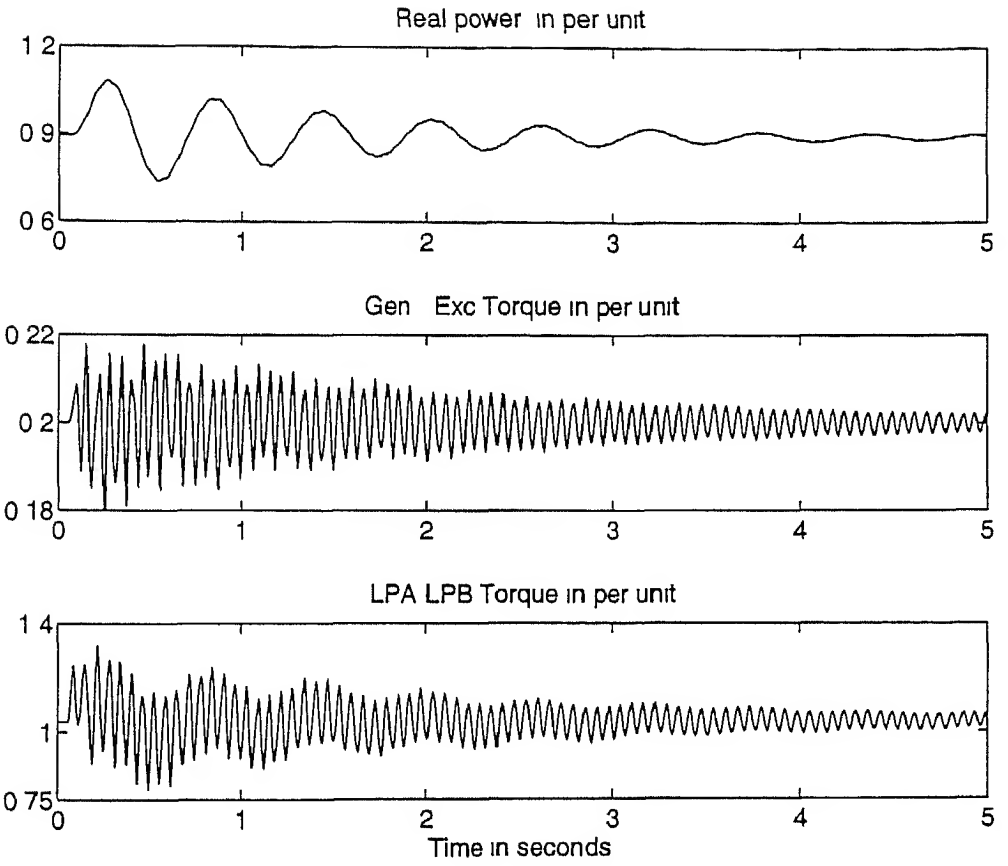


Figure 4 7 System response with $K_I$ =50 and $K_P$=0 067

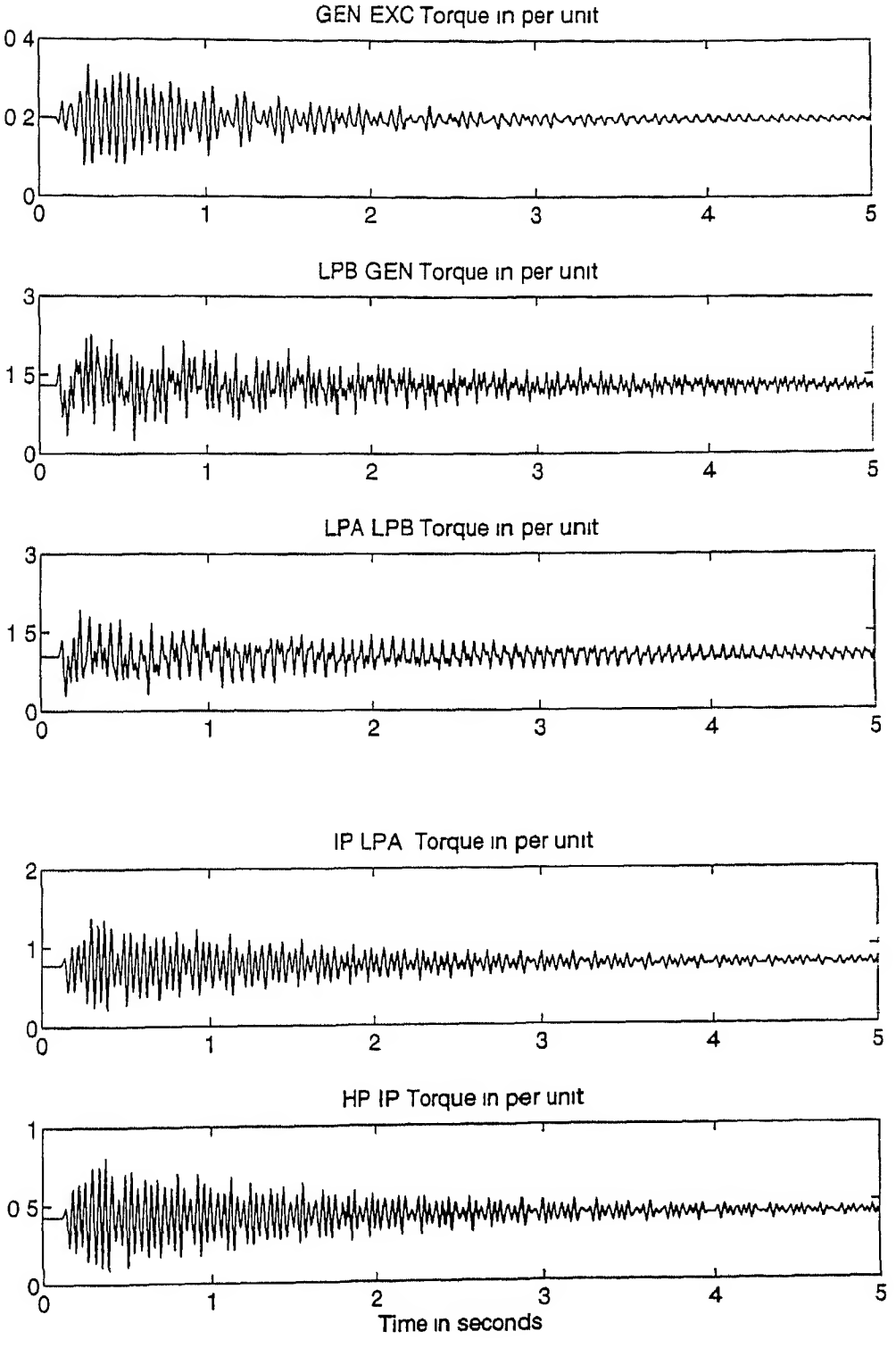


Figure 4 8 System response with Constant angle control based TCSC

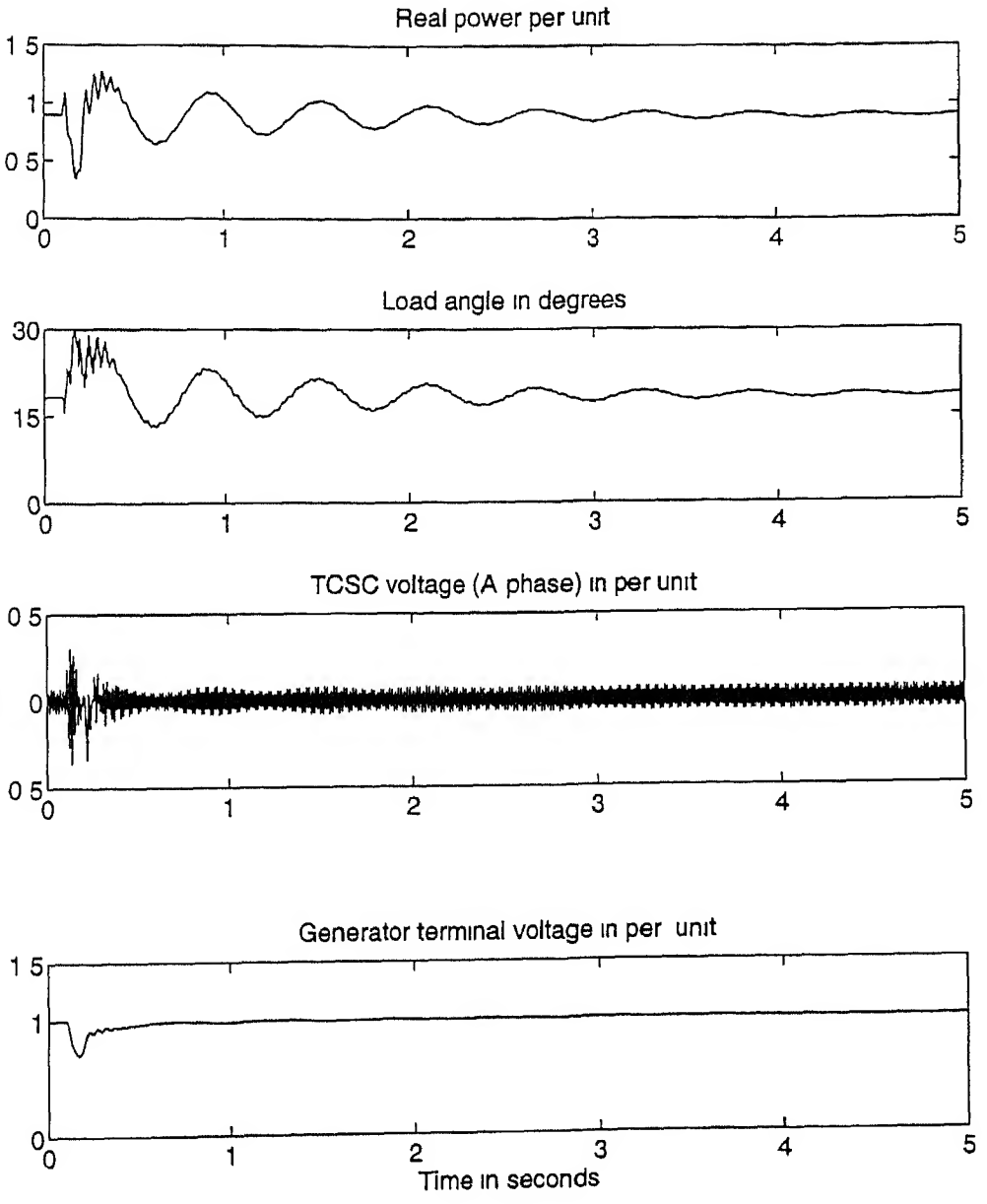


**Figure 4 9** System response with Constant angle control based TCSC

# Chapter 5

# SSR MITIGATION USING DIGITAL CONTROL OF TCSC

In the previous chapter, the efficacy of conventional TCSC control has been examined in damping SSR oscillations There has however been a trend to explore the suitability and use of digital control in controllable elements being employed in power transmission

In this chapter, a novel digital control scheme is proposed for TCSC Generally, in TCSC control the approach is to utilize a look up table in place of closed form transcendental expression to determine the firing angle for the desired TCSC reactance This is preferred as the solution of the closed form expression in real time is both computationally tedious and time consuming The look up table is generated off line for a given TCSC In this chapter use of an estimated characteristic of the TCSC is suggested to relate the TCSC reactance to the firing angle The estimated characteristic is incorporated in a $D-Q$ domain state space model of TCSC compensated transmission line The resulting nonlinear model is utilized to derive a linear discrete time domain state space model and the controller is designed using state feedback approach

The discrete time domain model of the TCSC compensated transmission line along with controller is converted into a continuous time domain model to interface with the synchronous machine model and obtain homogeneous state space equation Using the system model so derived, the eigenvalue analysis is carried out to observe the influence of

digital controller on torsional mode damping The results obtained through the eigenvalue analysis are validated with time domain simulation

## 5 1 Estimation of TCSC Characteristic

The TCSC consists of a capacitor in parallel with an inductor connected to a pair of anti parallel thyristors By varying the firing angle of the thyristors the inductor reactance is varied and which in turn changes the effective reactance of the TCSC Thus, we can represent the TCSC as a variable impedance device The TCSC is generally designed to operate in the capacitive region, while inductive mode operation can be used during the fault conditions In this section, the estimation of the TCSC characteristic in the capacitive operating region is described

Let us denote the TCSC capacitor reactance by $X_C$ the thyristor controlled inductor reactance by $X_P$ and the thyristor controlled reactor firing angle by $\alpha$ The overall TCSC reactance ($X_{TCSC}$) is given by [22]

$$X_{TCSC} = X_C - \eta_1(X_C + \eta_2) + \eta_4\eta_5 \tag{5 1}$$

where

$$\begin{aligned}
\eta_1 &= \frac{2(\pi - \alpha) + sin2(\pi - \alpha)}{\pi} \\
\eta_2 &= \frac{X_C X_P}{X_C - X_P} \\
\eta_3 &= \sqrt{\frac{X_C}{X_P}} \\
\eta_4 &= \eta_3 tan\{\eta_3(\pi - \alpha)\} - tan(\pi - \alpha) \\
\eta_5 &= \frac{4\eta_2^2 cos^2(\pi - \alpha)}{\pi X_P}
\end{aligned}$$

Th e variation in TCSC reactance with $\alpha$ is shown in Fig 5 1 This curve can now be

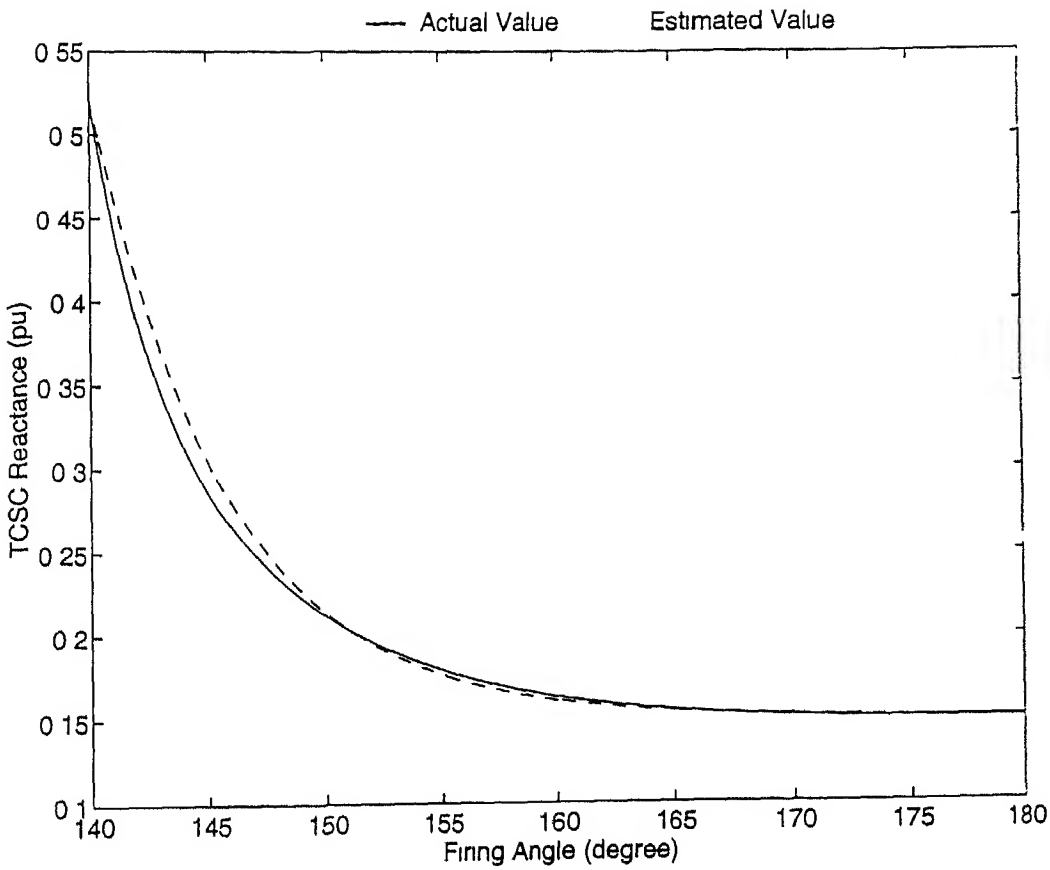


**Figure 5 1** The Actual and Estimated Characteristic of TCSC

approximated by an exponential function which is given by

$$X_{TCSC} = X_C + K_\beta \exp(-\frac{\alpha}{\alpha_c}) \qquad (5.2)$$

where

$$K_\beta = \frac{X_{TCSCmax} - X_C}{\beta},$$
$$\beta = \exp(-\frac{\alpha_{min}}{\alpha_c})$$

$X_{TCSCmax}$ is the maximum value of $X_{TCSC}$ $\alpha_{min}$ is the corresponding firing angle and $\alpha_c$ is called the $\alpha$ constant of this device The $\alpha$-constant is defined by the TCR firing angle $\alpha$ which is required to achieve the TCSC reactance of $X_C + 0.632(X_{TCSCmax} - X_C)$ Consequently, $\alpha_c$ is obtained as 0.632 The estimated curve is also shown in Fig. 5.1

## 5.2 TCSC Compensated Transmission Line Model

The system under study is shown in Fig. 5.2 This is essentially the IEEE FBM with a fixed series capacitor and a TCSC connected to it Let us denote the reactance of the fixed capacitor and TCSC respectively by $X_F$ and $X_{TCSC}$ The system equations are then written in the synchronously rotating $D-Q$ axis reference frame as

$$[\mathbf{x}] = [\mathbf{F}]\,\mathbf{x} + [\mathbf{G}]\,\mathbf{v} \qquad (5.3)$$

where the state vector $\mathbf{x}$ contains the $D-Q$ axes line currents and capacitor voltages i.e. $\mathbf{x}^T = [i_{LD}\ i_{LQ}\ v_{CD}\ v_{CQ}]$ and the vector $\mathbf{v}$ is given by $\mathbf{v}^T = [v_{gD} - v_{\infty D}\quad v_{gQ} - v_{\infty Q}]$ and the matrices [F] and [G] are given by

$$[\mathbf{F}] = \begin{bmatrix} -\frac{R}{L} & -\omega & -\frac{1}{L} & 0 \\ \omega & -\frac{R}{L} & 0 & -\frac{1}{L} \\ \frac{1}{C_F} + \frac{1}{C_{TCSC}} & 0 & 0 & -\omega \\ 0 & \frac{1}{C_F} + \frac{1}{C_{TCSC}} & \omega & 0 \end{bmatrix}, [\mathbf{G}] = \begin{bmatrix} \frac{1}{L} & 0 \\ 0 & \frac{1}{L} \\ 0 & 0 \\ 0 & 0 \end{bmatrix}$$

It is to be noted that $X_F = \frac{1}{\omega C_F}$, $X_{TCSC} = \frac{1}{\omega C_{TCSC}}$ and $L$ is the total inductance of the transmission line and the transformers Combining eqs (4.2) and (4.3) we get

$$\mathbf{x} = \mathbf{A}\mathbf{x} + \mathbf{B}\mathbf{v} + \mathbf{C}\mathbf{x}u \qquad (5.4)$$

where [B] = [G], $u = \exp(-\frac{\alpha}{\alpha})$ and the matrices [A], [B] and [C] are given by

$$[\mathrm{A}] = \begin{bmatrix} -\frac{R}{L} & -\omega & -\frac{1}{L} & 0 \\ \omega & -\frac{R}{L} & 0 & -\frac{1}{L} \\ \omega(X_F + X_{Cmin}) & 0 & 0 & -\omega \\ 0 & \omega(X_F + X_{Cmin}) & \omega & 0 \end{bmatrix}, [\mathrm{B}] = \begin{bmatrix} \frac{1}{L} & 0 \\ 0 & \frac{1}{L} \\ 0 & 0 \\ 0 & 0 \end{bmatrix},$$

$$[\mathrm{C}] = \begin{bmatrix} 0 & 0 & 0 & 0 \\ 0 & 0 & 0 & 0 \\ K_{beta}\omega & 0 & 0 & 0 \\ 0 & K_{beta}\omega & 0 & 0 \end{bmatrix}$$

Since $u$ is a scalar, the system eq (5 4) reduces to

$$\mathbf{x} = \left(\mathrm{A} + \mathrm{C}exp(-\frac{\alpha}{\alpha_c}\right)\mathbf{x} + \mathrm{B}\mathbf{v} \tag{5 5}$$

The matrix $\left[\mathrm{A} + \mathrm{C}\ exp(-\frac{\alpha}{\alpha})\right]$ has two pairs of eigenvalues It is observed from the root locus plot of the eigenvalues of the above matrix for various values of $\alpha$, that the real parts of the two pairs of eigenvalues are constant as $\alpha$ changes from $180^0$ to $140^0$ and one pair of eigenvalues moves towards the real axis while the other pair moves outwards [40]

### 5 2 1 Linearized Model of TCSC Compensated Transmission Line

The solution of eq (5 5) is given by

$$\begin{aligned} \mathbf{x}(t_f) &= \exp\{(\mathrm{A} + \mathrm{Cu})\triangle T\}\,\mathbf{x}(t_o) + \int_t^{t_f} \exp\{(\mathrm{A} + \mathrm{Cu})(t_f - \tau)\}\,\mathrm{B}\,\mathbf{v}(\tau)d\tau \\ &= \exp(\Gamma\triangle T)\,\mathbf{x}(t_o) + \int_{t_o}^{t_f} \exp\{\Gamma(t_f - \tau)\}\,\mathrm{B}\,\mathbf{v}(\tau)d\tau \end{aligned} \tag{5 6}$$

where $\Gamma = \mathrm{A} + \mathrm{C}\ exp\left(\frac{-\alpha_o}{\alpha_c}\right)$, $\triangle T = t_f - t_o$, and $t_0$ *and* $t_f$ are initial and final values of the sampling instants Equation (4 6) is nonlinear due to the presence of the term $u$ that is a function of the firing angle We now have to linearize eq (5 6) To do that we note that th independent variables are $\mathbf{x}(t_0)$, $\mathbf{v}$ and $\alpha$ Expanding eq (5 6) in Taylors series

around nominal values of $x_0$ $v_0$, $\alpha_0$ and neglecting the second and higher order terms we get

$$\begin{aligned} \Delta x(t_f) &= \frac{\partial x(t_f)}{\partial x(t_o)}\Delta x(t_o) + \frac{\partial x(t_f)}{\partial v}\Delta v(t_o) + \frac{\partial x(t_f)}{\partial \alpha}\Delta\alpha(t_o) \\ &= A\Delta x(t_o) + B\Delta v(t_o) + C\Delta\alpha(t_o) \end{aligned} \tag{5 7}$$

where $\Delta x$ $\Delta v$ and $\Delta\alpha$ denote the perturbations from the respective nominal values The derivation of the matrices A $\hat{B}$ and C are given below From the eq (5 6) we notice that the second term is independent of $x(t_o)$ Thus

$$\frac{\partial x(t_f)}{\partial x(t_o)} = A == \Delta A = \exp(\Gamma\Delta T)$$

Similarly the first term on the right hand side of eq (5 6) is independent of v Thus,

$$\frac{\partial x(t_f)}{\partial v} = \hat{B} = \int_o^{\Delta T} \exp\{\Gamma(\Delta T - \tau)\} B d\tau$$

Since $\Gamma$ is non singular, the above equation can be simplified as

$$B = \Delta B = \Gamma^{-1}(\Delta A - I)B$$

Now the matrix C is given by

$$C = \frac{\partial x(t_f)}{\partial \alpha}$$

C can be divided into two parts $C_1$ and $C_2$ such that $C = \Delta C = C_1 + C_2$ These two terms are given below

$$C_1 = \frac{\partial}{\partial \alpha}\left[\exp\left\{A + C\exp(-\frac{\alpha}{\alpha_c})\right\} x(t_o)\right] = -\frac{\Delta T}{\alpha_c}\Delta AC\exp(-\frac{\alpha_o}{\alpha_c})\, x_o$$

$$C_2 = \frac{\partial}{\partial \alpha}\int_o^{\Delta T} \exp\{A + Cu)(t_f - \tau)\} B\ v(\tau) d\tau$$

Assuming $v(t) = v_o, 0 \le t \le \Delta T$ and solving we get

$$C_2 = -\frac{\exp(-\frac{\alpha_o}{\alpha})}{\alpha_c}\Gamma^{-1}\left\{\Delta T\exp(\Gamma\Delta T) - \Gamma^{-1}\exp(\Gamma\Delta T) + \Gamma^{-1}\right\} C\ B\ v_o$$

It is assumed that the firing angle is generated based on the individual firing angle control such that $\alpha$ is updated six times in each cycle Now representing the eq (5 7) in discrete time domain as

$$\Delta \mathrm{x}(k+1) = \Delta \mathrm{A}\ \Delta \mathrm{x}(k) + \Delta \mathrm{B}\ \Delta \mathrm{v}(k) + \Delta \mathrm{C}\ \Delta \alpha(k) \tag{5 8}$$

It is to be noted that since the infinite bus voltage is assumed to be constant we can write $\Delta \mathrm{v}^T = [\Delta v_{gD}\ \Delta v_{gQ}]$

## 5 3 TCSC Control

The discrete time model of the system is used with a pole placement regulating control law of the form

$$\Delta \alpha(k) = -[\mathrm{K}]\ \Delta \mathrm{x}(k) \tag{5 9}$$

where [K] is a feed back gain matrix chosen using the pole shift control technique [41] In this method the open loop system poles are radially shifted to more stable locations in the closed loop Let the open loop characteristic equation of a discrete time system be given by

$$G_{OL}(z) = z^n + g_1 z^{n-1} + g_2 z^{n-2} + - - - g_{n-1} z + g_n$$

then in the pole shift control, the closed loop characteristic equation is specified by

$$G_{CL}(z) = z^n + g_1\ \lambda\ z^{n-1} + g_2\ \lambda^2\ z^{n-2} + - - - + g_{n-1}\ \lambda^{n-1}\ z + g_n\ \lambda^n$$

where $\lambda$ $(0 < \lambda < 1)$ is the pole shift factor It is to be noted that as $\lambda$ reduces, the penalty on the control also reduces

The TCSC control system block diagram is given in Fig 5 3 The three phase line currents and capacitor voltages are transformed in the $D - Q$ domain to obtain the vector x The vector x is compared with the nominal value $\mathrm{x}_o$ to obtain $\Delta \mathrm{x}$ The output $\Delta \alpha$

of the controller is added to the nominal value $\alpha_o$ to obtain TCSC firing angle Now the discrete time TCSC model incorporating the controller can be written as

$$\Delta \mathbf{x}(k+1) = (\Delta \mathbf{A} - \Delta \mathbf{CK})\, \Delta \mathbf{x}(k) + \Delta \mathbf{B}\, \Delta \mathbf{v}(k) \tag{5 10}$$

To interface the above discrete time model with the continuous time turbine generator

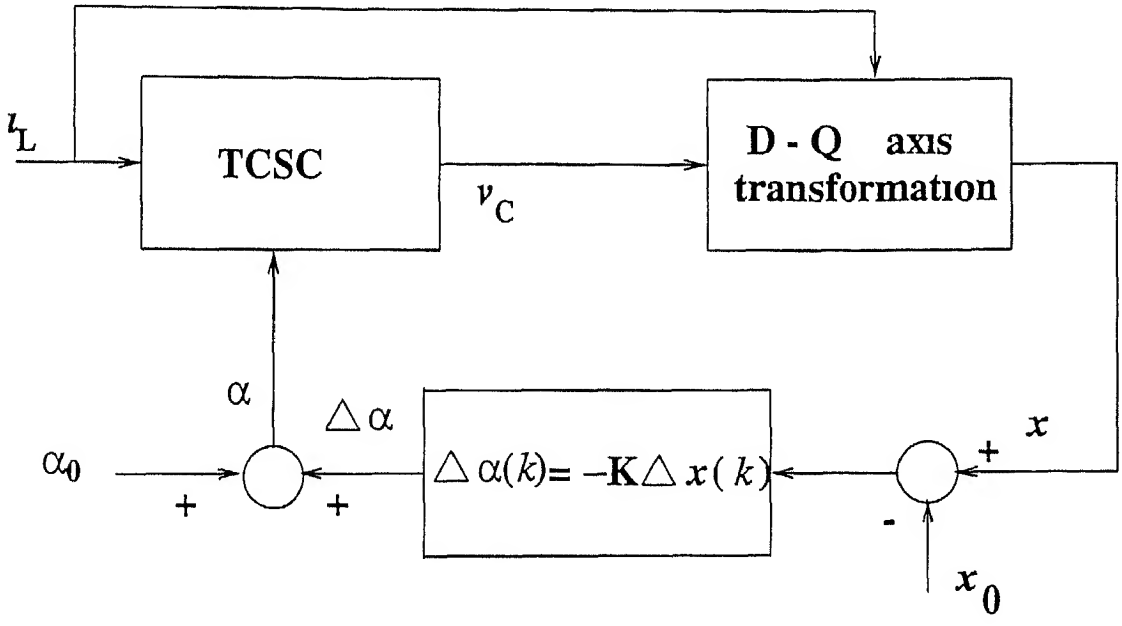


Figure 5 2 The schematic representation of TCSC control system

system model for eigenvalue analysis, we convert the above equation to continuous time and obtain the following equation

$$\Delta \mathbf{x} = \left[\mathbf{A}\right]\, \Delta \mathbf{x} + \left[\mathbf{B}\right]\, \Delta \mathbf{v} \tag{5 11}$$

where

$$\begin{bmatrix} \mathbf{A}' & \mathbf{B}' \\ \mathbf{0}_{24} & \mathbf{0}_{22} \end{bmatrix} = \frac{1}{\Delta T}\, log \begin{bmatrix} \Delta \mathbf{A} - \Delta \mathbf{C}\, \mathbf{K} & \Delta \mathbf{B} \\ \mathbf{0}_{24} & \mathbf{I}_{22} \end{bmatrix}$$

In the above equation $0_{i\,j}$ is a null matrix with $i$ rows and $j$ columns and $\mathrm{I}_{2\,2}$ is an identity matrix of order 2 It is to be noted that the sampling time $\triangle T$ defined before is used for the above transform

## 5 4 Combined Generator-Network System Model

The basic purpose of the generator network interface is to preserve the structure of the network given by eq (5 11), since this will allow us to check the validity of the state feedback controller vis a vis the stability of the system To facilitate such an interface we define a fictitious capacitor of value $c_n$ at the generator terminals The value of $c_n$ can be chosen to be arbitrarily small ($\lambda_c = 100$ per unit) as this is only used for interfacing The network equations then can be written from eq (5 11) as

$$\begin{aligned} \triangle \mathbf{x}_N &= [\mathbf{A}_N]\,\triangle \mathbf{x}_N + [\mathbf{B}_N]\,\triangle \mathbf{u}_N \\ \triangle \mathbf{y}_N &= [\mathbf{C}_N]\,\triangle \mathbf{x}_N \end{aligned} \tag{5 12}$$

where $\triangle \mathbf{x}_N = [\triangle i_{LD}\ \triangle i_{LQ}\ \triangle v_{CD}\ \triangle v_{CQ}\ \triangle v_{gD}\ \triangle v_{gQ}]^T$, $\triangle \mathbf{u}_N = [\triangle i_{GD}\ \triangle i_{GQ}]^T$ and $\triangle \mathbf{y}_N = [\triangle v_{gD}\ \triangle v_{gQ}]^T$ and the matrices are

$$[\mathbf{A}_N] = \begin{bmatrix} \mathbf{A} & \mathbf{B}' \\ 0 & \mathbf{A}_1 \end{bmatrix}$$

$$[\mathbf{A}_1] = \begin{bmatrix} -\frac{1}{c} & 0 & 0 & 0 & 0 & 0 \\ 0 & -\frac{1}{c_n} & 0 & 0 & 0 & 0 \end{bmatrix}$$

$$[\mathbf{B}_N] = \begin{bmatrix} 0 & 0 \\ 0 & 0 \\ 0 & 0 \\ 0 & 0 \\ \frac{1}{c_n} & 0 \\ 0 & \frac{1}{c_n} \end{bmatrix}$$

$$[\mathbf{C}_N] = \begin{bmatrix} 0 & 0 & 0 & 0 & 1 & 0 \\ 0 & 0 & 0 & 0 & 0 & 1 \end{bmatrix}$$

The state and output equations of generator system are mentioned in Chapter 2 (Section 2 1) and are reproduced here

$$\begin{aligned} \Delta \mathbf{x}_G &= [\mathbf{A}_G]\, \Delta \mathbf{x}_G + [\mathbf{B}_G]\, \Delta \mathbf{u}_G \\ \Delta \mathbf{y}_G &= [\mathbf{C}_G]\, \Delta \mathbf{x}_G \end{aligned} \tag{5 13}$$

where $\Delta \mathbf{x}_G^T = [\Delta x_{s1}^T \ \Delta x_m^T]$, $\Delta \mathbf{u}_G = [\Delta v_{gD} \ \Delta v_{gQ}]^T$, $\Delta \mathbf{y}_G = [\Delta i_D \ \Delta i_Q]^T$ $\Delta \mathbf{x}_{s1}$ is the state vector of stator and rotor variables and $\Delta \mathbf{x}_m$ is the state vector of mechanical system variables It is assumed that machine output currents $\Delta i_D$ and $\Delta i_Q$ are equal to the network injection currents i e , $\Delta i_{GD}$ and $\Delta i_{GQ}$ respectively It is to be mentioned here that the above output equation of the generator system is different to the one given in Chapter 2 (Section 2 1) Accordingly the dimension of the $[\mathbf{C}_G]$ matrix will change and also $[\mathbf{C}_G] = [\mathbf{C}_{G1}]$ The matrices $[\mathbf{A}_G]$, $[\mathbf{B}_G]$ and $[\mathbf{C}_{G1}]$ are defined in Chapter 2 We now combine eqs (4 12) and (4 13) to obtain the overall system model as

$$\Delta \mathbf{x} = [\mathbf{A}_T]\, \Delta \mathbf{x} \tag{5 14}$$

where $\Delta \mathbf{x}^T = [\Delta \mathbf{x}_G^T \ \Delta \mathbf{x}_N^T]$ and

$$[\ \mathbf{A}_T\ ] = \begin{bmatrix} \mathbf{A}_G & \\ & \mathbf{A}_N \end{bmatrix} + \begin{bmatrix} \mathbf{B}_G & \\ & \mathbf{B}_N \end{bmatrix} \begin{bmatrix} & \mathbf{C}_N \\ \mathbf{C}_G & \end{bmatrix}$$

## 5 5 Eigenvalue Analysis

The study of a IEEE-FBM is carried out to examine the performance of the proposed digital control in damping the SSR oscillations through real power modulation The study system configuration is shown in Fig 5 2 and the data is given in Appendix B The generator field voltage is assumed to be constant Series capacitive compensation is 70 9% of transmission line reactance Out of this 40% is in the form of fixed capacitive reactance $C_F$ and the rest is in the form of TCSC The generator is delivering 1 43 per unit power to

the infinite bus Self damping of 0 2 per unit and mutual damping of 0 3 per unit is added to the shaft to account for steam damping [13]

A pole shift controller is used for the state feedback control of eq (5 9) In this method the open loop system poles are radially shifted to more stable locations in the closed loop The pole shift factor value can be selected in the range between 0 and 1 As mentioned previously in Section 5 3, the control effort is less when the value of pole shift factor is close to 1 and the reduction in pole shift factor value increases the control effort The chosen value of pole shift factor must result in the stable system operation

System eigenvalues are listed in Table 5 1 for pole shift factors of 0 95 and 0 8 It is observed that the damping of supersynchronous and subsynchronous network modes are increased with the introduction of TCSC as compared to that obtained with fixed compensation For pole shift factor of 0 95, mode 1 and mode 2 are unstable All torsional modes are damped with a pole shift factor of 0 8 With the decrease of pole shift factor to 0 8, the mode 1 and mode 2 are damped but the damping of mode 0 is slightly reduced Also, the damping of supersynchronous and subsynchronous network modes is considerably increased The frequency of oscillation of subsynchronous network mode is increased with decrease of pole shift factor value from 0 95 to 0 8 The subsynchronous network mode for a pole shift factor of 0 8 has a time constant of 11 6 ms whereas without TCSC the value is around 0 5 sec This indicates fast damping of subsynchronous network mode

The requirements for SSR mitigation are either to increase mechanical damping, or reduce the electrical destabilization One of the major concerns of SSR control is the resonant response of the torsional system in the post fault state In the case of undischarged fixed capacitor, while returning to the post fault equilibrium state, it produces subsynchronous network currents and associated generated electromagnetic torque that may have frequ ncy components close to torsional frequency Even if the post fault state is stable, the effect of resonance causes very large shaft torques to build up The rapid discharge

Table 5 1 Eigenvalues of TCSC with digital control

| Fixed capacitance | Pole shift factor of 0 95 | Pole shift factor of 0 8 | Comments |
|---|---|---|---|
| 4 41 ± j612 432 | 22 79 ± j613 26 | 85 69 ± j612 13 | Supersyn Net Mode |
| 3 44 ± j141 11 | 22 10 ± j137 74 | 81 69 ± j145 74 | Subsyn Net Mode |
| 1 380 ± j298 15 | 1 380 ± j298 15 | 1 380 ± j298 15 | Mode 5 |
| 0 27 ± j203 03 | 0 244 ± j203 027 | 0 242 ± j203 10 | Mode 4 |
| 0 886 ± j1o9 11 | 0 787 ± j159 29 | 0 88 ± j159 43 | Mode 3 |
| 0 03 ± j129 142 | 0 079 ± j128 92 | 0 023 ± j128 875 | Mode 2 |
| 0 10 ± j98 64 | 0 088 ± j98 46 | 0 042 ± j98 04 | Mode 1 |
| 0 431 ± j10 oo | 0 3024 ± j9 938 | 0 2618± j8 16 | Mode 0 |
| | 2 93± j1798 95 | 4 67± j1797 64 | |
| | 3 57 ± j1378 81 | 2 93 ± j1378 47 | |
| 3 91 | 4 0 | 3 84 | |
| 0 19 | 0 11 | 0 058 | |

of capacitor energy by TCSC can eliminate subsynchronous currents quickly The time constant of subsynchronous network mode for a pole shift factor of 0 8 is less than one cycle This indicates that the subsynchronous currents are damped quickly Also the interaction between the torques produced by the subsynchronous currents and shaft torques is minimum

## 5 6 Time Domain Simulation

To observe the effectiveness of proposed TCSC controller, time domain simulation of the study system is carried out using PSCAD/EMTDC package version 3 0, by including the system non linearities The field voltage is assumed to be constant A 4 5 cycle, three phase to ground fault with 0 04 per unit fault impedance at the infinite bus is applied when the system is in steady state From the eigenvalue analysis, it can be observed that mode 1 and mode 2 are negatively damped for pole shift factor of 0 95 Fig 5 3 shows the shaft torques when TCSC is operating in feedback control mode with a pole shift factor of

0 95 It can be seen that the shaft torque oscillations are increasing These results are in agreement with the eigenvalue analysis results

The plots of the shaft torques with pole shift factor of 0 8 are shown in Fig 5 4 It can be observed from Fig 5 4 that with the introduction of TCSC all shaft modes are damped The settling time of LPA LPB torque is relatively large because of low damping The same observation is evident from the eigenvalues shown in Table 5 1 where the damping of mode 2 (which corresponds to LPA LPB torque) is poor The plots of generator real power and load angle are shown in Fig 5 5 for this stable case

## 5 7 Conclusions

A novel digital control scheme is proposed for TCSC control To study the performance of the control scheme a discrete time model of the TCSC has been developed and which is suitably interfaced with the generator system model The control is based on state feedback approach which utilizes capacitor voltage and current Eigenvalue analysis is carried out to examine the performance of the proposed digital control with TCSC in damping the SSR oscillations The variation in pole shift factor affects the damping of mode 1, mode 2 supersynchronous and subsynchronous network modes The TCSC contributes to the damping of network modes to a great extent, but at the same time it also reduces the damping of some of the stable torsional modes marginally The choice of pole shift factor, therefore, becomes critical Time domain simulations are carried out to study the transient torque case It is shown that the introduction of TCSC results in the stabilization of torsional modes with proper choice of pole shift factor

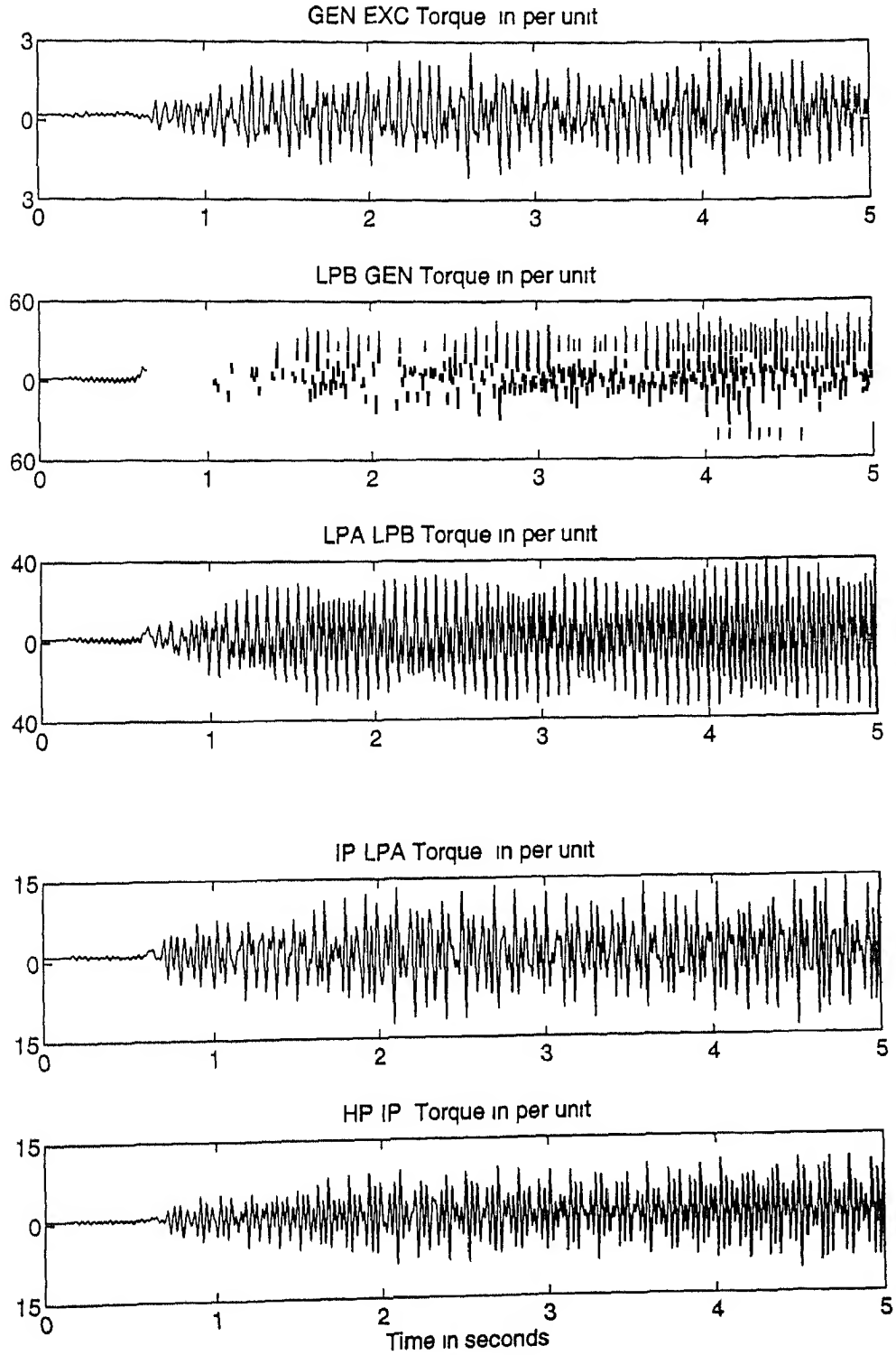


**Figure 5 3** System response with digital control based TCSC ( pole shift factor of 0 95)

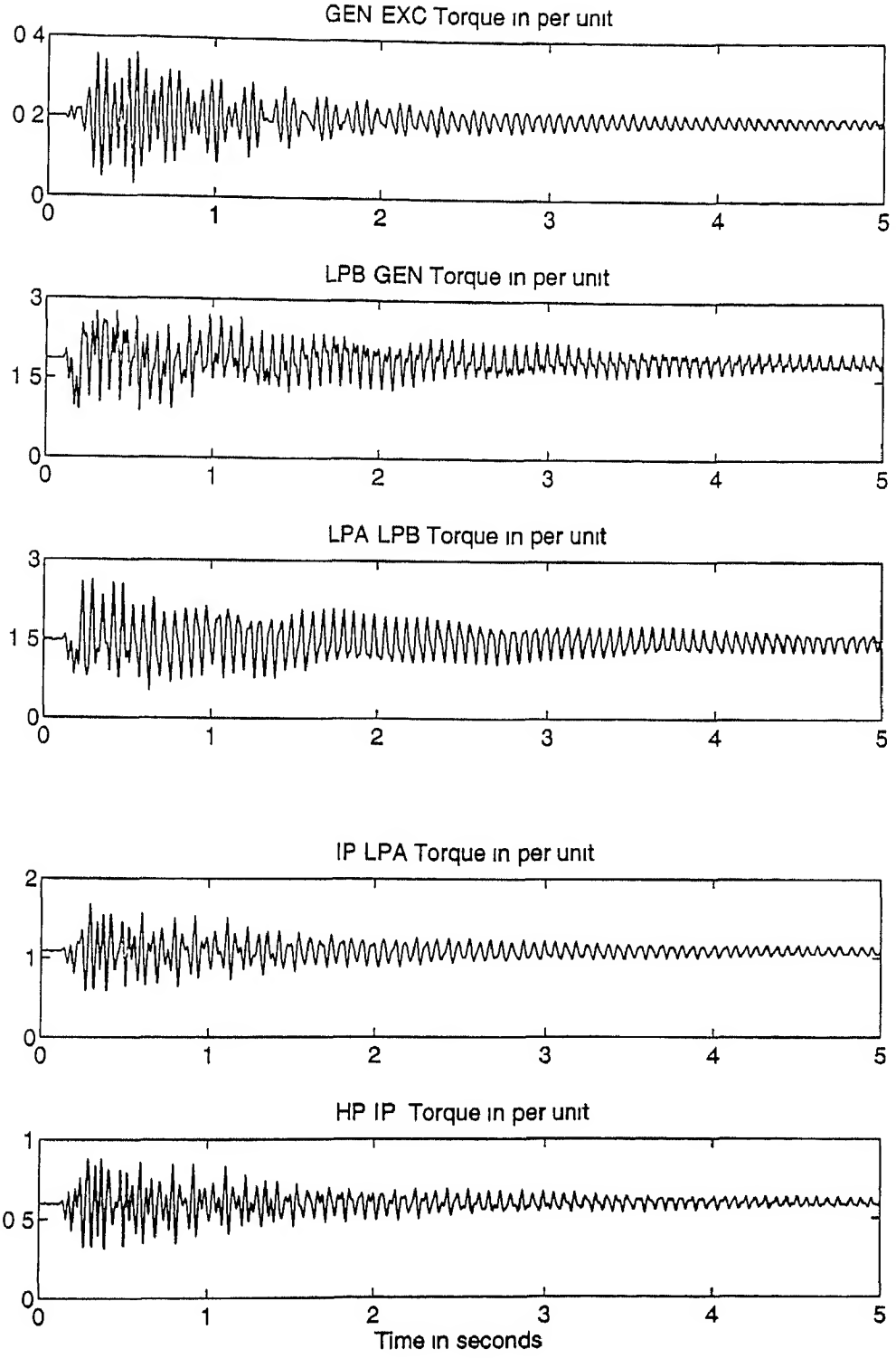


**Figure 5 4** System response with digital control based TCSC ( pole shift factor of 0 8)

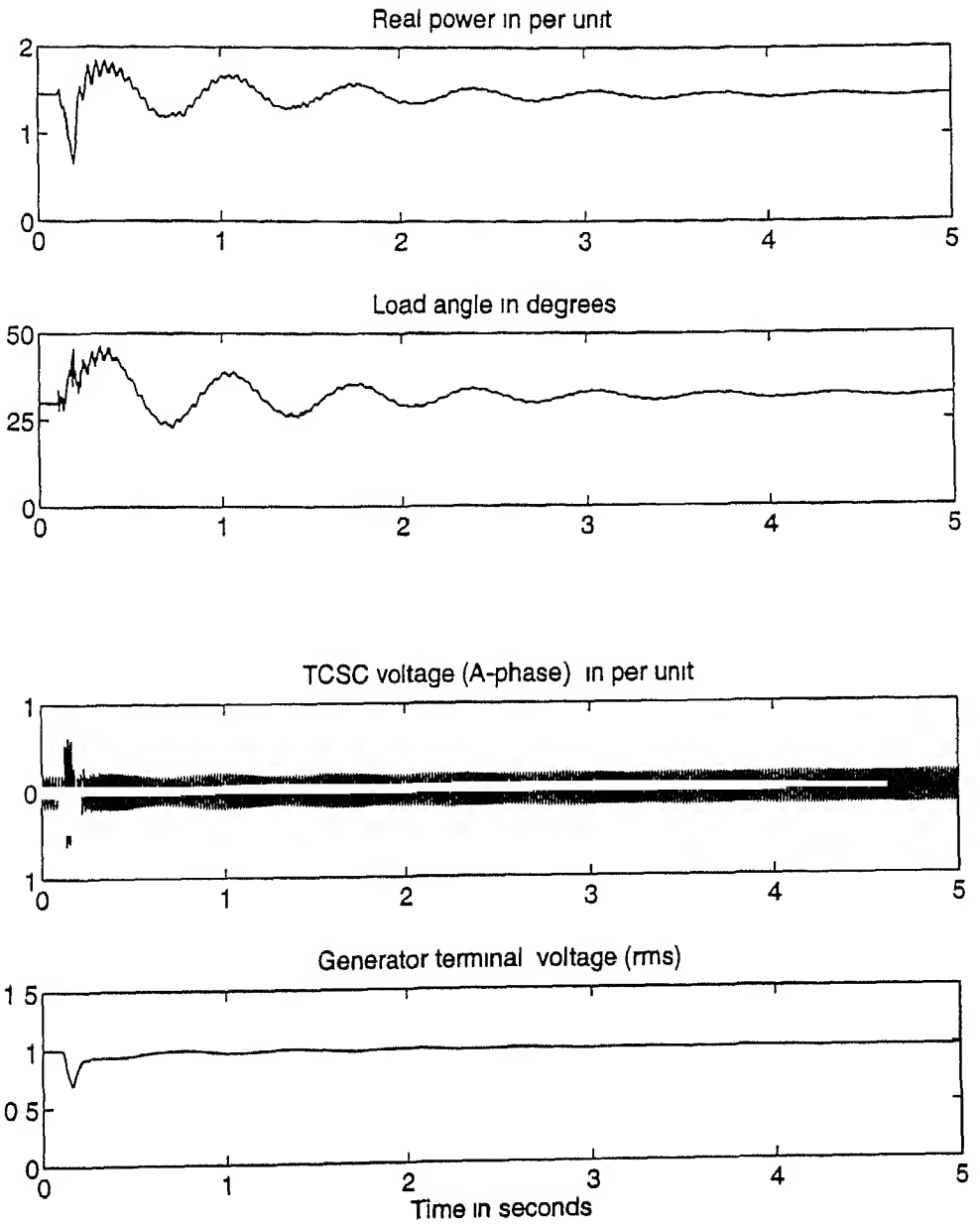


Figure 5 5 System response with digital control based TCSC ( pole shift factor of 0 8)

# Chapter 6

# TORSIONAL INTERACTION BETWEEN TCSC AND PSS

In the study presented in Chapters 4 and 5, the effect of excitation system and power system stabilizer is not considered The power system stabilizer (PSS) is generally used to damp the low frequency oscillations with generator speed as auxiliary signal The generator speed has the components of shaft modes and these components have significant effect on the performance of power system stabilizer When PSS is used with generator speed as supplementary signal there may be a possibility of it interacting with TCSC control in the range of torsional mode frequencies The control interaction study is, therefore, important to ensure proper design and coordination between various controllers

Power system stabilizers (PSS) can extend stability limits of systems that exhibit lightly damped oscillations in the low frequency (0 2 to 2 5 Hz) range This is accomplished via excitation control Torsional oscillations of turbine generators are inherently lightly damped There have been several instances of torsional mode instability due to interaction between generating unit excitation and nearby HVDC converter controls [42] In the previous chapters it has been shown that the TCSC with suitable control strategy provides positive damping to unstable torsional modes However, presence of PSS may influence this performance In this chapter, the extent and nature of control interaction between PSS and TCSC has been studied The TCSC considered to be equipped with the controllers as

described in Chapters 4 and 5

## 6 1 System Representation

As before, the study system considered is IEEE FBM For this system the various component models viz generator system model network model and TCSC model have been developed in the previous chapters These models are utilized here to develop the complete system model while suitably incorporating the excitation system and PSS

### 6 1 1 Excitation System and PSS Model

Consider a static exciter that includes a single time constant voltage regulator as shown in Fig 6 1 [4] In the block diagram of the exciter $v_g$ is the machine terminal voltage and $V_s$ is the output signal from auxiliary controllers such as PSS The excitation system dynamics can be written as

$$E_{FD} = -\frac{1}{T_R}E_{FD} + \frac{K_R}{T_R}(v_{ref} - v_g + v_s) \tag{6 1}$$

where $T_R$ is the exciter time constant Also $v_g$ is related to its $D$ and $Q$ axis components by

$$v_g = \sqrt{v_{gD}^2 + v_{gQ}^2} \tag{6 2}$$

Substituting eq (6 2) in eq (6 1) and linearizing we get

$$\triangle E_{FD} = -\frac{1}{T_R}\triangle E_{FD} + \frac{K_R}{T_R}\triangle v_s - \frac{K_R v_{gD0}}{T_R v_{g0}}\triangle v_{gD} - \frac{K_R v_{gQ0}}{T_R v_{g0}}\triangle v_{gQ} + \frac{K_R}{T_R}\triangle v_{ref} \tag{6 3}$$

The PSS consists of a washout circuit, lead/lag blocks and a limiter Its block diagram is shown in Fig 6 2 The input signal to the PSS is the generator slip For the sake of convenience in writing the state equations for PSS the block diagram of Fig 6 2 can be modified to the form shown in Fig 6 3 From this figure, it can be noticed that the

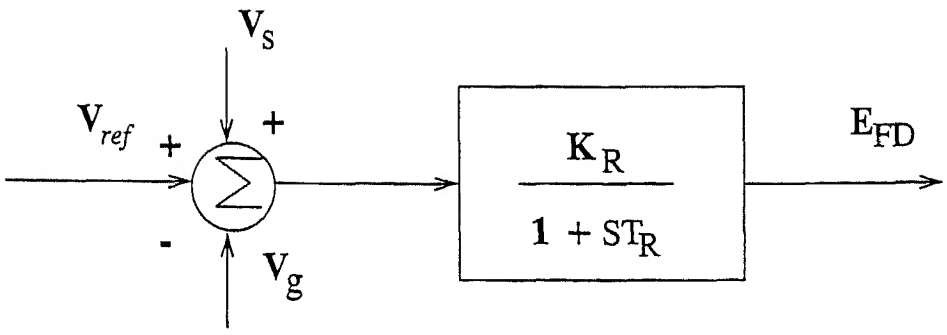


Figure 6 1 Static Exciter

system is having three poles and requires three state variables to describe its dynamics The following linearized state equations for the PSS can therefore be written as

$$\begin{aligned}
\Delta x_1 &= -C_1\Delta x_1 + C_4\Delta x_2 + K_s C_5\Delta x_3 + K_s C_5\Delta s_g \\
\Delta x_2 &= -C_1\Delta x_2 + K_s C_4\Delta x_3 + K_s C_4\Delta s_g \\
\Delta x_3 &= -\frac{1}{T_W}\Delta x_3 - \frac{1}{T_W}\Delta s_g \\
v_s &= x_1 + C_2 x_2 + K_s C_2^2 x_3 + K_s C_2^2 s_g
\end{aligned} \tag{6 4}$$

where $C_1 = \frac{1}{T_2}$ $C_2 = \frac{T_1}{T_2}$ $C_3 = 1 - \frac{T_1}{T_2}$, $C_4 = C_1 C_3$ $C_5 = C_1 C_2 C_3$ and $T_W$ is the washout time constant Combining eqs 6 3 and 6 4, we can write the following state space equation for the static exciter with PSS

$$\Delta \mathbf{x}_{e1} = [\mathbf{A}_{e1}]\,\Delta \mathbf{x}_{e1} + [\mathbf{B}_{e11}]\,\Delta \mathbf{u}_{e1} + [\mathbf{B}_{e12}]\,\Delta \mathbf{u}_G + [\mathbf{E}_{e1}]\,\Delta \mathbf{v}_{ref} \tag{6 5}$$

$$\Delta \mathbf{y}_{e1} = [\mathbf{C}_{e1}]\,\Delta \mathbf{x}_{e1} \tag{6 6}$$

where $\Delta \mathbf{x}_{e1} = [\Delta E_{FD}\ \ \Delta x_1\ \ \Delta x_2\ \ \Delta x_3]^T$, $\Delta \mathbf{u}_{e1} = \Delta s_g$ and $\Delta \mathbf{y}_{e1} = \Delta E_{FD}$ Since $\mathbf{v}_{ref}$ is assumed constant, $\Delta \mathbf{v}_{ref} = 0$ The matrices $[\mathbf{A}_{e1}]$, $[\mathbf{B}_{e11}]$, $[\mathbf{B}_{e12}]$, $[\mathbf{E}_{e1}]$ and $[\mathbf{C}_{e1}]$ are defined in Appendix F

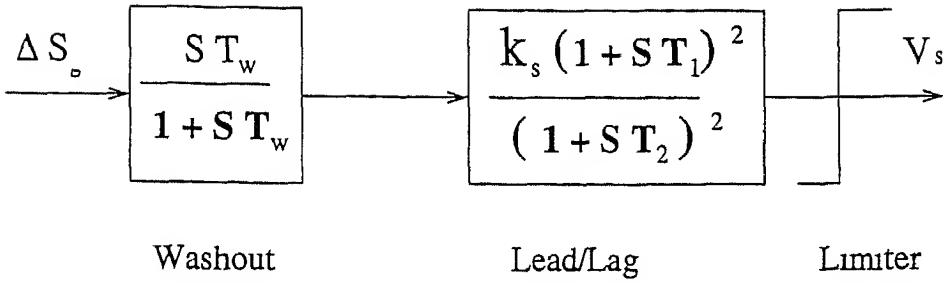


Figure 6 2 Block diagram of Power System Stabilizer

## 6 1 2 Complete Generator System Model with Excitation system

Defining state vector as $\mathbf{x}_G^T = [\mathbf{x}_{s1}^T \ \mathbf{x}_m^T \ \mathbf{x}_{e1}^T]$, and combining eqs (2 19) (6 5) and (6 6), we can write the following state space equation

$$\Delta \mathbf{x}_G = \begin{bmatrix} \mathbf{A}_{s1} & & \\ & \mathbf{A}_m & \\ & & \mathbf{A}_{e1} \end{bmatrix} \Delta \mathbf{x}_G + \begin{bmatrix} \mathbf{B}_{s11} \\ 0 \\ 0 \end{bmatrix} \Delta \mathbf{u}_{s11} + \begin{bmatrix} \mathbf{B}_{s12} \\ 0 \\ 0 \end{bmatrix} \Delta \mathbf{u}_{s12} + \begin{bmatrix} \mathbf{B}_{s13} \\ 0 \\ \mathbf{B}_{e12} \end{bmatrix} \Delta \mathbf{u}_G + \begin{bmatrix} 0 \\ \mathbf{B}_m \\ 0 \end{bmatrix} \Delta \mathbf{u}_m + \begin{bmatrix} 0 \\ 0 \\ \mathbf{B}_{e11} \end{bmatrix} \Delta \mathbf{u}_{e1} \tag{6 7}$$

Note that $\Delta \mathbf{u}_m = \Delta \mathrm{T}_e = \mathbf{C}_{me1} \Delta \mathbf{x}_{s1}$, $\Delta \mathbf{u}_{s11} = \Delta \mathbf{y}_m = \mathbf{C}_m \Delta \mathbf{x}_m$, $\Delta \mathbf{u}_{s12} = \Delta \mathbf{y}_{e1} = \mathbf{C}_{e1} \Delta \mathbf{x}_{e1}$, $\Delta \mathbf{u}_{e1} = \mathbf{C}_{m2} \Delta \mathbf{x}_m$ and $\mathbf{C}_{m2} = [0 \ 1]$ Hence we can rewrite the above equation as

$$\Delta \mathbf{x}_G = \begin{bmatrix} \mathbf{A}_{s1} & \mathbf{B}_{s11}\mathbf{C}_m & \mathbf{B}_{s12}\mathbf{C}_{e1} \\ \mathbf{B}_M \mathbf{C}_{me1} & \mathbf{A}_m & 0 \\ 0 & \mathbf{B}_{e11}\mathbf{C}_{m2} & \mathbf{A}_{e1} \end{bmatrix} \Delta \mathbf{x}_G + \begin{bmatrix} \mathbf{B}_{s13} \\ 0 \\ \mathbf{B}_{e12} \end{bmatrix} \Delta \mathbf{u}_G$$

$$= [\ \mathbf{A}_G\ ] \Delta \mathbf{x}_G + [\ \mathbf{B}_G\ ] \Delta \mathbf{u}_G \tag{6 8}$$

where $\Delta \mathbf{u}_G = [\Delta \upsilon_{gD} \ \ \Delta v_{gQ}]^T$ The output equation of the generator as defined in Chapter 2, is

$$\Delta \mathbf{y}_G = [\mathbf{C}_G] \Delta \mathbf{x}_G + [\mathbf{D}_G] \Delta \mathbf{u}_G \tag{6 9}$$

It may be noted that the dimensions of matrices $[\mathbf{C}_G]$ and $[\mathbf{D}_G]$ w ll get modified suitably in view of the inclusion of the excitation system and PSS model

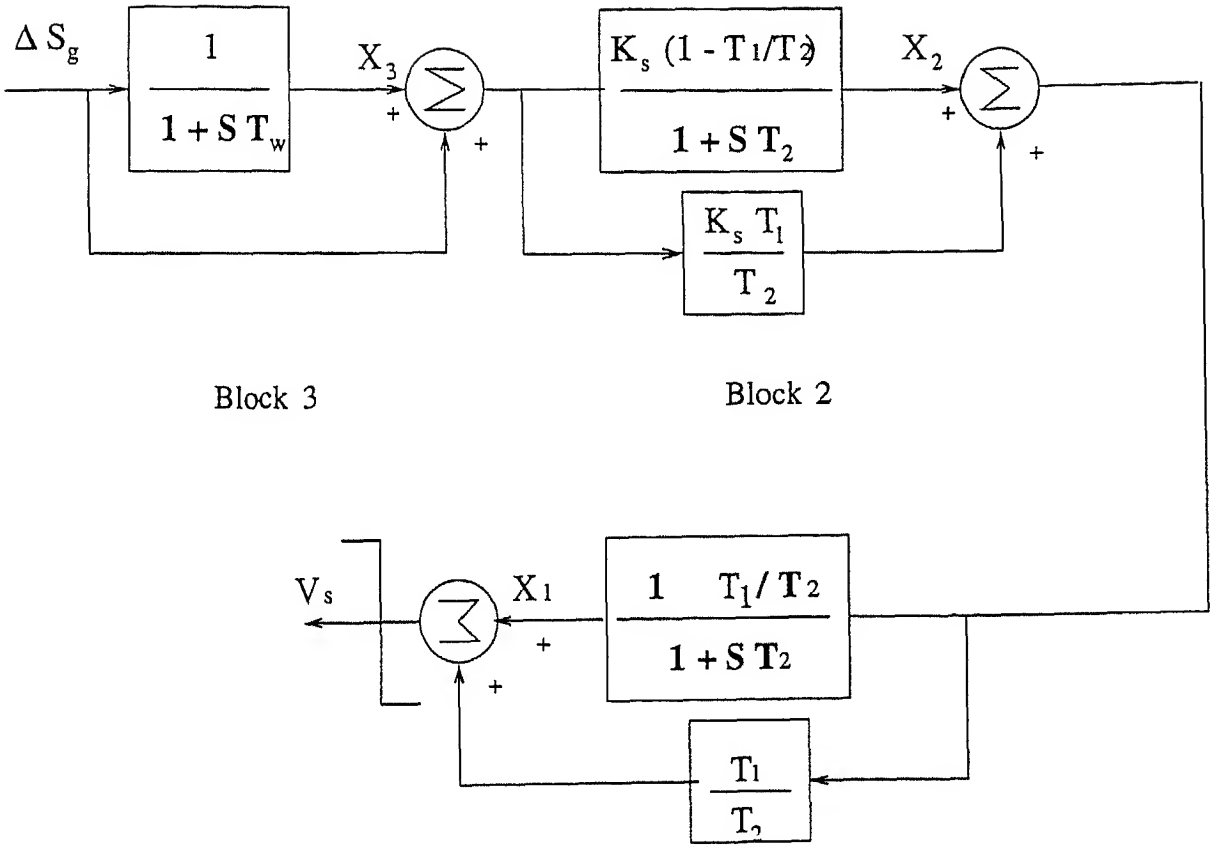


**Figure 6 3** Alternate method of PSS representation shown in Figure 6 2

## 6 2 Combined Generator - Network System Model

Constant angle control based TCSC

State space model of TCSC with constant angle control is derived in Chapter 4 (Section 4 1) This is reproduced below

$$\begin{aligned} \Delta \mathbf{x}_C &= [\mathbf{A}_C]\,\Delta \mathbf{x}_C + [\mathbf{B}_C]\,\Delta \mathbf{u}_C \\ \Delta \mathbf{y}_C &= [\mathbf{C}_C]\,\Delta \mathbf{x}_C \end{aligned}$$

where $\Delta \mathbf{x}_C = [\Delta x_1\ \Delta x_2]^T$, $\Delta \mathbf{u}_C = [\Delta v_{TCSCD}\ \Delta v_{TCSCQ}\ \Delta i_{GD}\ \Delta i_{GQ}]^T$ and $\Delta \mathbf{y}_C = \Delta \sigma$ The network model as derived in Chapter 4 is

$$\begin{aligned} \Delta \mathbf{x}_N &= [\mathbf{A}_N]\,\Delta \mathbf{x}_N + [\mathbf{B}_N]\,\Delta \mathbf{u}_N \\ \Delta \mathbf{y}_N &= [\mathbf{C}_N]\,\Delta \mathbf{x}_N + [\mathbf{D}_N]\,\Delta \mathbf{u}_N \end{aligned}$$

where

$\Delta \mathbf{x}_N = [\Delta v_{CFD}\ \Delta v_{CFQ}\ \Delta v_{TCSCD}\ \Delta v_{TCSCQ}]^T$, $\Delta \mathbf{u}_N = [\Delta i_{GD}\ \Delta i_{GQ}\ \Delta \sigma\ \Delta i_{GD}\ \Delta i_{GQ}]^T$

and $\Delta \mathbf{y}_N = [\Delta v_{gD}\ \Delta v_{gQ}\ \Delta v_{TCSCD}\ \Delta v_{TCSCQ}]^T$ Following the usual procedure network and TCSC system equations can be combined with eqs (6 8) and (6 9) to get the overall system model in the form $\Delta \mathbf{x} = [\mathbf{A}_T]\,\Delta \mathbf{x}$

Digital Control based TCSC

The network incorporating the model of TCSC based on digital control strategy has been derived in Chapter 5 (Section 5 4) For the sake of completeness the network model is given below

$$\begin{aligned} \Delta \mathbf{x}_N &= [\mathbf{A}_N]\,\Delta \mathbf{x}_N + [\mathbf{B}_N]\,\Delta \mathbf{u}_N \\ \Delta \mathbf{y}_N &= [\mathbf{C}_N]\,\Delta \mathbf{x}_N \end{aligned}$$

where

$$\Delta \mathbf{x}_N = [\Delta i_{LD}\ \Delta i_{LQ}\ \Delta v_{CD}\ \Delta v_{CQ}\ \Delta v_{gD}\ \Delta v_{gQ}]^T$$

$$\Delta \mathbf{u}_N = [\Delta i_{GD}\ \Delta i_{GQ}]^T \text{ and } \Delta \mathbf{y}_N = [\Delta v_{gD}\ \Delta v_{gQ}]^T$$

Following the usual procedure the network equations can be combined with eqs (6 8) and (6 9) to get the overall system model in the form $\Delta \mathbf{x} = [\mathbf{A}_T]\,\Delta \mathbf{x}$

It may be noted that the overall system matrix $[\mathbf{A}_T]$ used above has the same structure as the matrix $[\mathbf{A}_T]$ given in Chapters 4 and 5 except that its component matrix $[\mathbf{A}_G]$ now gets modified as per eqn (6 8) to consider inclusion of excitation system and PSS

## 6 3 Case Studies

To investigate the effect of excitation system (Automatic Voltage Regulator (AVR) and PSS), the following three situations are considered with the study system augmented to include

(1) Fixed series compensation

(2) Constant angle control based TCSC

(3) Digital control based TCSC

The study system is essentially the IEEE FBM The study is carried out using eigenvalue analysis The excitation system and PSS data is given in Appendix F and the FBM data is given in Appendix B

### 6 3 1 Fixed Series Compensation

Before proceeding with the analysis of the effect of AVR and PSS with TCSC controls, it would be beneficial to first examine the generator excitation controls with fixed series compensation Considering fixed series compensation in the study system the following three scenarios are examined

(i) without AVR and PSS

(ii) with AVR and without PSS

(iii) with AVR and PSS

The eigenvalue analysis result for these cases is given in Table 6 1 In the present study the stabilizer gain is chosen as $K_s = 3$

There are five pairs of torsional modes which are important from the view point of stabilizer application one pair of each supersynchronous network mode and subsynchronous network mode and one pair of zeroth mode The sixth mode identified as exciter mode primarily associated with field voltage and exist only in the presence of speed stabilization This mode is usually well damped like network modes

From the eigenvalue analysis results given in Table 6 1 it can be seen that mode 2 is unstable without AVR and PSS (case i ) This mode becomes stable when the AVR is introduced (case ii) However in this case the zeroth mode is destabilized The speed signal is the obvious choice for PSS to damp the zeroth mode Further introduction of PSS (case iii) stabilizes this mode, while modes 1 and 2 become unstable Thus, the PSS has adverse effect on torsional mode damping while contributing to the damping of zeroth mode Furthermore, the damping of modes 3 and 4 is reduced The speed signal is inherently sensitive to the presence of torsional oscillations and this is leading to negative damping of some of the torsional modes

From the results it is clear that the PSS has significant effect on torsional mode stability It is to be mentioned here that at lower values of PSS gain (i e $K_s < 1$) the torsional modes are not destabilized, but the damping of zeroth mode is poor The primary objective of the PSS is, however, to damp the zeroth mode Destabilization of torsional modes due to PSS is also observed in [43], but in case of an uncompensated transmission system

### 6 3 2 Constant angle control based TCSC

The effect of the stabilizer on torsional modes in the presence of TCSC control is analyzed The integral gain $K_I$ and proportional gain $K_P$ of TCSC controller are set at values of 10 and 0 01 respectively, and PSS gain is varied The results are given in Table 6 2 It can

Table 6 1 System eigenvalues with fixed series compensation

| Without AVR and PSS | With AVR and without PSS | With AVR and PSS | comments |
|---|---|---|---|
| 4 42± j612 43 | 4 4 ± j612 47 | 4 406 ± j612 47 | Supersyn Net Mode |
| 3 45± j141 11 | 2 72 ± j141 64 | 2 76 ± j141 63 | Subsyn Net Mode |
| 1 38 ± j298 16 | 2 04 ± j298 16 | 1 98 ± j298 16 | Mode 5 |
| 0 28 ± j203 03 | 0 27 ± j203 03 | 0 2 ± j203 03 | Mode 4 |
| 0 89 ± j159 12 | 0 99 ± j159 11 | 0 062 ± j1o9 12 | Mode 3 |
| 0 03 ± j129 14 | 0 019 ± j129 13 | 0 02 ± j129 12 | Mode 2 |
| 0 11 ± j98 651 | 0 28 ± j98 60 | 0 08 ± j98 60 | Mode 1 |
| 0 43 ± j10 56 | 0 05 ± j10 96 | 0 043 ± j10 62 | Mode 0 |
| | 23 35± j19 03 | 23 15±j18 95 | Exciter mode |
| 3 91 | 2 847 | 32 99 | |
| 0 20 | | 20 6 | |
| | | 0 87 | |
| | | 0 1 | |

**Table 6 2** System Eigenvalues with Constant angle Control based TCSC

| PSS gain $K_s$=2 | PSS gain $K_s$=4 | PSS gain $K_s$=10 | comments |
|---|---|---|---|
| 4 857 ± j497 878 | 4 8563 ± j497 878 | 4 853 ± j497 88 | Supsvn Net Mode |
| 3 301 ± j2oo 95 | 3 379 ± j255 95 | 3 409 ± j255 91 | Subsyn Net Mode |
| 1 38 ± j298 158 | 1 38 ± j298 158 | 1 38 ± j298 158 | Mode 5 |
| 0 24 ± j203 26 | 0 22 ± j203 274 | 0 164 ± j203 304 | Mode 4 |
| 0 90 ± j1o9 49 | 0 88 ± j1o9 503 | 0 83 ± j159 525 | Mode 3 |
| 0 03 ± j128 892 | 0 0254 ± j128 90 | 0 003 ± j128 91 | Mode 2 |
| 0 0795 ± j98 149 | 0 005 ± j98 20 | 0 26 ± j98 38 | Mode 1 |
| 0 316 ± j9 467 | 1 133 ± j9 79 | 4 66 ± j10 91 | Mode 0 |
| 21 62± j21 44 | 20 71± j20 75 | 17 33±j16 85 | Exciter mode |
| 0 ± j377 | 0 ± j377 | 0 ± j377 | |
| 2 8 +j 0 000 | 2 8 +j 0 00 | 2 75 +j 0 0 | |
| 0 005 + j 0 00 | 0 005 + j 0 0 | 0 005 + j 0 0 | |
| 0 10 j 0 0 | 0 1 j 0 0 | 0 1 j 0 0 | |

be seen hat with an increase in PSS gain, the damping of modes 1 and 2 decreases For a PSS g in $K_s = 4$, mode 1 has positive real part, indicating small signal instability while

both modes 1 and 2 become unstable for PSS gain of 10 Also, the damping of mode 3 and mode 4 is decreased with the increase of PSS gain These modes however remains stable The damping of the zeroth mode increases with stabilizer gain At a PSS gain value of 2 all torsional modes are stable It can be noted that with fixed series compensation the PSS has greater detrimental effect on the damping of modes 3 and 4 as compared to the present case In the presence of TCSC, PSS has detrimental effect on modes 1 and 2, but this effect is more pronounced at higher PSS gains

### 6.3.3 Digital Control based TCSC

The primary objective of the TCSC is to provide damping to torsional modes From the eigenvalue analysis results presented in Chapter 5, it is observed that the study system is stable for a pole shift factor of 0 8 Here the effect of PSS on torsional modes is examined by varying PSS gains while keeping the pole shift factor at a value of 0 8 The results are given in Table 6 3 It can be seen that with an increase in PSS gain, the damping of modes 1 and 2 decreases For a PSS gain $K_s = 2$, mode 1 has positive real part, indicating small signal instability while both modes 1 and 2 become unstable for PSS gain of 4 Furthermore, the damping of mode 3 and mode 4 is decreased with the increase of PSS gain These modes however remains stable On the positive side, the damping of the zeroth mode increases with stabilizer gain At a PSS gain value of 0 5 all torsional modes are stable, but the damping of mode 1 and mode 2 is poor

### 6.3.4 Discussion

From the case studies presented in the previous sections the following general observations can be made

1. The PSS has greater positive influence on zeroth mode(power swing mode) in the presence of TCSC as compared to the fixed series compensated system. This is

**Table 6.3:** System Eigenvalues with Digital Control based TCSC

| PSS gain $K_s = 0.5$ | PSS gain $K_s = 2$ | PSS gain $K_s = 4$ | comments |
|---|---|---|---|
| -85.65± j612.37 | -85.65± j612.37 | -85.64± j612.38 | Supersyn Net Mode |
| -80.624± j145.32 | -80.68± j145.36 | -80.75± j145.41 | Subsyn Net Mode |
| -1.38 ± j298.15 | -1.38 ± j298.15 | -1.38 ± j298.15 | Mode 5 |
| -0.241 ± j203.12 | -0.225 ± j203.11 | -0.20± j203.11 | Mode 4 |
| -0.8798 ± j159.44 | -0.861 ± j159.44 | -0.83 ± j159.43 | Mode 3 |
| -0.023 ± j128.80 | -0.011 ± j128.88 | 0.005 ± j128.88 | Mode 2 |
| -0.039 ± j98.08 | 0.063 ± j98.13 | 0.1994 ± j98.21 | Mode 1 |
| -0.0044 ± j9.06 | -0.8 ± j9.466 | -2.0 ± j10.06 | Mode 0 |
| -23.41 ± j19.55 | -22.47± j18.82 | -21.16±j17.73 | Exciter mode |
| -3.79 ±j1798.19 | -3.79 ±j1798.19 | -3.79 ±j11798.19 | |
| -2.22 ±j1377.30 | -2.2 ±j1377.3 | -2.2 ±j1377.3 | |
| -33.64 | -36.36 | -38.88 | |
| -29.064 | -26.88 | -24.83 | |
| -2.844 | -2.78 | -2.7 | |
| -0.1 | -0.1 | -0.1 | |

expected, as the basic function of the PSS is to damp the zeroth mode

2 In the presence of TCSC, PSS has detrimental effect primarily on some torsional modes ( mode 1 and mode 2), but this effect is prominent at higher values of PSS gains

To circumvent the detrimental impact of PSS on torsional modes, it is possible to use [4] torsional filter in the speed signal loop of PSS This aspect is examined in the next section.

## 6.4 Excitation System with PSS and Torsional filter

In this section the mathematical model of synchronous machine with excitation system, PSS and torsional filter is developed The schematic diagram of PSS with torsional filter is shown in Fig 6.4 The output of the PSS is denoted by $V_{s1}$ From this figure, it can be noticed that the torsional filter has two poles requiring two state variables to describe

its dynamics and three state variables are associated with PSS as mentioned before The state space equations for the static exciter have been given earlier in Section 6 1 The state

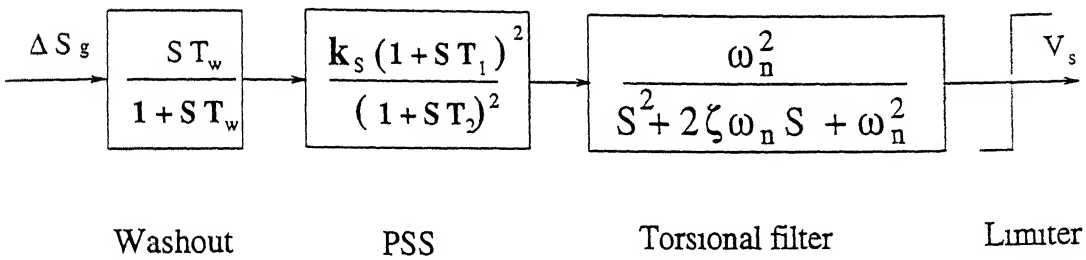


**Figure 6.4:** Power System Stabilizer

space equations for PSS with torsional filter are given by

$$\begin{aligned}
\dot{x}_1 &= x_2 \\
\dot{x}_2 &= -\omega_n^2 x_1 - 2\zeta\omega_n x_2 + \omega_n^2 v_{s1} \\
\dot{x}_3 &= -C_1 x_3 + C_4 x_4 + K_s C_5 x_5 + K_s C_5 s_g \\
\dot{x}_4 &= -C_1 x_4 + K_s C_4 x_5 + K_s C_4 s_g \\
\dot{x}_5 &= -\frac{1}{T_W} x_5 - \frac{1}{T_W} s_g \\
v_s &= x_1 \omega_n^2 \\
v_{s1} &= x_3 + C_2 x_4 + K_s C_2^2 x_5 + K_s C_2^2 s_g
\end{aligned} \tag{6 10}$$

where $C_1 = \frac{1}{T_2}$, $C_2 = \frac{T_1}{T_2}$, $C_3 = 1 - \frac{T_1}{T_2}$, $C_4 = C_1 C_3$, $C_5 = C_1 C_2 C_3$. In the above equations the state variables $x_1$ and $x_2$ are associated with torsional filter and $x_3$, $x_4$ and $x_5$ are associated with PSS and washout circuit

Now we linearize the above set of equations and combine with eq. (6 3) to get the following state space model of the excitation system that includes PSS and torsional filter

$$\Delta\dot{\mathbf{x}}_{e1} = [\mathbf{A}_{e1}]\,\Delta\mathbf{x}_{e1} + [\mathbf{B}_{e11}]\,\Delta\mathbf{u}_{e1} + [\mathbf{B}_{e12}]\,\Delta\mathbf{u}_G + [\mathbf{E}_{e1}]\,\Delta\mathbf{V}_{ref} \tag{6 11}$$

$$\Delta \mathbf{y}_{e1} = [\mathbf{C}_{e1}]\,\Delta \mathbf{x}_{e1} \tag{6 12}$$

where $\Delta \mathbf{x}_{e1} = [\Delta E_{FD}\ \Delta x_1\ \Delta x_2\ \Delta x_3\ \Delta x_4\ \Delta x_5]^T$, $\Delta \mathbf{u}_{e1} = \Delta s_g$ and $\Delta \mathbf{y}_{e1} = \Delta E_{FD}$ The matrices $[\mathbf{A}_{e1}]$, $[\mathbf{B}_{e11}]$, $[\mathbf{B}_{e12}]$, $[\mathbf{C}_{e1}]$ and $[\mathbf{E}_{e1}]$ are defined in Appendix F Since $\mathbf{v}_{ref}$ is assumed constant $\Delta \mathbf{v}_{ref} = 0$ Following the procedure given Section 6 1 we can write the state space equation for the combined generator system as

$$\begin{aligned} \Delta \mathbf{x}_G &= [\mathbf{A}_G]\,\Delta \mathbf{x}_G + [\mathbf{B}_G]\,\Delta \mathbf{u}_G \\ \Delta \mathbf{y}_G &= [\mathbf{C}_G]\,\Delta \mathbf{x}_G + [\mathbf{D}_G]\,\Delta \mathbf{u}_G \end{aligned} \tag{6 13}$$

where $\Delta \mathbf{x}_G = [\Delta x_{s1}\ \ \Delta x_m\ \ \Delta x_{e1}]^T$, and $\Delta \mathbf{u}_G = [\Delta v_{gD}\ \ \Delta v_{gQ}]^T$ Equation (6 13) can now be used to derive the complete system model as described in Section 6.1 considering both the constant angle control based TCSC and the digital control based TCSC

## 6.5 System Study

The overall system model as derived above is used to investigate the effect of torsional filter in the performance of PSS Two configurations of the study system are considered One with constant angle control based TCSC and the other with digital control based TCSC The excitation system and PSS data is given in Appendix F and the FBM data is given in Appendix B

### 6.5.1 System with Constant angle control based TCSC

From the analysis presented in the previous section, it is observed that the PSS is destabilizing some of the stable torsional modes in the presence of TCSC control The system eigenvalues with variation in torsional filter parameters ($\omega_n$ *and* $\zeta$) are given in Tables 6 4 and 6.5. Only torsional modes are given in the table. It can be noticed from the results that all the torsional modes are stable In this study the PSS gain is selected as 10 However, for this gain value mode 1 and mode 2 were unstable without torsional filter. This

shows that as expected, the filter makes the torsional modes insensitive to the speed signal stabilization

The study is carried out to further examine the effect of filter parameters on the system performance The analysis considered the effect of variation of filter parameters ($\omega_n$ *and* $\zeta$) Initially $\zeta$ is fixed at 0 5 and $\omega_n$ is varied For this three values of $\omega_n$ are considered varying $\omega_n$ The results are given in Table 6 4 It can be observed from the results that the damping order of torsional modes is same for different values of $\omega_n$ Variation of $\omega_n$ has a significant effect on zeroth mode and torsional filter mode damping However, its influence on the exciter mode damping is minimum Table 6 5 gives the results of variation of $\zeta$ with $\omega_n$ fixed at 7 rad/sec. Similar behavior can be found in this situation also The variation of $\zeta$ has significant influence on zeroth mode and torsional filter mode and its influence on exciter mode is small

**Table 6.4:** System eigenvalues for different values of $\omega_n$

| $\omega_n$ = 2 rad/sec | $\omega_n$ = 7 rad/sec | $\omega_n$ = 13 rad/sec | comments |
|---|---|---|---|
| -1 38 ± j298 16 | -1 38 ± j298 16 | -1 38 ± j298.16 | Mode 5 |
| -0 24 ± j202.82 | -0 24 ± j202 82 | -0 24 ± j202 82 | Mode 4 |
| -0 89 ± j159 67 | -0 89 ± j159 67 | -0 89 ± j159 67 | Mode 3 |
| -0 03 ± j128 93 | -0 03 ± j128 93 | -0 03 ± j128 93 | Mode 2 |
| -0 08 ± j98 26 | -0 08 ± j98 149 | -0 08 ± j98 36 | Mode 1 |
| 0 01 ± j9 94 | -2.14 ± j9 18 | -3 55 ± j10 38 | Mode 0 |
| -21.04 ± j20.78 | -22 32± j20.73 | -23 29±j20 46 | Exciter mode |
| -1.14 ±j1.61 | -2 29 ±j5 25 | 0 12 ±j7 18 | Torsional filter mode |

### 6.5.2 System with Digital Control based TCSC

The PSS gain value 4 is selected for the study For this value of gain mode 1 and mode 2 were unstable without torsional filter The study is carried out following the procedure mentioned in the previous case The results are given in Tables 6 6 and 6.7. From the results it can be observed that in this case also the torsional filter is preventing the PSS to

Table 6.5. System eigenvalues for different values of $\zeta$

| $\zeta = 0.1$ | $\zeta = 0.5$ | $\zeta = 0.8$ | comments |
|---|---|---|---|
| -1.38 ± j298.16 | -1.38 ± j298.16 | -1.38 ± j298.16 | Mode 5 |
| -0.24 ± j202.82 | -0.24 ± j202.82 | -0.24 ± j202.82 | Mode 4 |
| -0.89 ± j159.67 | -0.89 ± j159.67 | -0.89 ± j159.67 | Mode 3 |
| -0.03 ± j128.93 | -0.03 ± j128.93 | -0.03 ± j128.93 | Mode 2 |
| -0.08 ± j98.26 | -0.08 ± j98.149 | -0.08 ± j98.36 | Mode 1 |
| -1.51 ± j10.94 | -2.14 ± j9.18 | 0.055 ± j9.08 | Mode 0 |
| -22.84 ± j20.78 | -22.32± j20.73 | -22.29±j20.86 | Exciter mode |
| 0.57 ±j4.1 | -2.29 ±j5.25 | -2.59 ±j5.2 | Torsional filter mode |

interact with the torsional modes. The analysis also considered the effect of variation of filter parameters. From the results it can be noticed that the variation of filter parameters are affecting the zeroth mode and torsional filter mode and have minimum influence on the exciter mode.

Table 6.6: System eigenvalues for different values of $\omega_n$

| $\omega_n = 1$ rad/sec | $\omega_n = 5$ rad/sec | $\omega_n = 10$ rad/sec | comments |
|---|---|---|---|
| -85.65± j612.37 | -85.65± j612.37 | -85.64± j612.37 | Supersyn. Net Mode |
| -80.60± j145.31 | -80.60± j145.31 | -80.60± j145.31 | Subsyn. Net Mode |
| -1.38 ± j298.15 | -1.38 ± j298.15 | -1.38 ± j298.15 | Mode 5 |
| -0.247 ± j203.12 | -0.247 ± j203.12 | -0.247± j203.12 | Mode 4 |
| -0.88 ± j159.44 | -0.88 ± j159.44 | -0.88 ± j159.44 | Mode 3 |
| -0.027 ± j128.87 | -0.027 ± j128.87 | -0.027 ± j128.87 | Mode 2 |
| -0.07 ± j98.06 | -0.07 ± j98.06 | -0.07 ± j98.06 | Mode 1 |
| 0.23 ± j8.93 | -0.00002 ± j8.955 | -3.66 ± j10.23 | Mode 0 |
| -23.72 ± j19.78 | -23.78± j19.80 | -23.96±j19.87 | Exciter mode |
| -0.38 ± j0.92 | -1.69 ± j4.65 | 0.11 ± j8.131 | Torsional filter mode |

## 6.6 Conclusions

In this chapter, the linearized formulation of IEEE first benchmark model with TCSC, AVR and PSS for the study of control interactions is presented. Both constant angle control

Table 6.7. System eigenvalues for different values of $\zeta$

| $\zeta = 0\,1$ | $\zeta = 0\,4$ | $\zeta = 0\,9$ | comments |
|---|---|---|---|
| -85 65± j612 37 | -85 65± j612 37 | -85 65± j612 37 | Supersyn Net Mode |
| -80 60± j145 31 | -80 60± j145 31 | -80 60± j145 31 | Subsyn Net Mode |
| -1 38 ± j298 15 | -1 38 ± j298 15 | -1 38 ± j298 15 | Mode 5 |
| -0 247 ± j203 12 | -0 247 ± j203 12 | -0 247± j203 12 | Mode 4 |
| -0 88 ± j159 44 | -0 88 ± j159 44 | -0 88 ± j159 44 | Mode 3 |
| -0 027 ± j128 87 | -0 027 ± j128 87 | -0 027 ± j128 87 | Mode 2 |
| -0 07 ± j98 06 | -0 07 ± j98 06 | -0 07 ± j98 06 | Mode 1 |
| -1 061 ± j10 45 | -3 1 ± j9 26 | 0 031 ± j8 63 | Mode 0 |
| -23 88 ± j19 86 | -23 91± j19 85 | -23 98±j19 79 | Exciter mode |
| 0 55 ± j7 56 | -0 08 ± j8 14 | -7 77 ± j5 024 | Torsional filter mode |

based TCSC and digital control based TCSC have been considered It can be observed from the study, that in the case of fixed series compensation, the AVR is damping torsional mode 2, while at the same time it is undamping the zeroth mode The introduction of PSS in this case results in damping of the zeroth mode, but it is destabilizing mode 1 and mode 2 Higher values of PSS gain has beneficial effect on zeroth mode damping in the presence of TCSC but at the same time this results in the destabilization of some of the stable torsional modes With the torsional filter all the torsional modes are stable, but the variation in filter parameters affect significantly the zeroth mode and the torsional filter mode The filter parameters can be selected such that the maximum damping can be achieved for the zeroth mode without adversely affecting the system stability

# Chapter 7

# CONCLUSIONS

The objective of the work reported in the thesis is to investigate the occurance of SSR phenomenon in a series compensated power system and to examine the effectiveness of the controllable devices in mitigating SSR namely (1) NGH damping scheme (2) STATCOM (3) TCSC

## 7.1 Occurance of SSR

The occurance of SSR has been studied in case of IEEE-FBM. For this purpose development of system model with fixed series compensated line is presented in Chapter 2 The system model developed in linear state space domain and the modular approach adopted in developing the system model permits the representation of a subsystem to any desired degree of detail

The eigenvalue analysis results show that the machine network interaction in the presence of fixed series compensation destabilizes the torsional modes This fact is validated and the occurance of instability due to SSR is evident in the time domain results obtained

## 7.2 Mitigation of SSR

The effect of NGH damping scheme in mitigating SSR due to fixed series compensation has been examined in Chapter 2 It is observed that although the growth of transient torque

oscillations due to SSR are arrested with the NGH damping scheme, but the reduction in peak torques is only moderate

Use of STATCOM has been considered in power system to provide dynamic reactive support Coupled with its basic function the effectiveness of STATCOM in mitigating SSR has been investigated in Chapter 3 For this purpose a supplementary control based on reactive current has been considered It is seen that the voltage control alone is inadequate in damping the torsional modes This situation significantly improves when the control is affected using reactive current along with the voltage control Detailed simulation studies also validate this observation and demonstrate the STATCOM capability with reactive current control effectively mitigating SSR while simultaneously providing dynamic reactive power support It has also been observed that the STATCOM is more effective in damping torsional oscillations compared to NGH damping scheme

Another controllable device which is gaining prominence for enhancement of power transfer capability on a transmission line is TCSC While performing this task the TCSC is expected to avoid occurance of SSR The study presented in Chapter 4 demonstrate this aspect by considering a constant angle control of TCSC which is based on the philosophy of maintaining the voltage drop across the compensated line constant The extent to which the power transfer over the line increases would depend upon the level of fixed series compensation considered while the vernier control of TCSC would help in decoupling the network modes from the mechanical modes While the control design is based on eigenvalue analysis, its performance in the event of large disturbances has been quite satisfactory

For the control of TCSC, from the view point of SSR mitigation, a new digital control strategy based on state feedback involving, line current and capacitor voltage has been proposed in Chapter 5 To investigate the SSR mitigation capability of TCSC, the model of TCSC along with the proposed controller is developed in discrete time linearized domain. The results of the analysis show that the digital control scheme makes TCSC extremely

effective in damping torsional modes It has also been seen that the TCSC contributes very significantly to the damping of network modes

The investigations on the effectiveness of the various controllable devices mentioned above did not consider the presence of excitation system The design of a controllable device (STATCOM or TCSC) should generally consider the presence of any other control present in the system primarily to ensure that the two controls do not have conflicting contributions to the system performance

The interaction between the generator excitation system (AVR and PSS) and TCSC has been studied and it is observed that while PSS has favorable impact on the zeroth mode (power swing mode). and it has a detrimental effect on the torsional modes This impact of PSS conflicts with that of TCSC This situation can overcome with the use of torsional filter along with the PSS has shown in Chapter 6 The torsional filter makes the PSS insensitive to torsional modes however, the parameters of torsional filter need to be carefully chosen to ensure overall system stability

## 7.3 Suggestions for future work

1 The effectiveness of TCSC or STATCOM in mitigating SSR need to be examined in multi machine environment This investigation also result in alternate control strategies

2 Application of the generator rotor speed synthesized from locally measurable quantities, as supplementary signal in mitigating SSR can be examined

3 The frequency scan method provides information regarding possible problems with torsional interaction and transient torques The study can be made with the frequency scanning technique to further examine the effec iveness TCSC in mitigating the SSR

# Appendix A

# Generator System Matrices

In this appendix generator system matrices are given

## A.1 Synchronous machine model matrices

The Synchronous machine model matrices are given below

$$[\mathbf{A}_{s1}] = \begin{bmatrix} -\frac{R_a\omega_B}{x'_d} & -\omega_B & 0 & \frac{R_a\omega_B}{x'_d} \\ \omega_B & -\frac{R_a\omega_B}{x'_q} & -\frac{R_a\omega_B}{x'_q} & 0 \\ 0 & -\frac{1}{T'_{qo}}\left(\frac{x_q}{x'_q}-1\right) & -\frac{x_q}{T'_{qo}x'_q} & 0 \\ \frac{1}{T'_{qo}}\left(\frac{x_d}{x'_d}-1\right) & 0 & 0 & -\frac{x_d}{T'_{do}x_d} \end{bmatrix}$$

$$[\mathbf{B}_{s11}] = \begin{bmatrix} \omega_B V_{gq} & -\omega_B \Psi_q \\ -\omega_B V_{gd} & \omega_B \Psi_d \\ 0 & 0 \\ 0 & 0 \end{bmatrix}$$

$$[\mathbf{B}_{s12}] = \begin{bmatrix} 0 \\ 0 \\ 0 \\ \frac{1}{T'_{do}} \end{bmatrix}$$

$$[\mathbf{B}_{s13}] = \begin{bmatrix} -\omega_B cos\delta & \omega_B sin\delta \\ -\omega_B sin\delta & -\omega_B cos\delta \\ 0 & 0 \\ 0 & 0 \end{bmatrix}$$

## A.2 Mechanical System Matrices

For the six mass mechanical system non-zero entries of the matrix $A_m$ $B_m$ and $C_m$ are given below

$A_m$ is a 12 X 12 matrix

$A_m(1,1) = -\frac{(D_e+D_{ge})}{2H_e}$

$A_m(1,2) = \frac{D_{ge}}{2H_e}$

$A_m(1,7) = \frac{1}{2H_e}$

$A_m(2,1) = \frac{D_{ge}}{2H_g}$

$A_m(2,2) = -\frac{(D_g+D_{ge}+D_{gLPB})}{2H_g}$

$A_m(2,3) = \frac{D_{gLPB}}{2H_g}$

$A_m(2,7) = -\frac{1}{2H_g}$

$A_m(2,8) = \frac{1}{2H_g}$

$A_m(3,2) = \frac{D_{gLPB}}{2H_{LPB}}$

$A_m(3\ 3) = -\frac{(D_{LPB}+D_{gLPB}+D_{LPBLPA})}{2H_{LPB}}$

$A_m(3,4) = \frac{D_{LPBLPA})}{2H_{LPB}}$

$A_m(3,8) = -\frac{1}{2H_{LPB}}$

$A_m(3,9) = \frac{1}{2H_{LPB}}$

$A_m(4,3) = \frac{(D_{LPBLPA})}{2H_{LPA}}$

$A_m(4,4) = -\frac{(D_{IPA}+D_{LPALPB}+D_{LPAIP})}{2H_{LPA}}$

$A_m(4,5) = \frac{D_{LPAIP})}{2H_{LPA}}$

$A_m(4,5) = -\frac{1}{2H_{LPA}}$

$A_m(4,10) = \frac{1}{2H_{LPA}}$

$A_m(5,4) = \frac{D_{LPAIP})}{2H_{IP}}$

$A_m(5,5) = -\frac{(D_{IP}+D_{LPAIP}+D_{IPHP})}{2H_{IP}}$

$A_m(5,6) = \frac{D_{IPHP})}{2H_{IP}}$

$A_m(5,10) = -\frac{1}{2H_{IP}}$

$A_m(5,11) = \frac{1}{2H_{IP}}$

$A_m(6,5) = \frac{D_{IPHP}}{2H_{HP}}$

$A_m(6,6) = -\frac{(D_{HP}-D_{IPHP}+D_{HP})}{2H_{HP}}$

$A_m(6,11) = -\frac{1}{2H_{HP}}$

$A_m(7,1) = -K_{ge}$

$A_m(7,2) = K_{ge}$

$A_m(8,2) = -K_{gLPB}$

$A_m(8,3) = K_{gLPB}$

$A_m(9,3) = -K_{LPBLPA}$

$A_m(9,4) = K_{LPBLPA}$

$A_m(10,4) = -K_{LPAIP}$

$A_m(10,5) = K_{LPAIP}$

$A_m(11,5) = -K_{IPHP}$

$A_m(11,6) = K_{IPHP}$

$A_m(12,2) = \omega_B$

$[\mathbf{B}_m]$ is a 12X1 matrix with non-zero entry

$B_m(2,1) = -\frac{1}{2H_g}$

$[\mathbf{C}_m]$ is a 2X12 matrix with non-zero entry

$C_m(1,12) = 1$

$C_m(2,2) = 1$

The matrix $[\mathbf{C}_{G1}]$ is defined as

$$[\mathbf{C}_{G1}] = [\mathbf{C}_{G1s}]\,\Delta\mathbf{x}_{s1} + [\mathbf{C}_{G1m}]\,\Delta\mathbf{x}_m$$

where

$$[\mathbf{C}_{G1s}] = \begin{bmatrix} \frac{cos\delta}{x'_d} & \frac{sin\delta}{x'_q} & \frac{sin\delta}{x'_q} & -\frac{cos\delta}{x'_d} \\ -\frac{sin\delta}{x'_d} & \frac{cos\delta}{x'_q} & \frac{cos\delta}{x'_q} & \frac{sin\delta}{x'_d} \end{bmatrix}$$

For a six mass system

$[\mathbf{C}_{G1m}]$ is a 2X12 matrix with non-zero entries

$C_{G1m}(1,12) = \imath_{Qo}$

$C_{G1m}(2,12) = -\imath_{Do}$

The synchronous machine output matrices are given below

$$[\ \mathbf{C}_G\ ] = \begin{bmatrix} \mathbf{C}_{G1} \\ \mathbf{C}_{G1}\mathbf{A}_G \end{bmatrix} and [\ \mathbf{D}_G\ ] = \begin{bmatrix} 0 \\ \mathbf{C}_{G1}\mathbf{B}_G \end{bmatrix}$$

In Chapter 5 the following synchronous machine output equation is used to get the overall system model

$$\Delta \mathbf{y}_G = [\mathbf{C}_G]\, \Delta \mathbf{x}_G$$

where $\Delta \mathbf{y}_G = [\Delta \imath_D\ \Delta \imath_Q]$ and $[\mathbf{C}_G] = [\mathbf{C}_{G1}]$

The interface matrix $[\mathbf{F}]$ for the IEEE-FBM is given by

$$[\mathbf{F}] = \begin{bmatrix} R_L & X_L & L_L & 0 & 1 & 0 \\ -X_L & R_L & 0 & L_L & 0 & 1 \\ 1 & 0 & 0 & 0 & 0 & 0 \\ 0 & 1 & 0 & 0 & 0 & 0 \end{bmatrix}$$

# Appendix B

# IEEE First bench mark model data

The data for the Synchronous machine is adapted from IEEE first benchmark model [1]

The data is given on 892 4 MVA base

(i) Generator data

$f = 60$ Hz, $R_a = 0$

$x_d = 1\ 79$ per unit , $x_d' = 0\ 169$ per unit, $T_{do}' = 4\ 3$ sec $x_q = 1\ 71$ per unit, $x_q' = 0\ 228$ per unit, $T_{qo}' = 0\ 85$ sec,

**Table B.1:** Mechanical system data

| Mass | Shaft | H (second) | K (per unit) |
|---|---|---|---|
| HP | | 0 092897 | |
| | HP-IP | | 7277 |
| IP | | 0 155589 | |
| | IP-LPA | | 13168 |
| LPA | | 0 85867 | |
| | LPA-LPB | | 19618 |
| LPB | | 0 884215 | |
| | LPB-GEN | | 26713 |
| GEN | | 0 868495 | |
| | GEN-EXC | | 1064 |
| EXC | | 0 0342165 | |

(ii) Transmission line data

$R_L = 0\ 02$ per unit , $X_L = 0\ 5$ per unit

(iii) Transformer reactance

$X_T = 0\ 2$ per unit

(iii) Operating point data

$V_g = 1$ per unit $P = 0\ 9$ per unit , at 0 9 p f lag

# Appendix C

# Synchronous machine initial condition calculation

The vector diagram for the generator is shown in Fig C 1 The generator terminal voltage $V_g\angle\theta$ and current $I_g\angle\theta'$ is known in phasor form from the initial conditions of the network variables and power flow through the transmission lines The rotor angle $\delta$ and the initial values of $E_q'$, $E_d'$ $v_d$ and $\psi_q$ are calculated as follows

$$E_q\angle\delta = V_g\angle\theta + I_g\angle\theta'(R_a + jx_q)$$

$$V_{gq} = V_g cos(\delta - \theta)$$

$$V_{gd} = -V_g sin(\delta - \theta)$$

$$i_q = I_g cos(\delta - \theta')$$

$$i_d = -I_g sin(\delta - \theta')$$

$$E_q' = V_{gq} - x_d' i_d + R_a i_q$$

$$E_d' = V_{gd} - x_q' i_q + R_a i_d$$

$$\psi_d = x_d' i_d + E_q'$$

$$\psi_q = x_q' i_q - E_d'$$

where $V_{gd}$ and $V_{gq}$ are the $d_q$ components of the generator voltage and $i_d$ and $i_q$ are the corresponding current quantities

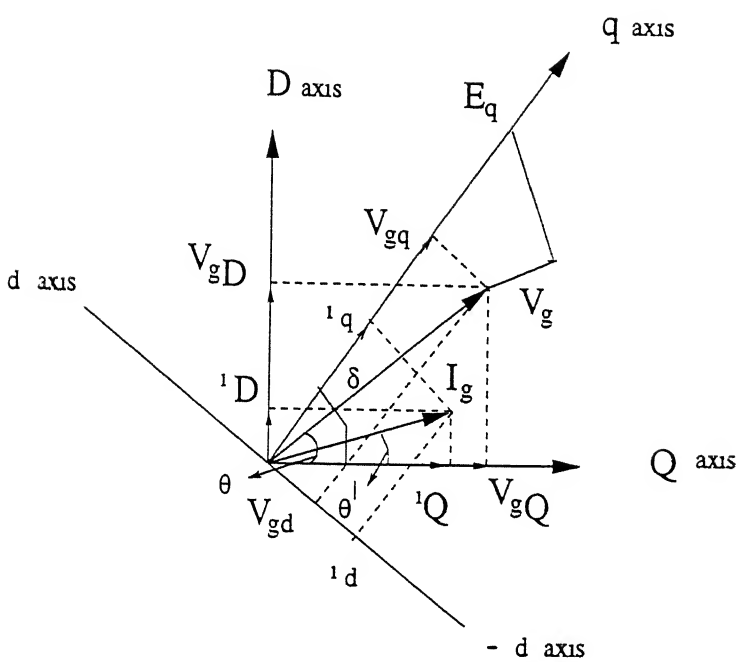


**Figure C 1:** Synchronous machine phasor diagram

# Appendix D

# STATCOM Controller and Interconnection Matrices

This appendix deals with the STATCOM controller matrices interconnection matrices initial condition calculation and STATCOM data

## D.1 STATCOM Controller Matrices

The matrices related to STATCOM controller are given below

$$[\mathrm{A}_{SC}] = \begin{bmatrix} -\frac{1}{T_m} & 0 & 0 & 0 \\ -K_I & 0 & 0 & 0 \\ 0 & 0 & -\frac{1}{T_m} & 0 \\ -K_pK_2 & K_2 & -K_2 & 0 \end{bmatrix}$$

$$[\mathrm{B}_{SC1}] = \begin{bmatrix} -\frac{K_DV_{sQ}}{V_sT_m} & \frac{K_DV_{sD}}{V_sT_m} \\ 0 & 0 \\ \frac{V_{sQ}}{V_sT_m} & -\frac{V_{sD}}{V_sT_m} \\ 0 & 0 \end{bmatrix}$$

$$[\mathrm{B}_{SC2}] = \begin{bmatrix} \frac{V_{sD}}{V_sT_m} - \frac{K_Dc_2}{T_m} & \frac{V_{sQ}}{V_sT_m} - \frac{K_Dc_3}{T_m} \\ 0 & 0 \\ \frac{c_2}{T_m} & \frac{c_3}{T_m} \\ 0 & 0 \end{bmatrix}$$

where

$$c_2 = -\frac{i_{sQ}}{V_s} - \frac{i_RV_{sD}}{V_s^2}$$

and

$$c_3 = \frac{i_{sD}}{V_s} - \frac{i_R V_{sQ}}{V_s^2}$$

$$[\mathrm{C}_{SC}] = \begin{bmatrix} -K_p K_1 & K_1 & -K_1 & 1 \end{bmatrix}$$

$$[\mathrm{C}_{S1}] = \begin{bmatrix} 1 & 0 & 0 & 0 & 0 & 0 & 0 \\ 0 & 1 & 0 & 0 & 0 & 0 & 0 \end{bmatrix}$$

$$[\mathrm{C}_{S2}^T] = [1^{st} row\ all\ columns\ of\ \mathrm{A}_S, 2^{nd}\ row\ all\ columns\ of\ \mathrm{A}_S]$$

$$[\mathrm{C}_S] = \begin{bmatrix} \mathrm{C}_{S1} \\ \mathrm{C}_{S2} \end{bmatrix}$$

$[\mathrm{D}_{S1}]$ is null matrix of size (2x2)

$$[\mathrm{D}_{S2}^T] = [1^{st}\ row\ all\ columns\ of\ \mathrm{B}_S, 2^{nd}\ row\ all\ columns\ of\ \mathrm{B}_S]$$

$$[\mathrm{D}_S] = \begin{bmatrix} \mathrm{D}_{S1} \\ \mathrm{D}_{S2} \end{bmatrix}$$

## D.2 Details of interconnection matrices

The [F] matrix describes the interconnection between inputs and outputs of various subsystems, is given by

$$[\mathrm{F}] = \begin{bmatrix} \mathrm{F}_{11} & \mathrm{F}_{12} & \mathrm{F}_{13} \\ \mathrm{F}_{21} & \mathrm{F}_{22} & \mathrm{F}_{23} \\ \mathrm{F}_{31} & \mathrm{F}_{32} & \mathrm{F}_{33} \end{bmatrix}$$

The elements of the [F] matrix are mentioned below

$$[\mathrm{F}_{11}] = \begin{bmatrix} R_L & X_L & L_L & 0 \\ -X_L & R_L & 0 & L_L \end{bmatrix}$$

$$[\mathrm{F}_{12}] = \begin{bmatrix} R_L & X_L & L_L & 0 \\ -X_L & R_L & 0 & L_L \end{bmatrix}$$

$$[\mathrm{F}_{13}] = \begin{bmatrix} 1 & 0 \\ 0 & 1 \end{bmatrix}$$

$$[\mathrm{F}_{21}] = \begin{bmatrix} R_L & X_L & L_L & 0 \\ -X_L & R_L & 0 & L_L \end{bmatrix}$$

$$[\mathbf{F}_{22}] = \begin{bmatrix} R_L & X_L & L_L & 0 \\ -X_L & R_L & 0 & L_L \end{bmatrix}$$

$$[\mathbf{F}_{23}] = \begin{bmatrix} 1 & 0 \\ 0 & 1 \end{bmatrix}$$

$$[\mathbf{F}_{31}] = \begin{bmatrix} 1 & 0 & 0 & 0 \\ 0 & 1 & 0 & 0 \end{bmatrix}$$

$$[\mathbf{F}_{32}] = \begin{bmatrix} -1 & 0 & 0 & 0 \\ 0 & -1 & 0 & 0 \end{bmatrix}$$

$$[\mathbf{F}_{33}] = \begin{bmatrix} 0 & 0 \\ 0 & 0 \end{bmatrix}$$

## D.3 STATCOM Initial condition calculation

The procedure for caluculating the initial conditions is mentioned below From load flow studies, $P_s$, $V_s$ and $Q_s$ at STATCOM bus are obtained

$B_s$ which is the susceptance of the STATCOM is given by

$$B_s = \frac{Q_s}{v_s^2}$$

The current $\imath_s$ through the STATCOM is given by

$$\imath_s = \jmath B_s v_s$$

The DC voltage $v_{dc}$ is given by

$$v_{dc} = \frac{|v_s - \imath_s(R + \jmath x_l)|}{k}$$

and the angle $\beta$ is given by

$$\beta = \angle v_s - \angle (v_s - \imath_s(R + \jmath x_l))$$

# Appendix E

# TCSC Controller and Interconnection Matrices

This appendix deals with the network matrices, derivation of continuous time TCSC model given in Chapter 5 and interconnection matrices

## E.1 MATRICES FOR TCSC CONTROL

The network matrices are given below

$$\mathbf{A}_N = \begin{bmatrix} 0 & -\omega_B & 0 & 0 \\ \omega_B & 0 & 0 & 0 \\ 0 & 0 & 0 & -\omega_B \\ 0 & 0 & \omega_B & 0 \end{bmatrix}$$

$$\mathbf{B}_N = \begin{bmatrix} \omega_B X_{CF} & 0 & 0 & 0 & 0 \\ 0 & \omega_B X_{CF} & 0 & 0 & 0 \\ \omega_B X_{TCSC} & 0 & -v_{TCSCD}\, \omega_B X_{TCSC}\, k & 0 & 0 \\ 0 & \omega_B X_{TCSC} & -v_{TCSCQ}\, \omega_B X_{TCSC}\, k & 0 & 0 \end{bmatrix}$$

$$\frac{\partial X_{TCSCeff}(\sigma)}{\partial \sigma} = k$$

where

$$k = \frac{1}{k_3^2}\left[\frac{cos\sigma}{\pi}(X_C + k_1) + \frac{4k_1^2}{\pi x_p}\left[\frac{cos\sigma}{2} - k_2 sin\sigma\, tan\left(\frac{k_2\sigma}{2}\right) + cos^2\left(\frac{\sigma}{2}\right) k_2 \frac{1}{sec^2\left(\frac{k_2\sigma}{2}\right)}\right]\right]$$

$$X_{TCSCeff}(c) = X_c - \frac{(\sigma + sin\sigma)}{\pi}[X_c + k_1] + \frac{4k_1^2}{\pi x_p} cos^2\left(\frac{\sigma}{2}\right)\left[tan\left(\frac{\sigma}{2}\right) - k_2 tan\left(\frac{k_2\sigma}{2}\right)\right]$$

$$k_1 = \frac{X_c X_p}{X_c - X_p}$$

$$k_2 = \sqrt{\frac{X_c}{X_p}}$$

$$k_3 = X_{TCSCeff}(\sigma)$$

$$C_N = \begin{bmatrix} 1 & 0 & 1 & 0 \\ 0 & 1 & 0 & 1 \\ 0 & 0 & 1 & 0 \\ 0 & 0 & 0 & 1 \end{bmatrix}$$

$$D_N = \begin{bmatrix} R_L & \omega_B L_L & 0 & L_L & 0 \\ -\omega_B L_L & R_L & 0 & 0 & L_L \\ 0 & 0 & 0 & 0 & 0 \\ 0 & 0 & 0 & 0 & 0 \end{bmatrix}$$

### E.1.1 Derivation of TCSC Voltage

The TCSC model is developed based on dynamic phasor approach In this approach a waveform $x(.)$ can be represented on the interval $(t-T, t)$ using a Fourier series of the form

$$x(\tau) = Re\left[\Sigma X_k(t) e^{j-B\tau}\right]$$

where $k \geq 0$, $Re$ denotes the real part, $\omega_B = \frac{2\pi}{T}$, $\tau \in (t-T, T)$. and $X_k$ are the Fourier coefficients, which are referred as phasors These Fourier coefficients are functions of time since the interval under consideration slides as a function of time The $k$-th coefficient (or $k-phasor$) at time $t$ is determined by the following averaging operation

$$X_k(t) = \frac{c}{T}\int_{t-T}^{t} x(\tau) e^{-jk\omega_B \tau} d\tau =< x >_k (t)$$

where $c = 1$ for $k = 0$ and $c = 2$ for $k > 0$ The derivative of the $k$-th Fourier coefficient is given by the following expression

$$\frac{dX_k}{dt} =< \frac{d}{dt}x >_k - jk\omega_B X_k$$

The TCSC capacitor voltage and parallel inductor current are denoted by $v_{TCSC}$ and $i_p$ respectively The parallel inductor is denoted by $L_p$ The line current is denoted by $i_G$ The state space model is given by

$$C_{TCSC}\frac{dv_{TCSC}}{dt} = i_G - i_p$$

$$L_p\frac{di_p}{dt} = qv$$

where $q$ is a switching function that denotes the thyristor status $q = 1$ when one thyristor is on, and $q = 0$ when both thyristors are off The line current is assumed sinusoidal over any interval of length $T = \frac{2\pi}{\omega_B}$ The state space model is obtained by applying averaging operation to the above equation resulting in

$$CTCSC\frac{dv_{TCSC1}}{dt} = i_G - i_{p1} - j\omega_B C_{TCSC} v_{TCSC1}$$

$$LP\frac{di_{p1}}{dt} = < qv_{TCSC} >_1 - j\omega_B L_P i_{p1}$$

The quasi steady state model of TCSC is obtained with the following assumption

$$i_{p1} \approx \frac{v_{TCSC1}}{j\omega_B L_{eff(\sigma)}}$$

where

$$L_{eff(\sigma)} = \frac{1}{\omega_B{}^2(C_{TCSC} - C_{TCSCeff(\sigma)})}$$

The quasi steady state model of the TCSC is obtained using the above approximation as

$$C_{TCSC}\frac{dv_{TCSC1}}{dt} = i_G - (j\omega_B C_{TCSC} + \frac{1}{j\omega_B L_{eff(\sigma)}})v_{TCSC1} = i_G - j\omega_B C_{TCSCeff(\sigma} v_{TCSC1}$$

In the above equation the TCSC voltage and line current are fundamental phasor quantities i e , $k = 1$ The above equation is derived in synchronously rotating reference frame and can be written as

$$C_{TCSC}\, v_{TCSC} = i_G + \frac{v_{TCSC}}{X_{TCSCeff}(\sigma)}$$

where, $\sigma = \sigma_{ref} + 2arg\,(-ji_G v_{TCSC})$

## E.2 Details of Interconnection matrices

The [F] matrix which describes the interconnection between inputs and outputs of the various subsystems is given by

$$[\mathbf{F}] = \begin{bmatrix} \mathbf{F}_{11} & \mathbf{F}_{12} & \mathbf{F}_{13} \\ \mathbf{F}_{21} & \mathbf{F}_{22} & \mathbf{F}_{23} \\ \mathbf{F}_{31} & \mathbf{F}_{32} & \mathbf{F}_{33} \end{bmatrix}$$

where, for the study system $\mathbf{F}_{11} = \mathbf{F}_{13} = \mathbf{F}_{22} = \mathbf{F}_{33} = 0$

$$[\mathbf{F}_{21}] = \begin{bmatrix} 1 & 0 & 0 & 0 \\ 0 & 1 & 0 & 0 \\ 0 & 0 & 0 & 0 \\ 0 & 0 & 1 & 0 \\ 0 & 0 & 0 & 1 \end{bmatrix}$$

$$[\mathbf{F}_{12}] = \begin{bmatrix} 1 & 0 & 0 & 0 \\ 0 & 1 & 0 & 0 \end{bmatrix}$$

$$[\mathbf{F}_{23}] = \begin{bmatrix} 0 \\ 0 \\ 1 \\ 0 \\ 0 \end{bmatrix}$$

$$[\mathbf{F}_{31}] = \begin{bmatrix} 0 & 0 & 0 & 0 \\ 0 & 0 & 0 & 0 \\ 1 & 0 & 0 & 0 \\ 0 & 1 & 0 & 0 \end{bmatrix}$$

$$[\mathbf{F}_{32}] = \begin{bmatrix} 0 & 0 & 1 & 0 \\ 0 & 0 & 0 & 1 \\ 0 & 0 & 0 & 0 \\ 0 & 0 & 0 & 0 \end{bmatrix}$$

# Appendix F

# Excitation System and PSS Matrices

In this appendix the matrices associated with chapter 6 and data of exciter and PSS are mentioned

## F.1 Exciter and PSS Matrices

The matrices related to excitation system and PSS are given below

$$\mathbf{A}_{e1} = \begin{bmatrix} -\frac{1}{T_R} & \frac{K_R}{T_R} & \frac{K_R}{T_R}C_2 & K_s\frac{K_R}{T_R}C_2^2 \\ 0 & -C_1 & C_4 & K_sC_5 \\ 0 & 0 & -C_1 & K_sC_4 \\ 0 & 0 & 0 & -\frac{1}{T_w} \end{bmatrix}$$

$$\mathbf{B}_{e11} = \begin{bmatrix} \frac{K_R}{T_R}C_2^2K_s \\ K_sC_5 \\ K_sC_4 \\ -\frac{1}{T_w} \end{bmatrix}$$

$$\mathbf{B}_{e12} = \begin{bmatrix} -\frac{K_Rv_{gD}}{T_Rv_g} & -\frac{K_Rv_{gQ}}{T_Rv_g} \\ 0 & 0 \\ 0 & 0 \\ 0 & 0 \end{bmatrix}$$

$$\mathbf{E}_{e1} = \begin{bmatrix} \frac{K_R}{T_R} \\ 0 \\ 0 \\ 0 \end{bmatrix}$$

$$\mathbf{C}_{e1} = \begin{bmatrix} 1 & 0 & 0 & 0 \end{bmatrix}$$

where $C_1 = \frac{1}{T_2}$, $C_2 = \frac{T_1}{T_2}$, $C_3 = 1 - \frac{T_1}{T_2}$, $C_4 = C_1 C_3$, $C_5 = C_1 C_2 C_3$ and $T_W$ is the washout time constant

## F.2 Exciter PSS and Torsional filter matrices

The matrices related to excitation system, PSS and torsional filter are given below

$$\mathbf{A}_{e1} = \begin{bmatrix} -\frac{1}{T_R} & \frac{K_R}{T_R}\omega_n^2 & 0 & 0 & 0 & 0 \\ 0 & 0 & 1 & 0 & 0 & 0 \\ 0 & -\omega_n^2 & -2\zeta\omega_n & \omega_n^2 & \omega_n^2 C_2 & \omega_n^2 C_2^2 K_s \\ 0 & 0 & 0 & -C_1 & C_4 & C_5 K_s \\ 0 & 0 & 0 & 0 & -C_1 & C_4 K_s \\ 0 & 0 & 0 & 0 & 0 & -\frac{1}{T_w} \end{bmatrix}$$

$$\mathbf{B}_{e11} = \begin{bmatrix} 0 \\ 0 \\ \omega_n^2 C_2^2 K_s \\ K_s C_5 \\ K_s C_4 \\ -\frac{1}{T_w} \end{bmatrix}$$

$$\mathbf{B}_{e12} = \begin{bmatrix} -\frac{K_R v_{gD}}{T_R v_g} & -\frac{K_R v_{gQ}}{T_R v_g} \\ 0 & 0 \\ 0 & 0 \\ 0 & 0 \\ 0 & 0 \\ 0 & 0 \end{bmatrix}$$

$$\mathbf{E}_{e1} = \begin{bmatrix} \frac{K_R}{T_R} \\ 0 \\ 0 \\ 0 \\ 0 \\ 0 \end{bmatrix}$$

$$\mathbf{C}_{e1} = \begin{bmatrix} 1 & 0 & 0 & 0 & 0 & 0 \end{bmatrix}$$

where $C_1 = \frac{1}{T_2}$, $C_2 = \frac{T_1}{T_2}$, $C_3 = 1 - \frac{T_1}{T_2}$, $C_4 = C_1 C_3$, $C_5 = C_1 C_2 C_3$ and $T_W$ is the washout time constant

## F.3 Exciter and PSS Data

The excitation system and PSS data is given below

**Exciter Data**

$K_R = 200$, $T_R = 0.025s$, $T_W = 10$

**PSS Data**

$T_1 = 0.048s$, $T_2 = 0.032$

# References


[1] M Hall and D Hodges "Experience with 500 kv subsynchronous resonance and resulting turbine generator shaft damage at mohave generating station," in *IEEE 1976 winter meeting and Tesla symposium*, pp 22–29, 1976

[2] IEEE SSR Task Force. "Proposed terms and definitions for subsynchronous resonance in series compensated power systems," *IEEE Trans on Power Apparatus and Systems*, vol PAS-92, pp 506–511, 1980

[3] IEEE Committee Report, "Reader's guide to subsynchronous resonance." *IEEE Trans on Power Systems*, vol 7, no 1, pp 150–157, 1992

[4] K R Padiyar, *Power system dynamics, stability and control* Bangalore· Interline publishing private limited, 1996

[5] P Andersonand B L Agrawal, and J Vanness, *Subsynchronous Resonance in Power Systems* Newyork IEEE Press, 1990

[6] L Kilgore, L Elliott, and E R Taylor, "The prediction and control of self excited oscillations·due to series capacitors in power systems *IEEE Trans on Power Apparatus and Systems*, vol PAS-90, pp 1305–1311, 1971

[7] A Fouad and K Khu, "Subsynchronous resonance zones in the ieee first bench mark power system," *IEEE Trans on Power Apparatus and Systems*, vol PAS-97 no 3, pp 754–762, 1997

[8] R G Farmer, A L Schwalb, and E Katz, "Navajo project report on subsynchronous resonance analysis and solutions," *IEEE Trans on Power Apparatus and Systems*, vol PAS-96, no 4, pp 1226–1232, 1977

[9] IEEE SSR Working Group. "Countermeasures to subsynchronous resonance problems." *IEEE Trans on Power Apparatus and Systems*, vol PAS-99, pp 1810–1818, 1980

[10] L Wang, "Damping of torsional oscillations using Excitation control of synchronous generator the IEEE second bench mark model investigation " *IEEE Trans. on Energy Conversion*, vol 6, no 1, pp 47–54, 1991

[11] A A Edris, "Subsynchronous resonance counterr ieasure using phase imbalance." *IEEE Trans on Power Systems*, vol 8, no 4, pp 1433–1447, 1993

[12] M.R Iravani et al, "Damping of subsynchronou s oscillations in power system using static phase shifter," *IEEE Trans on Power Systems*, vol 1, no 2, pp 76–82, 1986.

[27] P E Krause et al, "ASC with thyristor controlled impeadance," in *CIGRE International conference France 1992*, 1992

[28] C E J Bowler et al, "FACTS and SSR - focus on TCSC application and mitigation of ssr problems," in *EPRI FACTS Conference Boston*, 1992

[29] R A Heidin et al, "SSR characteristics of alternative types of series compensation schemes," *IEEE Trans on Power Systems*, vol 10, no 2, pp 845–852, 1995

[30] C W Edwards et al, "Advanced static VAR generator employing GTO thyristors," *IEEE Trans on Power Delivery*, vol 3, no 4, pp 1622–1627, 1988

[31] C Schauder and H Mehta, "Vector analysis and control of advanced static var generator," *IEE Proc c*, vol 140, no 4, pp 299–306, 1993

[32] C Schauder et al, "Development of a 100 MVAR static condensor for voltage control of transmission systems," *IEEE Trans on Power Delivery*, vol 10, no 3 pp 1486–1496, 1995

[33] B Das, A Ghosh, and Sachchidanand, "Suitable configuration of ASVC for power transmission application," *Electic Power System Research*, vol 49, pp 107–122, 1999

[34] B M Han, G C Karady, and J K Park, "Interaction analysis model for transmission static compensator with EMTP," *IEEE Trans on Power Delivery* vol 13, no 4, pp 1297 1302, 1998

[35] K V Patil et al , "Damping of torsional oscillations in ac system using STATCOM," in *National Power System Conference, Kanpur, India*, pp 243–247, 1996

[36] IEEE committee Report, "First benchmark model for computer simulation of subsynchronous resonance," *IEEE Trans on Power Apparatus and Systems*, vol PAS-96, pp 1565 1570, 1977

[37] O Wasynczuk, "Damping of Subsynchronous Resonance using Energy storage," *IEEE Trans on Power Apparatus and Systems*, vol PAS-101, no 4, pp 905–914, 1982

[38] D G Ramey et.al, "Dynamic stabilizer verification tests at san juan station," *IEEE Trans on Power Apparatus and Systems*, vol PAS-100, no 12, pp 5011–5019, 1981

[39] E V. Larsen, K Clark, J S A Miske, and J Urbanek, "Characteristics and rating considerations of thyristor controlled series compensation," *IEEE Trans on Power Delivery*, vol 9, no 2, pp 992–1000, 1994

[40] P C Srivastava, A Ghosh, and S V Jayaramkumar, "Model based control design of a TCSC compensated power system," *International journal of Electric power and Energy systems*, vol 21, no 4, pp 299–307, 1999

[41] A Ghosh, G Ledwich, GS Hope and OP Malik, "Powersystem stabilizer for large distrubances," *IEE Proc - Generation Transmission and Distribution*, vol 132, no 1, pp 14 -19, 1985

[42] K R Padiyar and A G Kothari, "Study of HVDC torsional interactions through digital dynamic simulation," *Electric machines and Power systems*, vol 14, no 5, 1989

[43] P Kundur, *Power system stability and control* New York McGraw-Hill Inc, 1994

## LIST OF PUBLICATIONS

[1] P C Srivastava A Ghosh and S V Jayaram Kumar Model based control design of a TCSC compensated power system International journal of Electric Power and Energy systems, Vol 21 No 1 pp 299-307, 1999

[2] S V Jayaram Kumar, A Ghosh and Sachchidanand Damping of Subsynchronous Transient torque oscillations using STATCOM To appear in Journal of Institution of Engineers (India)

[3] A Ghosh, S V Jayaram Kumar and Sachchidanand Subsynchronous Resonance Analysis using a Discrete Time TCSC Model To appear in International journal of Electric Power and Energy systems

[1] S V Jayaram Kumar, A Ghosh and Sachchidanand Damping of Subsynchronous Resonance Oscillations with TCSC and PSS and their control interaction To appear in Electric Power System Research